Bacillus cereus: emetic toxin production and gamma hypothesis for growth

Elisabeth G. Biesta-Peters

Thesis committee

Thesis supervisors
Prof dr. ir. M.H. Zwietering
Professor of Food Microbiology
Wageningen University

Prof. dr. L.G.M. Gorris
Professor of Food Microbiology
Wageningen University

Thesis co-supervisor
Dr. ir. M.W. Reij
Lecturer at the Laboratory of Food Microbiology
Wageningen University

Other members
Prof. dr. ir. M.A.J.S. van Boekel, Wageningen University, Wageningen, The Netherlands
Prof. dr. S. Brul, University of Amsterdam, Amsterdam, The Netherlands
Prof. dr. D.W. Schaffner, Rutgers University, New Brunswick, United States of America
Dr. Msc. ing. A. Rajkovic, Ghent University, Ghent, Belgium

This research was conducted under the auspices of the Graduate School of advanced studies in Food Technology, Agrobiotechnology, Nutrition and Health Sciences (VLAG)

Bacillus cereus: emetic toxin production and gamma hypothesis for growth

Elisabeth G. Biesta-Peters

Thesis
submitted in fulfilment of the requirements for the degree of doctor
at Wageningen University
by the authority of the Rector Magnificus
Prof. dr. M.J. Kropff,
in the presence of the
Thesis Committee appointed by the Academic Board
to be defended in public
on Friday September 16, 2011
at 1.30 PM in the Aula.

Elisabeth G. Biesta-Peters
Bacillus cereus: emetic toxin production and gamma hypothesis for growth
192 pages

Thesis Wageningen University, Wageningen, NL (2011)
With references, with summaries in Dutch and English

ISBN 978-90-8585-993-2

"Yesterday is history. Tomorrow is a mystery. Today is a gift. That's why it is called 'The Present'."

-Eleanor Roosevelt-

To my grandfather
To my parents
To Wouter

Contents

Abstract

Bacillus cereus is a food spoilage microorganism and a pathogen. Growth of *B. cereus* can be prevented or delayed by adding growth limiting compounds to the food product or by altered storage conditions. Combinations of growth limiting factors can show synergy, or be multiplicative without synergy (gamma hypothesis). For food safety management, it is important to understand if combinations are synergistic or not, to avoid making fail-dangerous or overly fail-safe predictions. Therefore, the aim of this PhD project was to validate the gamma hypothesis for specific combinations of hurdles commonly used in food production. Since the relationship between growth and toxin production of *B. cereus* is little understood, a second aim was to investigate the production of the emetic toxin cereulide in more detail. Several new lines of research were set-up to deliver on these aims. For growth data collection to quantify hurdle effects and to study combinations of hurdles, the relative rate to detection method was found to be preferred over two other methods evaluated. The gamma hypothesis was validated for combinations of pH and undissociated acid. For combinations of pH and water activity lowering solutes, the gamma hypothesis could neither be validated nor rejected. The validity of the gamma hypothesis appeared to be dependent on the models chosen for the single hurdle effects, which are subsequently combined into the gamma model. A systematic way of model selection is therefore advocated. Investigating cells in the transition from lag phase (λ) to exponential growth phase, it was found that trends in physiological processes could be observed for different culture conditions, independent of the duration of λ. Esterase activity and electron transport chain activity were found to be useful quantitative markers for this transition phase. A new method to produce synthetic cereulide showing biological activity was developed, allowing accurate quantification of cereulide in samples. The use of valinomycin as a standard, the current procedure, underestimates the amount of cereulide by approximately 10 %. Considering the onset of emetic toxin production, LC-MS analysis of *B. cereus* F4810/72 grown in BHI showed that cereulide production does not start before cells are in mid to late stationary phase, although significant variation was noted possibly related to variability in the growth parameters maximum specific growth rate (μ_{max}) and λ. Addition of salt to the growth medium delayed the production of cereulide. This research has been able to deliver several new insights and tools that are useful for food safety management of the emetic toxin producer *B. cereus*.

Chapter 1

Introduction and thesis outline

1

Abstract

The safety and shelf life of food products are impacted by the possible presence and growth of microorganisms. To assess their impact, the ecology of microorganisms in foods and their ability to survive and multiply at different stages of the food supply chain up to consumption needs to be assessed. In this assessment, mathematical modeling (or quantitative microbiology) has become a powerful tool that finds good use in food industry as well as in the governmental/regulatory context. Modeling often focuses on quantifying numbers of viable bacteria in foods and food environments. This thesis addresses the aspect of mathematical modeling of bacterial growth when growth rate limiting compounds are used to delay or prevent growth. It is essential to be able to determine the level of the actual hazard present in foods at the time of consumption, in order to make a risk-based assessment of the safety of the product. For microorganisms that produce toxins the actual hazard is the toxin that they produce. Therefore, the need to more accurately assess the health impact conveyed through bacterial toxins of concern, an area relatively new in terms of the application of mathematical modeling, is addressed as well. The toxigenic microorganism Bacillus cereus *was chosen as the model organism. This introduction covers relevant background aspects for the work presented in this thesis, i.e. food related bacteria, food preservation, quantitative microbiology, the model organism* B. cereus *and the toxins this microorganism can produce.*

Food related bacteria and the bacterial life cycle

Almost every food product contains bacteria. The types of bacteria present, the microflora, is highly dependent on the microflora in the raw materials, the processing, preservation techniques used and storage conditions. Bacteria can have positive effects on foods for instance due to food fermentation, since fermentation can add flavor to the product and prevents spoilage (38). Fermentation also improves digestibility and availability of nutrients. Examples of fermented foods are yoghurt and cheese, both products of fermented milk, and the fermentation of barley to beer and of grapes to wine (18). Amongst the typical spoilage organisms of foods is *Bacillus cereus*, which can spoil pasteurized milk when the spores survive the thermal treatment of the milk (23, 35). *B. cereus* can also be a food pathogen, potentially causing illness upon ingestion. The presence of pathogens is not necessarily related to spoilage of food products, since a food product containing pathogens might still be sensory acceptable or a spoiled food product might be free of pathogens.

Viable cells of different bacterial species have comparable life cycles. When microorganisms are present in a growth promoting environment, they often first need time to adapt to this environment, which results in a so-called lag phase (λ) (83). The duration of the lag phase depends on the difference in growth promoting conditions before and after bacteria transfer to a new environment. When the lag phase has elapsed, microorganisms start to grow exponentially; this is the so- called exponential growth phase (61). The speed of growing is reported as the maximum specific growth rate (μ_{max}) per hour, i.e. the growth rate once accelerated to the maximal value. When there are no nutrient limitations or unfavorable growth conditions for a bacterial culture the maximum specific growth rate is displayed as μ_{opt}. When microorganisms reach a level of approximately 10^9 (log 9) colony forming units (CFU) per ml or per g of food, generally, they will enter the stationary phase and the population as a whole will no longer increase in numbers. Depending on the specific conditions of the environment in and outside the food, sooner or later the microorganisms reach the starvation phase, in which the level of living microorganisms decreases. This bacterial life-cycle is depicted in Figure 1.

The particular set of environmental conditions inside and outside a food product (together referred to as the culture conditions) have a major impact on the survival and growth of microorganisms. Culture conditions affect both the length of the lag phase and the maximum specific growth rate of microorganisms. For example, when the pH of food

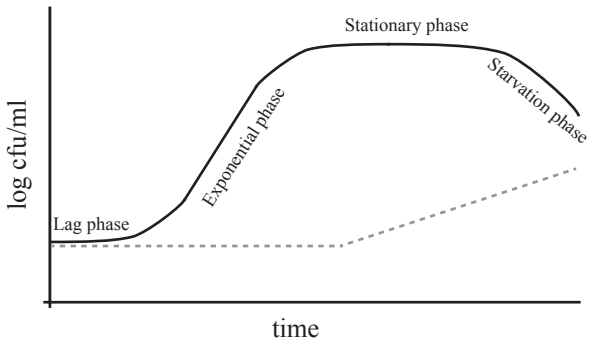

Figure 1. The bacterial life cycle with a lag phase, exponential growth phase, stationary phase and starvation phase (black line) and the effect of non-optimal conditions on the lag phase and the exponential phase (gray dashed line).

or of a growth medium decreases from neutral to pH values of around pH 5, the length of the lag phase substantially increases as indicated in Figure 1 by the gray dashed line. In the case of *B. cereus* F4810/72, such an increase is from 2.4 h to 7.6 h (17). Simultaneously μ_{max} decreases and for *B. cereus* F4810/72 this is from values of 2.42 h^{-1} to 0.63 h^{-1} (17). This effect is also indicated in Figure 1 by the reduced slope of the exponential growth phase depicted by the gray dashed line. The final number of microorganisms, which depends on the initial number and the culture conditions, can be calculated using for example Equation 1, the modified Gompertz equation, when μ_{max}, λ and A are known (97).

$$\ln\left(\frac{N_t}{N_0}\right) = A\,\exp\left\{-\exp\left[\frac{\mu_{max}\mathrm{e}}{A}(\lambda - t)+1\right]\right\} \quad (1)$$

Where N_t is the number of microorganisms (CFU/ml) at time t (h), N_0 is the number of microorganisms at the time of inoculation, A is the dimensionless asymptotic value of $\ln(N_t/N_0)$ (97), μ_{max} is the maximum specific growth rate (h^{-1}) and λ is the lag time (h).

Some microorganisms are able to produce spores which can be present in dormant forms in media or food products until the conditions become favorable (8). Then they will germinate and a growth pattern similar to Figure 1 will occur.

Food preservation

Food preservation techniques have been used by mankind for ages. One of the oldest preservation techniques is food fermentation, for example fermentation of beverages, bread and fish (38). Example of other preservation techniques include salting of fish to avoid spoilage (96) and cooking fruit with sugar to make jam which is not vulnerable to rotting anymore (62). These techniques all rely on the principle that if the conditions are non-optimal for microorganisms, they will have a longer lag phase and/or a lower growth rate, which both enhance the shelf life of a food product and impacts on food safety. Several growth limiting factors can be used to ensure food stability and safety, such as modified atmosphere packaging (MAP), chilling, lowering pH, drying, and the use of organic acids (34, 79). Contrary to cooking, baking or pasteurizing a food product before consumption, the addition of food preservatives targets on slowing down or blocking growth rather than killing microorganisms present. The various individual preservation methods are often referred to as ''hurdles", as they impact directly on the ability of microorganisms to survive and proliferate. The effectiveness of a hurdle mainly depends on the intensity of the hurdle and on the possible resistance of the particular microorganism to that hurdle. In case of, for example, the hurdle pH, *B. cereus* is still able to grow at a pH of 5.0, (set with strong acid), whilst no growth is observed anymore at a pH of 4.7 (17). This situation is sketched in Figure 2, where the intensity of the hurdle determines whether growth is possible or not. The hurdles pH, undissociated acid concentration and water activity will be discussed below in more detail, since they were used in the research conducted in this thesis.

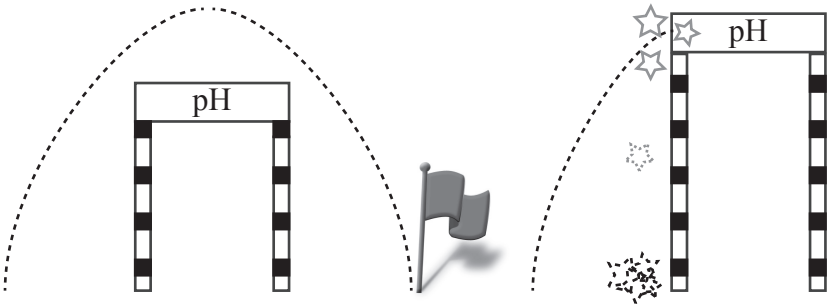

Figure 2. Author's impression of hurdle technology. The hurdle pH at two different intensities, where the left hurdle is not high enough to avoid microbial growth, the right hurdle is of a high enough intensity to limit the growth of the specific microorganism.

Hurdles

pH

The pH is a measure for the acidity or the basicity of a food or solution. It is the negative logarithm (p) of the molar concentration of the hydrogen ion ($[H^+]$) (12). Hydrogen ions can be added to the solution as strong or weak acids. Strong acids dissociate easily into the hydrogen ion and the anion part, and will therefore completely dissociate when added to a non-saturated solution. A drop in pH of medium or a food product may cause changes in the microorganism's internal pH or in its membrane fatty acid profile, which may lead to a rerouting of the ATP generating pathway, allowing less energy for biomass synthesis and therefore eventually eliminating growth (22).

Undissociated organic acids

Organic acids have a COOH functional group with an attached organic group or hydrogen atom, which distinguishes them from other acids. The organic acids are called weak acids since they do not easily donate protons in an aqueous solution. Weak acids only partly dissociate in water, e.g. only a percentage of the molecules splits into the proton (H^+) and the anion (A^-) (19). The level of dissociation depends on the dissociation constant (pK_a) of the particular acid and the pH of the medium. The concentrations of both the undissociated and dissociated forms of the acid can be calculated according to the Henderson-Hasselbalch equation (Equation 2).

$$\mathrm{pH} = \mathrm{p}K_a + \log\frac{[\mathrm{A}^-]}{[\mathrm{HA}]} \qquad (2)$$

Where pK_a is the acid dissociation constant, $[A^-]$ is the concentration of anions and [HA] is the concentration of the undissociated acid (12).

Organic acids can act both as a source of carbon and energy or as inhibitory agents for microorganisms. The obtained effect greatly depends on the concentration of the acid, but also depends on the survival capabilities of the microorganism. The mechanism of action of an undissociated acid is that it crosses the lipid bilayer of the cell membrane and dissociates in the cell cytoplasm, causing a decrease of the internal pH (19). The inhibitory action of undissociated acids generally is bigger than that of the dissociated acid at equal pH values (28).

Water activity

Water is present in all foods and food ingredients at different levels. Levels may vary from trace amounts, such as in dried soups or biscuits, to high moisture contents, for example in fresh fruits and vegetables. Water in foods is important for production, processing and microbial safety, as well as for chemical and physical stability of the product. The mobility of water molecules in a food product can be influenced when components such as sugar or salt are added to the product (76). Water content and mobility are reflected in the so-called water activity (a_w) of a food. The definition of a_w is the ratio of the vapor pressure (fugacity) of water in the system at a given temperature and the vapor pressure of pure liquid water at the same temperature. It is the measure of the tendency of water to escape from the food product, e.g. the “free” water (74). Water activity can be measured using a hygrometer. The material is placed in a sealed chamber and a sensor measures the changes in electrical response as a function of the relative humidity. Depending on the water vapor pressure of the air surrounding the product, water will absorb or desorb within the sensor and alter the electrical properties of the hygroscopic material in the sensor (33). Water activity is a major factor in preventing or limiting microbial growth. Spore production and toxin formation of bacteria is a_w dependent, and so is microbial growth (85).

Quantitative microbiology

Data and knowledge on the response of microorganisms to different culture conditions can be systematically assessed and captured in mathematical models that take account of the key growth promoting or inhibiting conditions. Such models can be used to determine or predict potential responses under particular conditions. This modeling approach is often referred to as "quantitative microbiology" or "predictive microbiology". Predictive microbiology relies on the concept that the responses of microorganisms to factors in the environment are to a large extent reproducible. Thus, knowledge about past behavior can be used to predict how a population will react to environmental changes in the future (75). Therefore predictive microbiology can be used to, for example, asses the likely shelf life of newly developed food products. Predictive microbiology can be used as kinetic modeling, modeling the growth rate and level of microorganisms, and as probability modeling, modeling the likelihood of growth or inactivation occurring under defined circumstances (75). Mathematical models are best used additionally to conducting

biological experiments. As they are a simplification of reality, still some (but often less) biological data are needed to get a good view on the response of microorganisms. Two types of models can be distinguished: empirical models, which describe observations without taking into account the mechanisms underlying the microbial response, and mechanistic models that describe the main mechanisms for the observed behavior (15). Models describing the bacterial growth or death curve are considered primary models and models describing how environmental factors affect growth parameters or starvation parameters are considered secondary models (15).

Predictive microbiology has many benefits, since it may significantly reduce the need for expensive, slow and skill demanding biological experiments such as shelf life tests and challenge tests. A drawback may be that environmental factors are not always accurately measured and that the heterogeneity of a microbial population may generate a different response then expected (56). Many experts therefore advocate that it is important to validate predictive models (64, 66, 67). These validation studies will eventually help to increase the accuracy and predictive capacity of the models and therefore contribute to accurate predictions that are useful in shelf life assessment and for food safety assurance.

Hurdle technology and the gamma hypothesis

Combining hurdles to achieve food stability and safety, known as hurdle technology, can be used to achieve an overall level of protection in food while minimizing impacts on food quality (52). When a combination of hurdles is used, generally, the intensity of the individual hurdles may be lower but together still have a comparable preservative effect as compared to the intensity of those hurdles when used as single hurdles (52). Though the concept of hurdle technology is rather well established, the quantification of the combined impact of hurdles on growth of microorganisms is still being investigated. A significant problem is that there are two opposite views of how antimicrobial factors combine in a hurdle technology approach. One view states that there are interactive effects between hurdles such that when they are applied together they give a significantly greater protection than expected on the basis of the application of the individual hurdles. This phenomenon is called “synergy”. The alternative view considers that the combined effect may be complex, and apparently synergistic, but that there are no interactive effects resulting in true synergy. The latter view is called the gamma hypothesis (98),

and states that inhibitory environmental factors combine in a multiplicative manner to produce the observed overall microbial inhibition. Figure 3 represents both views on hurdle technology, where the first result of the combination of the hurdle pH and a_w is without synergy, and the second result is the combination of both hurdles plus a little extra representing synergy, resulting in a higher hurdle then the first combination. Several studies in literature support the non-synergy concept for hurdle technology (48, 49, 57, 86, 94). Other studies support the view that there is synergy between hurdles, for example when using a mixture of nisin and lactates, salts, or lysozyme and nisin (7, 21, 55). Conceivably, the gamma hypothesis may be true for certain combinations of hurdles, while for other combinations synergy actually does exist.

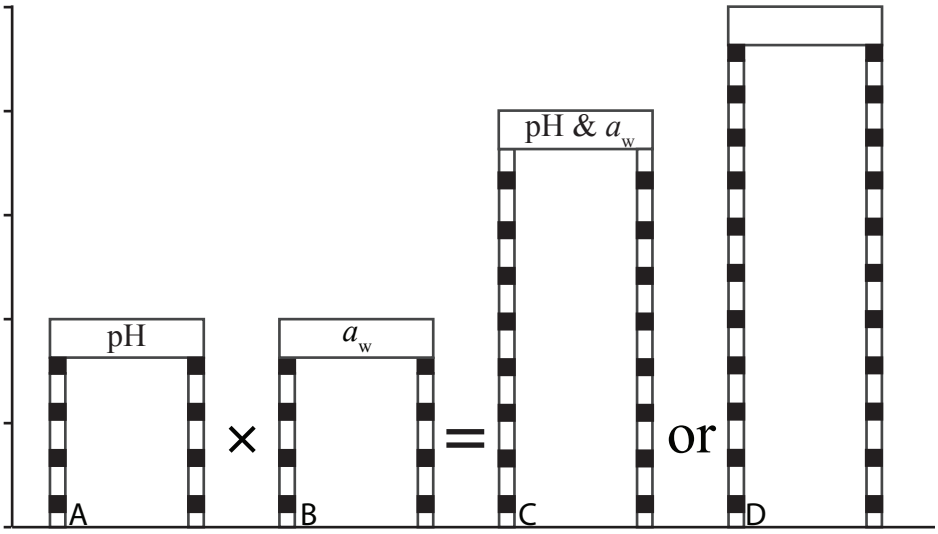

Figure 3. Combined effect of single hurdles pH (A) and a_w (B), resulting in higher total hurdles, without synergy (C) and with synergy (D). The lower the pH or a_w, the higher the hurdle becomes for a microorganism.

The gamma hypothesis owes its name to the ratio between the growth rate of a microorganism when growing with one hurdle (μ_{max}) and the optimal growth rate when no hurdles are present (μ_{opt}), since this ratio is called the gamma (γ) factor. When multiple hurdles are present, the growth rate of a microorganism can be calculated by multiplying all gamma factors for the single hurdles and multiplying this again with μ_{opt}. The gamma hypothesis is expressed mathematically as shown in Equation 3:

$$\mu_{max}(x,y) = \mu_{opt}\ \gamma(x)\ \gamma(y) \quad (3A)$$

with $\gamma(x) = \frac{\mu_{max}(x)}{\mu_{opt}}$ where y is optimal (3B)

and $\gamma(y) = \frac{\mu_{max}(y)}{\mu_{opt}}$ where x is optimal (3C)

Where μ_{max} is the maximum specific growth rate at the tested condition and μ_{opt} is the maximum specific growth rate in medium for optimal growth conditions.

Three classes of interaction can be defined when applying hurdle technology: "no interaction", in which the effect of a combination is as expected from the response of the separate factors; "synergy", in which the effect is greater than expected; and "antagonism", in which the effect is less than expected (16). Some models, like the model of Le Marc *et al*. (Equation 4) (51) and the model of Augustin and Carlier (Equation 5) (13, 14), have the same principle as the gamma model, but they include a synergy factor. This synergy factor represents the synergy between the combined hurdles, and which limits microbial growth more than expected, based on the separate effects only.

$$\mu_{max} = \mu_{opt}\ \gamma(x)\ \gamma(y)\ \xi(x,y) \quad (4)$$

Where ζ (*x*,*y*) is a synergy factor derived from Le Marc *et al*. (51).

$$\mu_{max} = \mu_{opt}\ \gamma_{new}(x)\ \gamma_{new}(y) \quad (5A)$$

with $x_{min,new} = x_{opt,fit} - (x_{opt,fit} - x_{min,fit})\left(1 - \frac{y}{y_{max,fit}}\right)^{1/3}$ (5B)

and $y_{max,new} = y_{max}\left(1 - \left(\frac{x_{opt,fit} - x}{x_{opt,fit} - x_{min,fit}}\right)^3\right)$ (5C)

Where $x_{min,new}$ and $y_{max,new}$ are taken from Augustin and Carlier (13, 14).

Bacillus cereus

B. cereus is a Gram positive, facultative anaerobic, spore-forming rod (46). The cells are relatively large, 1.0 µm by 3.0-5.0 µm, and the cells can appear in chains (Figure 4). The temperature range for growth is 8-55°C (optimum around 28-35°C). *B. cereus* can grow at pH values as low as pH 5 or pH 6 (depending on acidulant) and a_w values as low as 0.95 (1). Cells can be found in for example soil, food, and the human gastrointestinal tract (47, 50). Foods such as milk and milk products and ready-to-eat foods have a relatively high prevalence of the microorganism (93), but toxin producing strains of *B. cereus* are generally rare in milk (82).

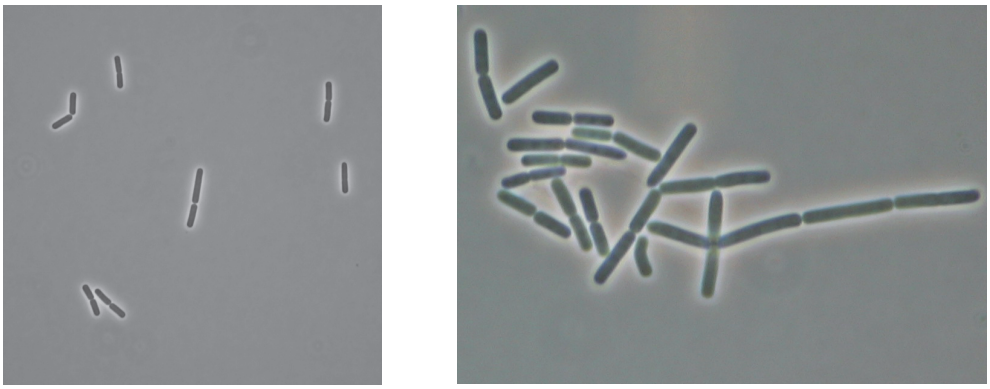

Figure 4. A: Microscopic pictures of *B. cereus* F4810/72 cells in an exponential growing culture, and B: *B. cereus* F4810/72 cells in chains.

B. cereus may cause problems for the food industry because the spores are very hydrophobic, which supports adherence to processing surfaces such as pipelines. The attached spores may detach and contaminate the food product when there is direct contact possible. Pasteurization does not inactivate the spores, while competing vegetative bacteria may be eliminated (8). The spores that survive such thermal treatment may germinate in the food. The vegetative cells can subsequently grow if conditions are favorable, which can lead to spoilage of the food product and possible production of toxins in the food or in the host (1, 20, 46, 50, 80). *B. cereus* can produce two types of toxins: enterotoxin and emetic toxin.

Toxins

Enterotoxins

B. cereus can produce three different enterotoxins in the gastro intestinal tract, causing diarrhea to the host (36). These toxins are the proteins haemolysin BL (Hbl), nonhaemolytic enterotoxin (Nhe) and cytotoxin K (CytK). HBl and Nhe are related three component toxins and CytK is a single pore-forming component toxin (80). Generally, a level of 10^5-10^8 cells or spores in a food product is sufficient to generate these toxins at a concentration able to cause the diarrheal type food poisoning (80). The incubation time is 8 to 16 h, after which typical symptoms of abdominal pain occur, watery diarrhea, and sometimes nausea. The duration of the illness is usually several days. The foods most implicated with this type of food poisoning are proteinaceous foods such as meat and fish (36).

Emetic toxin

The emetic toxin was first characterized and distinguished from the enterotoxin in the late seventies (58, 91). The emetic toxin, called cereulide, is mainly produced in farinaceous foods such as pasta, noodles and rice (6, 36, 47). It has also been found in some infant food formulas (77) and bakery products (43). Cereulide was discovered and named in 1994 by Agata *et al*. (2). Contrary to the enterotoxins, the emetic toxin is extremely heat stable as well as extremely resistant to high alkaline pH values (73). Cereulide is also very stable to digestion with proteolytic enzymes, indicating that the cereulide is also not broken down in the stomach and gastro-intestinal tract of the host (78). Emetic toxin producing *B. cereus* strains can be distinguished from the other strains by their characteristic ribotype and by their inability to hydrolyse starch (3, 69). They can also be detected using a PCR based assay (27, 63). The dose causing illness is estimated to be 8-10 µg cereulide/kg body weight (estimated based on animal models). The effective dose for induction of emesis in 50 % of the musk shrews was calculated to be 12.9 µg/kg, when administered orally, and 9.8 µg/kg when injected intraperitoneal (4). The incubation time is 0.5 to 6 h and the symptoms, nausea, vomiting and malaise, last up to 24 h.

Outbreaks

Data on the true frequency of outbreaks of food poisoning due to *B. cereus* are scarce, since the symptoms are often mild and therefore not reported. A few outbreaks, both enterotoxin and emetic toxin related, have however been reported in literature. In

February 1995 an enterotoxin food poisoning outbreak occurred during a ski championship for juniors and 152 people got ill (53). Enterotoxigenic *B. cereus* was also found in stool samples during investigation of a gastroenteritis outbreak in a chronic care institution (45). Emetic toxin poisonings have been reported more regularly. One fatal outbreak was reported in Belgium in 2003, where a child died due to the presence of emetic toxin in pasta-salad eaten during a picnic (24). In the Netherlands an outbreak occurred in 2000, where 116 students got ill after consumption of a rice dish containing emetic toxin (29). Production of cereulide in an infant breakfast cereal product caused projectile vomiting in two children of 9 and 12 month-old respectively (26). In Helsinki 122 people got ill after consumption of a pasta and meat dish (68), and emetic *B. cereus* was detected in the product.

Cereulide

Structure and mechanism of action

The emetic toxin cereulide is a cyclic dodecadepsipeptide (D-*O*-Leu-D-Ala-L-*O*-Val-L-Val)$_3$ (Figure 5A) (2). Cereulide is produced by a nonribosomal peptide synthetase (NRPS) (90) and the genes involved in cereulide production are located on a plasmid named pCERE01 (40). Cereulide structurally resembles valinomycin (Figure 5B), another cyclic potassium ionophore produced by *Streptomyces* (2). The difference between the two components is three amino acids and the stereo-chemistry. Both toxins form complexes with alkali metal ions (81), but cereulide has been suggested to have a higher toxicity than valinomycin due to its higher affinity for potassium (87). Valinomycin needed 20-30 mM KCl for substantial toxic effects, but cereulide already showed effects at 1-3 mM KCl. This level is close to levels present in the blood, explaining why cereulide is more toxic to humans than valinomycin at low levels. Cereulide forms adducts with Na^+ and NH_4^+ (60). The binding structures of NH_4^+ and K^+ with cereulide are however similar, but the molecular weights of the complexes are different, 1170.79 vs. 1191.72 (70).

The toxic effects of cereulide are caused by the ionophoric uptake of K^+, resulting in dissipation of the transmembrane potential, stimulating swelling and respiration in mitochondria, finally resulting in their inactivation (60). Cereulide caused pathological changes in the mitochondria of hepatocytes in mice after injection with cereulide. After four weeks all mice were recovered from the pathological changes (54, 95). Also toxicity

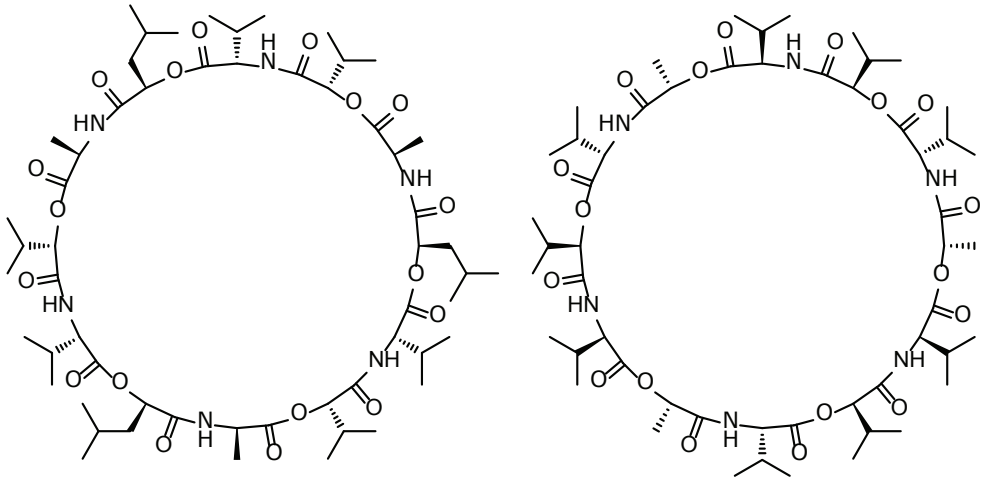

Figure 5. A: Chemical structure of cereulide and B: chemical structure of valinomycin.

against pancreas cells has been observed. The Langerhans islets in the culture died, since the insulin content in the cells was decreased (92). Also human natural killer cells, important components against infections and malignancy, are inhibited by cereulide (65).

Production conditions

Cereulide production is often considered to commence at the end of the exponential phase, but to be independent of sporulation (30, 37). According to Dommel *et al*. (25) the *ces* gene transcription was detectable during mid- to late exponential growth, while the cereulide amount increased during the stationary phase. Production of cereulide is dependent on the type of medium, solid or liquid, the medium chosen and its composition, the amount of oxygen present in the media or headspace, the culturing temperature and the addition of specific amino acids to the medium (11, 31, 37, 42). Experiments in which rice, beans and tryptic soy broth were inoculated with a cereulide producing strain, and subsequently incubated with oxygen or nitrogen, showed clear differences. The oxygen incubated samples contained 2 to 7 µg/ml or /g wet wt after 4 days of incubation, and the nitrogen incubated samples contained less than 0.05 µg/ml or per g wet wt. On solid medium cereulide production occurred overnight, whereas production in liquid medium commenced after 16 to 24 h (42). Toxin production is reduced at lower incubation temperature and also the type of agar used effects the production. Tryptic soy agar gives

usually considerable higher levels compared to milk agar and nutrient agar, but it has to be noted that this is also strain dependent (72). Milk and BHI broth proved to support production of high levels of cereulide production by *B. cereus* F4810/72, as well as rice. Temperatures between 25 and 30°C afforded the highest yield for this strain. Production in BHI occurred after 12 h and in milk after 9 h (84). Three amino acids, valine, leucine and threonine, are essential for growth and toxin production of *B. cereus* (5). The $[K^+]$:$[Na^+]$ ratio is also of importance, as well as the contents of glycine and the $[Na^+]$ (11). Addition of glucose to the medium also proved to enhance cereulide production (5).

Cereulide quantification

The three most used methods to quantify cereulide are the boar semen method, the HEp-2 cell assay and the LC-MS method. The three methods are explained in more detail below. All the described methods measure cereulide as a valinomycin equivalent.

Boar semen

The boar sperm motility assay is based on the loss of motility of boar spermatozoa upon exposure to extracts of emetic *B. cereus* strains or contaminated food. Cereulide acts as a membrane channel forming ionophore, this way damaging the mitochondria, which causes mitochondrial swelling, and blocking the oxidative phosphorylation required for the motility. No decrease in cellular ATP or damages to the plasma membrane was observed (10). The detection threshold of the sperm motility assay was 0.3 ± 0.1 ng of cereulide per 5.4×10^6 sperm cells per 0.2 ml, which equals 0.9 ng of cereulide per mg of *B. cereus* biomass (9) or 2 ng of cereulide per ml of extended boar sperm (44). The presence of food debris did not enhance or mask the effects of cereulide on the boar sperm (44). The boar sperm motility assay was also tested for robustness by addition of other toxins, of for example *Staphylococcus aureus* and *B. cereus* enterotoxins and mycotoxins, commonly used food preservatives and the food components acrylamide and dioxins. The other toxins did not induce a response to the semen and also none of the other components induced a motility loss to the cells in levels maximally allowed to be prevalent in food products (71). The (human) cell lines HeLa, Caco-2, Calu-3 and Paju showed the same response of mitochondrial swelling to the cereulide, whereas bull semen were 100 times less sensitive to cereulide (44).

HEp-2 cell assay

The HEp-2 cell assay has been developed by Hughes *et al*. in 1988 when investigating the use of tissue culture to investigate food poisoning toxins, to avoid feeding of the toxin to primates (41). It appeared that culture filtrates of emetic *B. cereus* caused the production of vacuoles in HEp-2 cells. The HEp-2 cells and the culture filtrate were incubated overnight at 37 °C, and the number of vacuoles per cell was determined. Non-emetic *B. cereus* culture filtrates had no effect on the HEp-2 cells. Apart from vacuolation, cereulide causes also granulation, cell rounding, acid production and reduced multiplication to the cell lines (84). The production of acids due to addition of cereulide can also be used in the HEp-2 cell assay. When the cells and the cereulide are incubated in Basal Eagle's minimum essential (BME) medium the production of acid changes the color of the medium, and this change in color can be measured and related to toxin concentrations (59). Finlay *et al*. developed a nowadays often used semiautomated metabolic staining acid (32). This assay is based on the transition of the water soluble tetrazolium salt 3-(4,5-Dimethylthiazol-2-yl)-2,5-diphenyltetrazolium bromide (MTT) from yellow to purple when the cells are metabolically active. Since the cereulide effects the mitochondrial function, and since MTT is regarded as a cell viability and cytotoxicity indicator, the cereulide affects the MTT conversion as well.

LC-MS

In 2002 a paper describing a quantitative and sensitive assay for cereulide was published by Häggblom *et al*. (37). High-performance liquid chromatography (HPLC) was used to separate the fractions in the sample by polarity. Subsequent mass spectrometry (MS) was used to ionize the fraction in order to identify the different compounds by mass and to quantify the compound by the intensity of the signal. This LC-MS method gave similar results as the boar sperm motility assay. Cereulide was extracted from the food matrix using pentane. The solvents used for the HPLC was a mixture of 95% acetonitrile, 4.9% water, and 0.1 % trifluoroacetic acid at a flow rate of 0.15 ml/min. A C_8 column was used for separation of the compounds. The detection limit using this method was 10 pg per injection into the LC-MS for 1 µl of sample. The LC-MS method as proposed by Häggblom *et al*. is nowadays used in most studies to quantify cereulide. Changes to the method are however also made, to optimize the measurements. Thorsen *et al*. used 96% ethanol to extract cereulide from the biomass and changed the eluens to water

buffered with 10 mM ammonium formate (NH_4HCO_2) and 20 mM formic acid (CH_2O_2), and acetonitrile (CH_3CN) buffered with 20 mM CH_2O_2. The flow rate was 0.3 ml/min and a gradient was used to elute the column (88, 89). Hormazábal *et al*. (2004) used a mixture of acetone-tetrahydrofurane, methanol and water to extract cereulide. A C_{18} column was eluted isocratic with a flow-rate of 0.8 ml/min with a mobile phase of a mixture of 92 % methanol and 8 % water containing 100 µl/l trifluoroacetic acid. The detection limit was 1 ng/g (39).

Aim and impact of the thesis

The aim of the project was to examine the emetic toxin production by *B. cereus* and to test the gamma hypothesis for microbial growth. The gamma hypothesis will be validated for combinations of the hurdles pH and undissociated acid and the hurdles pH and water activity. A validation of the gamma hypothesis will reduce the need for time consuming challenge tests for *B. cereus*, which is of benefit for food industry since it will limit the testing of combinations and intensities of preservatives. This research also contributes to an improved strategy for selection of models for validation studies, which will in turn contribute to an improved testing of the gamma hypothesis for future studies. The experiments to be performed in order to test the gamma hypothesis stress the necessity of evaluating new and less labor intensive methods to obtain growth parameters. The testing of different methods to obtain parameters for growth may be of general benefit, since a new method to obtain parameters for growth can be used, instead of resource intensive plate counting. Method testing in turn raised questions about the lag phase occurring when microorganisms are cultured at conditions close to the growth boundary. Therefore, the physiological processes occurring during the lag phase were investigated. The results can be used by scientists generally and food industry in particular to aid in the identification of novel targets interfering with bacterial exit from the lag phase. Research on the parameters influencing toxin production and time to onset of the production is of general importance for scientists such as in regulatory bodies or in food industry, since it might be possible that small numbers of microorganisms already produce cereulide, but that the level is too low to be measured. This effect might be interpreted as a lack of production during growth of cultures and that toxin production only starts when the cells are in their stationary phase. More exact knowledge about the onset of production may help to establish whether it is possible that low numbers of cells can produce toxins in

a food product to such a level that consumers get ill. The results can help to determine the need for new safety levels regarding the presence and number of *B. cereus* in foods. While working on the detection and quantification of cereulide, the lack of a cereulide standard became apparent. The production of a cereulide standard with known purity and concentration will allow directly expressing the amount of cereulide detected, instead of expressing the level in valinomycine equivalents. This will then help to avoid differences occurring in estimated doses causing illness upon ingestion of the toxin due to the use of different standards.

Overall, the results of this research can benefit scientists, competent authorities and industry when using quantitative risk assessments, since it will allow them to better estimate bacterial behavior in food environments.

Thesis outline

General principles about microbial life cycles, hurdle technology, *B. cereus* and cereulide production are described in this Chapter 1, the introduction to this thesis. The selection and development of a method to obtain parameters for growth is described in Chapter 2 of this thesis. Chapter 3 investigates and describes the processes in *B. cereus* cells during the lag phase and the onset to the growth phase, both under optimal and pH stressed condition. Chapter 4 describes a systematic way to select models for gamma hypothesis validation and subsequently tests the hypothesis for the hurdles pH and undissociated acid concentration. Chapter 5 continues on the theme of the previous chapter by testing the model selection method and the gamma hypothesis validation for the hurdles pH and water activity. Chapter 6 describes the chemical synthesis of cereulide and the testing of the biological activity of the compound. The impact of salt stress on growth and cereulide production is assessed in Chapter 7. Finally, Chapter 8 provides a general discussion incorporating all topics addressed in this thesis.

References

1. **Adams, M. R., and M. O. Moss.** 2000. Food Microbiology, 2 ed. The Royal Society of Chemistry.

2. **Agata, N., M. Mori, M. Ohta, S. Suwan, I. Ohtani, and M. Isobe.** 1994. A novel dodecadepsipeptide, cereulide, isolated from *Bacillus cereus* causes vacuole formation in HEp-2 cells. FEMS Microbiol. Lett. 121:31-34.

3. **Agata, N., M. Ohta, and M. Mori.** 1996. Production of an emetic toxin, cereulide, is associated with a specific class of *Bacillus cereus*. Curr. Microbiol. 33:67-69.

4. **Agata, N., M. Ohta, M. Mori, and M. Isobe.** 1995. A novel dodecadepsipeptide, cereulide, is an emetic toxin of *Bacillus cereus*. FEMS Microbiol. Lett. 129:17-20.

5. **Agata, N., M. Ohta, M. Mori, and K. Shibayama.** 1999. Growth conditions of and emetic toxin production by *Bacillus cereus* in a defined medium with amino acids. Microbiol. Immunol. 43:15-18.

6. **Agata, N., M. Ohta, and K. Yokoyama.** 2002. Production of *Bacillus cereus* emetic toxin (cereulide) in various foods. Int. J. Food Microbiol. 73:23-27.

7. **Almagro, A., C. Prista, S. Castro, C. Quintas, A. Madeira-Lopes, J. Ramos, and M. C. Loureiro-Dias.** 2000. Effects of salts on *Debaryomyces hansenii* and *Saccharomyces cerevisiae* under stress conditions. Int. J. Food Microbiol. 56:191-197.

8. **Andersson, A., U. Rönner, and P. E. Granum.** 1995. What problems does the food industry have with the spore-forming pathogens *Bacillus cereus* and *Clostridium perfringens*? Int. J. Food Microbiol. 28:145-155.

9. **Andersson, M. A., E. L. Jääskeläinen, R. Shaheen, T. Pirhonen, L. M. Wijnands, and S. Salkinoja-Salonen.** 2004. Sperm bioassay for rapid detection of cereulide-producing *Bacillus cereus* in food and related articles. Int. J. Food Microbiol. 94:175-183.

10. **Andersson, M. A., R. Mikkola, J. Helin, M. C. Andersson, and M. Salkinoja-Salonen.** 1998. A novel sensitive bioassay for detection of *Bacillus cereus* emetic toxin and related depsipeptide ionophores. Appl. Environ. Microbiol. 64:1338-1343.

11. **Apetroaie-Constantin, C., R. Shaheen, L. Andrup, L. Smidt, H. Rita, and M. Salkinoja-Salonen.** 2008. Environment driven cereulide production by emetic strains of *Bacillus cereus*. Int. J. Food Microbiol. 127:60-67.

12. **Atkins, P., and J. de Paula.** 2002. Physical Chemistry, 7th edition. Oxford University Press.

13. **Augustin, J.-C., and V. Carlier.** 2000. Mathematical modelling of the growth rate and lag time for *Listeria monocytogenes*. Int. J. Food Microbiol. 56:29-51.

14. **Augustin, J.-C., and V. Carlier.** 2000. Modelling the growth rate of *Listeria monocytogenes* with a multiplicative type model including interactions between environmental factors. Int. J. Food Microbiol. 56:53-70.

15. **Baranyi, J.** 2004. Predictive modelling to control microbial hazards in the food processing industry, p. 145-156. *In* F. J. M. Smulders and J. D. Collins (ed.), Safety assurance during food processing: food safety assurance and veterinary public

health, vol. 2. Wageningen Academic Publishers, Wageningen.

16. **Berenbaum, M. C.** 1989. What is synergy? Pharmacol. Rev. 41:93-141.

17. **Biesta-Peters, E. G., M. W. Reij, H. Joosten, L. G. M. Gorris, and M. H. Zwietering.** 2010. Comparison of two optical density methods and a plate count method for estimation of growth parameters of *Bacillus cereus*. Appl. Environ. Microbiol. 76:1399-1405.

18. **Campbell-Platt, G.** 1994. Fermented foods - a world perspective. Food Res. Int. 27:253-257.

19. **Cherrington, C. A., M. Hinton, G. C. Mead, and I. Chopra.** 1991. Organic acids: chemistry, antibacterial activity and practical applications. Adv. Microb. Physiol. 32:87-108.

20. **Choma, C., T. Clavel, H. Dominguez, N. Razafindramboa, H. Soumille, C. Nguyen-the, and P. Schmitt.** 2000. Effect of temperature on growth characteristics of *Bacillus cereus* TZ415. Int. J. Food Microbiol. 55:73-77.

21. **Chung, W., and R. E. W. Hancock.** 2000. Action of lysozyme and nisin mixtures against lactic acid bacteria. Int. J. Food Microbiol. 60:25-32.

22. **Cotter, P. D., and C. Hill.** 2003. Surviving the acid test: responses of Gram-positive bacteria to low pH. Microbiol. Mol. Biol. Rev. 67:429-453.

23. **Crielly, E. M., N. A. Logan, and A. Anderton.** 1994. Studies on the *Bacillus* flora of milk and milk products. J. Appl. Bacteriol. 77:256-263.

24. **Dierick, K., E. Van Coillie, I. Swiecicka, G. Meyfroidt, H. Devlieger, A. Meulemans, G. Hoedemaekers, L. Fourie, M. Heyndrickx, and J. Mahillon.** 2005. Fatal family outbreak of *Bacillus cereus*-associated food poisoning. J. Clin. Microbiol. 43:4277-4279.

25. **Dommel, M. K., G. Lücking, S. Scherer, and M. Ehling-Schulz.** 2011. Transcriptional kinetic analyses of cereulide synthetase genes with respect to growth, sporulation and emetic toxin production in *Bacillus cereus*. Food Microbiol. 28:284-290.

26. **Duc, L. H., T. C. Dong, N. A. Logan, A. D. Sutherland, J. Taylor, and S. M. Cutting.** 2005. Cases of emesis associated with bacterial contamination of an infant breakfast cereal product. Int. J. Food Microbiol. 102:245-251.

27. **Ehling-Schulz, M., M. Fricker, and S. Scherer.** 2004. identification of emetic toxin producing *Bacillus cereus* strain by a novel molecular assay. FEMS Microbiol. Lett. 232:189-195.

28. **Eklund, T.** 1983. The antimicrobial effect of dissociated and undissociated sorbic acid at different pH levels. J. Appl. Microbiol. 54:383-389.

29. **Essen, R., de Ruiter, C., and de Wit, M.** 2000. Massale voedselvergiftiging in het

Kotterbos te Almere. Infectieziekten bulletin 11:205-207.

30. **Finlay, W. J. J., N. A. Logan, and A. D. Sutherland.** 2002. *Bacillus cereus* emetic toxin production in relation to dissolved oxygen tension and sporulation. Food Microbiol. 19:423-430.

31. **Finlay, W. J. J., N. A. Logan, and A. D. Sutherland.** 2000. *Bacillus cereus* produces most emetic toxin at lower temperatures. Lett. Appl. Microbiol. 31:385-389.

32. **Finlay, W. J. J., N. A. Logan, and A. D. Sutherland.** 1999. Semiautomated metabolic staining assay for *Bacillus cereus* emetic toxin. Appl. Environ. Microbiol. 65:1811-1812.

33. **Fontana, A. J. Jr.** 2007. Measurement of water activity, moisture sorption isotherms, and moisture content of foods, p. 155-171. *In* G. V. Barbosa-Cánovas, A. J. Fontana Jr., S. J. Schmidt, and T. P. Labuza (ed.), Water activity in foods: fundamentals and applications, 1st ed. Blackwell Publishing, Iowa, USA.

34. **Gould, G. W.** 1996. Methods for preservation and extension of shelf life. Int. J. Food Microbiol. 33:51-64.

35. **Gram, L., L. Ravn, M. Rasch, J. B. Bruhn, A. B. Christensen, and M. Givskov.** 2002. Food spoilage - interactions between food spoilage bacteria. Int. J. Food Microbiol. 78:79-97.

36. **Granum, P. E., and T. Lund.** 1997. *Bacillus cereus* and its food poisoning toxins. FEMS Microbiol. Lett. 157:223-228.

37. **Häggblom, M. M., C. Apetroaie, M. A. Andersson, and M. S. Salkinoja-Salonen.** 2002. Quantitative analysis of cereulide, the emetic toxin of *Bacillus cereus* produced under various conditions. Appl. Environ. Microbiol. 68:2479-2483.

38. **Hesseltine, C. W., and H. L. Wang.** 1967. Traditional fermented foods. Biotechnol. Bioeng. 9:275-288.

39. **Hormazábal, V., Ø. Østensvik, K. O' Sullivan, and P. E. Granum.** 2004. Quantification of *Bacillus cereus* emetic toxin (cereulide) in figs using LC-MS. J. Liq. Chromatogr. Related Technol. 27:2531-2538.

40. **Hoton, F. M., L. Andrup, I. Swiecicka, and J. Mahillon.** 2005. The cereulide genetic determinants of emetic *Bacillus cereus* are plasmid-borne. Microbiol. 151:2121-2124.

41. **Hughes, S., B. Bartholomew, J. C. Hardy, and J. M. Kramer.** 1988. Potential application of a HEp-2 cell assay in the investigation of *Bacillus cereus* emetic-syndrome food poisoning. FEMS Microbiol. Lett. 52:7-11.

42. **Jääskeläinen, E. L., M. M. Häggblom, M. A. Andersson, and M. S. Salkinoja-Salonen.** 2004. Atmospheric oxygen and other conditions affecting the

production of cereulide by *Bacillus cereus* in food. Int. J. Food Microbiol. 96:75-83.

43. **Jääskeläinen, E. L., M. M. Häggblom, M. A. Andersson, L. Vanne, and M. S. Salkinoja-Salonen.** 2003. Potential of *Bacillus cereus* for producing an emetic toxin, cereulide, in bakery products: Quantitative analysis by chemical and biological methods. J. Food Prot. 66:1047-1054.

44. **Jääskeläinen, E. L., V. Teplova, M. A. Andersson, L. C. Andersson, P. Tammela, M. C. Andersson, T. I. Pirhonen, N. E. L. Saris, P. Vuorela, and M. S. Salkinoja-Salonen.** 2003. In vitro assay for human toxicity of cereulide, the emetic mitochondrial toxin produced by food poisoning *Bacillus cereus*. Toxicol. in Vitro 17:737-744.

45. **Jackson, S. G., R. B. Goodbrand, R. Ahmed, and S. Kasatiya.** 1995. *Bacillus cereus* and *Bacillus thuringiensis* isolated in a gastroenteritis outbreak investigation. Lett. Appl. Microbiol. 21:103-105.

46. **Kotiranta, A., K. Lounatmaa, and M. Haapasalo.** 2000. Epidemiology and pathogenesis of *Bacillus cereus* infections. Microb. Infect. **2:**189-198.

47. **Kramer, J. M., and R. J. Gilbert.** 1989. *Bacillus cereus* and other *Bacillus* species. M. Dekker, New York (USA).

48. **Lambert, R. J. W., and E. Bidlas.** 2007. An investigation of the gamma hypothesis: A predictive modelling study of the effect of combined inhibitors (salt, pH and weak acids) on the growth of *Aeromonas hydrophila*. Int. J. Food Microbiol. 115:12-28.

49. **Lambert, R. J. W., and E. Bidlas.** 2007. A study of the gamma hypothesis: Predictive modelling of the growth and inhibition of *Enterobacter sakazakii*. Int. J. Food Microbiol. 115:204-213.

50. **Larsen, H. D., and K. Jørgensen.** 1999. Growth of *Bacillus cereus* in pasteurized milk products. Int. J. Food Microbiol. 46:173-176.

51. **Le Marc, Y., V. Huchet, C. M. Bourgeois, J. P. Guyonnet, P. Mafart, and D. Thuault.** 2002. Modelling the growth kinetics of *Listeria* as a function of temperature, pH and organic acid concentration. Int. J. Food Microbiol. 73:219-237.

52. **Leistner, L., and L. G. M. Gorris.** 1995. Food preservation by hurdle technology. Trends Food Sci. Technol. 6:41-46.

53. **Lund, T., and P. E. Granum.** 1996. Characterisation of a non-haemolytic enterotoxin complex from *Bacillus cereus* isolated after a foodborne outbreak. FEMS Microbiol. Lett. 141:151-156.

54. **Mahler, H., A. Pasi, J. M. Kramer, P. Schulte, A. C. Scoging, W. Bär, and S. Krähenbühl.** 1997. Fulminant liver failure in association with the emetic toxin of

Bacillus cereus. N. Engl. J. Med. 336:1142-1148.

55. **McEntire, J. C., T. J. Montville, and M. L. Chikindas.** 2003. Synergy between nisin and select lactates against *Listeria monocytogenes* is due to the metal cations. J. Food Prot. 66:1631-1636.

56. **McMeekin, T. A., J. Brown, K. Krist, D. Miles, K. Neumeyer, D. S. Nichols, J. Olley, K. Presser, D. A. Ratkowsky, T. Ross, M. Salter, and S. Soontranon** 1997. Quantitative microbiology: a basis for food safety. Emerg. Infect. Diseases 3:541-549.

57. **McMeekin, T. A., K. Presser, D. A. Ratkowsky, T. Ross, M. Salter, and S. Tienungoon.** 2000. Quantifying the hurdle concept by modelling the bacterial growth/no growth interface. Int. J. Food Microbiol. 55:93-98.

58. **Melling, J., and B. J. Capel.** 1978. Characteristics of *Bacillus cereus* emetics toxin. FEMS Microbiol. Lett. 4:133-135.

59. **Mikami, T., T. Horikawa, T. Murakami, T. Matsumoto, A. Yamakawa, S. Murayama, S. Katagiri, K. Shinagawa, and M. Suzuki.** 1994. An improved method for detecting cytostatic toxin (emetic toxin) of *Bacillus cereus* and its application to food samples. FEMS Microbiol. Lett. 119:53-58.

60. **Mikkola, R., N. E. L. Saris, P. A. Grigoriev, M. A. Andersson, and M. S. Salkinoja-Salonen.** 1999. Ionophoretic properties and mitochondrial effects of cereulide. Eur. J. Biochem. 263:112-117.

61. **Monod, J.** 1949. The growth of bacterial cultures. Annu. Rev. Microbiol. 3:371-394.

62. **Morris, T. N.** 1946. Principles of food preservation, 2nd ed. Chapman & Hall, London.

63. **Nakano, S., H. Maeshima, A. Matsumura, K. Ohno, S. Ueda, Y. Kuwabara, and T. Yamada.** 2004. A PCR assay based on a sequence-characterized amplified region marker for detection of emetic *Bacillus cereus*. J. Food Prot. 67:1694-1701.

64. **Neumeyer, K., T. Ross, G. Thomson, and T. A. McMeekin.** 1997. Validation of a model describing the effects of temperature and water activity on the growth of psychrotrophic pseudomonads. Int. J. Food Microbiol. 38:55-63.

65. **Paananen, A., R. Mikkola, T. Sareneva, S. Matikainen, M. Hess, M. Andersson, I. Julkunen, M. S. Salkinoja-Salonen, and T. Timonen.** 2002. Inhibition of human natural killer cell activity by cereulide, an emetic toxin from *Bacillus cereus*. Clin. Exp. Immunol. 129:420-428.

66. **Pin, C., J. P. Sutherland, and J. Baranyi.** 1999. Validating predictive models of food spoilage organisms. J. Appl. Microbiol. 87:491-499.

67. **Pinon, A., M. Zwietering, L. Perrier, J. M. Membré, B. Leporq, E. Mettler, D. Thuault, L. Coroller, V. Stahl, and M. Vialette.** 2004. Development and validation of experimental protocols for use of cardinal models for prediction of microorganism growth in food products. Appl. Environ. Microbiol. 70:1081-1087.

68. **Pirhonen, T. I., M. A. Andersson, E. L. Jääskeläinen, M. S. Salkinoja-Salonen, T. Honkanen-Buzalski, and T. M. L. Johansson.** 2005. Biochemical and toxic diversity of *Bacillus cereus* in a pasta and meat dish associated with a food-poisoning case. Food Microbiol. 22:87-91.

69. **Pirttijarvi, T. S. M., M. A. Andersson, A. C. Scoging, and M. S. Salkinoja Salonen.** 1999. Evaluation of methods for recognising strains of the *Bacillus cereus* group with food poisoning potential among industrial and environmental contaminants. Syst. Appl. Microbiol. 22:133-144.

70. **Pitchayawasin, S., M. Kuse, K. Koga, M. Isobe, N. Agata, and M. Ohta.** 2003. Complexation of cyclic dodecadepsipeptide, cereulide with ammonium salts. Bioorg. Med. Chem. Lett. 13:3507-3512.

71. **Rajkovic, A., M. Uyttendaele, and J. Debevere.** 2007. Computer aided boar semen motility analysis for cereulide detection in different food matrices. Int. J. Food Microbiol. 114:92-99.

72. **Rajkovic, A., M. Uyttendaele, W. Deley, A. Van Soom, T. Rijsselaere, and J. Debevere.** 2006. Dynamics of boar semen motility inhibition as a semi-quantitative measurement of *Bacillus cereus* emetic toxin (cereulide). J. Microbiol. Meth. 65:525-534.

73. **Rajkovic, A., M. Uyttendaelle, A. Vermeulen, M. Andjelkovic, I. Fitz-James, P. in 't Veld, Q. Denon, R. Vérhe, and J. Debevere.** 2008. Heat resistance of *Bacillus cereus* emetic toxin, cereulide. Lett. Appl. Microbiol. 46:536-541.

74. **Reid, D. S.** 2007. Water activity: fundamentals and relationships, p. 15-28. *In* G. V. Barbosa-Cánovas, A. J. Fontana Jr., S. J. Schmidt, and T. P. Labuza (ed.), Water activity in foods: fundamentals and applications, 1st ed. Blackwell Publishing, Iowa, USA.

75. **Ross, T., and T. A. McMeekin.** 1994. Predictive microbiology. Int. J. Food Microbiol. 23:241-264.

76. **Schmidt, S. J.** 2007. Water mobility in foods, p. 47-108. *In* G. V. Barbosa-Cánovas, A. J. Fontana Jr., S. J. Schmidt, and T. P. Labuza (ed.), Water activity in foods: fundamentals and applications, 1st ed. Blackwell Publishing, Iowa, USA.

77. **Shaheen, R., W. A. Anderson, C. Apetroaie, A. Schulz, M. Ehling-Schulz, V. M. Ollilainen, and M. Salkinoja-Salonen.** 2006. Potential of selected infant food formulas for production of *Bacillus cereus* emetic toxin cereulide. Int. J. Food

Microbiol. **107:**287-294.

78. **Shinagawa, K., H. Konuma, H. Sekita, and S. Sugii.** 1995. Emesis of rhesus monkeys induced by intragastric administration with the HEp-2 vacuolation factor (cereulide) produced by *Bacillus cereus*. FEMS Microbiol. Lett. 130:87-90.

79. **Sofos, J. N.** 1993. Current microbiological considerations in food preservation. Int. J. Food Microbiol. 19:87-108.

80. **Stenfors Arnesen, L. P., A. Fagerlund, and P. E. Granum.** 2008. From soil to gut: *Bacillus cereus* and its food poisoning toxins. FEMS Microbiol. Rev. 32:579-606.

81. **Suwan, S., M. Isobe, I. Ohtani, N. Agata, M. Mori, and M. Ohta.** 1995. Structure of cereulide, a cyclic dodecadepsipeptide toxin from *Bacillus cereus* and studies on NMR characteristics of its alkali metal complexes including a conformational structure of the K^+ complex. J. Chem. Soc. 7:765-775.

82. **Svensson, B., A. Monthán, R. Shaheen, M. A. Andersson, M. Salkinoja-Salonen, and A. Christiansson.** 2006. Occurrence of emetic toxin producing *Bacillus cereus* in the dairy production chain. Int. Dairy J. 16:740-749.

83. **Swinnen, I. A. M., K. Bernaerts, E. J. J. Dens, A. H. Geeraerd, and J. F. van Impe.** 2004. Predictive modelling of the microbial lag phase: a review. Int. J. Food Microbiol. 94:137-159.

84. **Szabo, R. A., J. I. Speirs, and M. Akhtar.** 1991. Cell culture detection and conditions for production of a *Bacillus cereus* heat-stabile toxin. J. Food Prot. 54:272-276.

85. **Tapia, M. S., S. M. Alzamora, and J. Chirife.** 2007. Effects of water activity (a_w) on microbial stability - as a hurdle in food preservation, p. 239-271. *In* G. V. Barbosa-Cánovas, A. J. Fontana Jr., S. J. Schmidt, and T. P. Labuza (ed.), Water activity in foods: fundamentals and applications, 1st ed. Blackwell Publishing, Iowa, USA.

86. **Te Giffel, M. C., and M. H. Zwietering.** 1999. Validation of predictive models describing the growth of *Listeria monocytogenes*. Int. J. Food Microbiol. 46:135-149.

87. **Teplova, V., R. Mikkola, A. Tonshin, N. Saris, and M. Salkinoja Salonen.** 2006. The higher toxicity of cereulide relative to valinomycin is due to its higher affinity for potassium at physiological plasma concentration. Toxicol. Appl. Pharmacol. 210:39-46.

88. **Thorsen, L., B. B. Budde, L. Henrichsen, T. Martinussen, and M. Jakobsen.** 2009. Cereulide formation by *Bacillus weihenstephanensis* and mesophilic emetic *Bacillus cereus* at temperature abuse depends on pre-incubation conditions. Int. J. Food Microbiol. 134:133-139.

89. **Thorsen, L., B. M. Hansen, K. F. Nielsen, N. B. Hendriksen, R. K. Phipps, and B.**

B. Budde. 2006. Characterization of emetic *Bacillus weihenstephanensis* a new cereulide-producing bacterium. Appl. Environ. Microbiol. 72:5118-5121.

90. **Toh, M., M. C. Moffitt, L. Henrichsen, M. Raftery, K. Barrow, J. M. Cox, C. P. Marquis, and B. A. Neilan.** 2004. Cereulide, the emetic toxin of *Bacillus cereus*, is putatively a product of nonribosomal peptide synthesis. J. Appl. Microbiol. 97:992-1000.

91. **Turnbull, P. C., J. M. Kramer, K. Jorgensen, R. J. Gilbert, and J. Melling.** 1979. Properties and production characteristics of vomiting, diarrheal, and necrotizing toxins of *Bacillus cereus*. Am. J. Clin. Nutr. 32:219-228.

92. **Virtanen, S. M., M. Roivainen, M. A. Andersson, P. Ylipaasto, D. Hoornstra, R. Mikkola, and M. S. Salkinoja-Salonen.** 2008. In vitro toxicity of cereulide on porcine pancreatic Langerhans islets. Toxicon 51:1029-1037.

93. **Wijnands, L. M., J. B. Dufrenne, F. M. Rombouts, P. H. in 't Veld, and F. M. van Leusden.** 2006. Prevalence of potentially pathogenic *Bacillus cereus* in food commodities in The Netherlands. J. Food Prot. 69:2587-2594.

94. **Wijtzes, T., F. M. Rombouts, M. L. T. Kant-Muermans, K. van 't Riet, and M. H. Zwietering.** 2001. Development and validation of a combined temperature, water activity, pH model for bacterial growth rate of *Lactobacillus curvatus*. Int. J. Food Microbiol. 63:57-64.

95. **Yokoyama, K., M. Ito, N. Agata, M. Isobe, K. Shibayama, and T. Horii.** 1999. Pathological effect of synthetic cereulide, an emetic toxin of *Bacillus cereus*, is reversible in mice. FEMS Immunol. Med. Microbiol. 24:115-120.

96. **Zugarramurdi, A., and H. M. Lupín.** 1980. A model to explain observed behavior on fish salting. J. Food Sci. 45:1305-1311.

97. **Zwietering, M. H., I. Jongenburger, F. M. Rombouts, and K. van 't Riet.** 1990. Modeling the bacterial growth curve. Appl. Environ. Microbiol. 56:1875-1881.

98. **Zwietering, M. H., T. Wijtzes, J. C. de Wit, and K. van 't Riet.** 1992. A decision support system for prediction of the microbial spoilage in foods. J. Food Prot. 55:973-979.

Chapter 2

Comparison of two optical-density-based methods and a plate count method for estimation of growth parameters of *Bacillus cereus*

2

Elisabeth G. Biesta-Peters, Martine W. Reij, Han Joosten, Leon G. M. Gorris, Marcel H. Zwietering

Published in Applied and Environmental Microbiology (2010), Vol. 76, No. 5, p. 1399-1405

Abstract

Quantitative microbiological models predicting proliferation of microorganisms relevant for food safety and/or food stability are useful tools to limit the need for generation of biological data through challenge testing and shelf life testing. The use of these models requires quick and reliable methods for the generation of growth data and estimation of growth parameters. Growth parameter estimation can be achieved using methods based on plate counting and methods based on measuring the optical density. This research compares the plate count method with two optical density methods, namely, the 2-fold dilution (2FD) method and the relative rate to detection (RRD) method. For model organism Bacillus cereus *F4810/72, the plate count method and both optical density methods gave comparable estimates for key growth parameters. Values for the maximum specific growth rate (μ_{max}) derived by the 2FD method and by the RRD method were of the same order of magnitude, but some marked differences between the two approaches were apparent. Whereas the 2FD method allowed the derivation of values for lag time (λ) from the data, this was not possible with the RRD method. However, the RRD method gave many more data points per experiment and also gave more data points close to the growth boundary. This research shows that all three proposed methods can be used for parameter estimation but that the choice of method depends on the objectives of the research.*

Introduction

Food products are required to be safe and sufficiently stable within their given shelf lives. For this reason, generally some kind of preservation is applied. An often-used preservation method is mild heat treatment, such as pasteurization, which inactivates vegetative microbial pathogens and spoilage microorganisms. *Bacillus cereus* is a Gram positive, facultative anaerobic, spore-forming rod (17) that can be found in, for example, soil, food, and the human gastrointestinal tract (23). Viable spores present in a food product may germinate, and the vegetative cells may grow if conditions are favorable. In order to delay or prevent this, one or more hurdles for germination and outgrowth need to be present in the food or food environment. Examples of such hurdles are the acidification of food and addition of salt (12). When a combination of hurdles is used, generally the intensity of the hurdles may be lower to show a preservative effect comparable to the level of those hurdles when they are used individually (24).

In this investigation, the use of acidification as a hurdle to prevent growth of *B. cereus* was studied. The amount of acid to be added to the food product is of importance for both safety reasons and organoleptic properties. *B. cereus* will not be able to grow at low pH values (pH 5 to 6, depending on the acidulant) (1), but, on the other hand, the food product should not be too acid, given consumer preferences. Research showed that children do not like orange juice with concentrations of citric acid above 0.02 M; for adults this value is 0.04 M (25). The lowest pH value allowing growth of *B. cereus* can be investigated by experiments culturing the microorganism in a suitable growth medium or food product with different pH values and using the viable plate count method for enumeration (33). Using such an approach to generate biological data for safety or shelf life evaluations is considered both slow and human resource-intensive since experiments have to be repeated for every new condition. Quantitative microbiological modeling can speed up experimentation and reduce the resources required. Should modeling make it possible to predict the behavior of *B. cereus* over a wide range and a variety of conditions, then it would help to limit the need for experimentation to the point where just validation of predictions is needed.

For successful use of modeling, the maximum specific growth rate (μ_{max}) and, preferably, also the lag time (λ) have to be known. These parameters can be determined using different techniques. Plate counting can be used to generate the data points μ_{max} and λ by fitting of the growth curve (15, 33). Often, automated optical density (OD)

measurements are used to determine parameters for growth as they allow quicker data generation with less need for human resources (22). It is not possible, however, to directly translate OD values to μ_{max} values due to the high detection limit of OD readers of ~10^7 viable cells. When cells reach their maximum cell density, they proliferate at a progressively slower rate. Consequently, values for μ_{max} would be consistently underestimated by using OD values. For this reason, OD measurements are often used in combination with time-to-detection (TTD) measurements (5). Values for μ_{max} can be derived from OD measurements and TTD measurements by the 2-fold dilution (2FD) method (5, 28, 36). The 2FD method uses TTD and inoculum size variations to obtain values for both μ_{max} and λ. The relative rate to detection (RRD) method also uses OD measurements and TTD measurements to obtain parameters for growth. This method uses the ratio between TTD at the tested and the optimal conditions and can compute μ_{max} but not λ (20, 21, 37). Notably, plate count data allow both μ_{max} and λ to be derived, and this method is required as an addition to the RRD method.

Although both the 2FD method and the RRD method make use of OD measurements, it is not known whether the two techniques result in comparable estimates of growth parameters and whether these values match values obtained with plate counts. Growth parameters determined by plate count and the 2FD method were previously compared in several studies (5, 27). The present study set out to compare the three different methods for the assessment of parameters for growth on the basis of the following, mainly measureable, criteria: the number of data points obtained per experiment, the measuring intensity, the time consumption per experiment, the reproducibility of the method as determined by comparing the standard deviations of the average μ_{max} at pH 7, the number of parameters obtained, and the number of criteria necessary for data analysis. *B. cereus* F4810/72 was used as the model organism. It was cultured at different pH values, a common hurdle in food products, to obtain a variety of growth rates.

Materials and Methods

Bacterial strain and preparation of the standardized bacterial suspension

B. cereus F4810/72, an emetic toxin producer, was originally isolated from human vomit (34). This strain is also known as *B. cereus* NCTC 11143, DSM 4312, and PAL 25 (35; Health Protection Agency Culture Collections [www.nctc.org.uk]). The culture was stored frozen

at -80°C in cryovials (Greiner Bio-one GmbH; Frickenhausen, Germany) containing 0.3 ml of glycerol (87%; Fluka-Chemica GmbH, Buchs, Switzerland) and 0.7 ml of bacterial culture in brain heart infusion (BHI) broth (Becton Dickinson and Co.; Le Pont de Claix, France). For every experiment, a loopful of microorganisms was inoculated in a 500-ml Erlenmeyer flask containing 100 ml of BHI broth and incubated for 16 h at 30°C with shaking at 200 rpm (Julabo SW20; Julabo Labortechnik GmbH, Germany). The overnight culture was standardized by transferring the culture in equal portions to four 50-ml centrifuge tubes and centrifuging for 15 min at 15°C and 3,000 x *g* (Mistral 3000i; MSE, Leicester, United Kingdom). The supernatant was discarded, and the pellets were resuspended in 1 ml of 1% (wt/vol) peptone physiological salt (PPS) solution. The cell suspensions were then pooled and diluted to an OD at 600 nm (OD_{600}) of 0.5 (Novaspec II spectrophotometer; Pharmacia Biotech, United Kingdom) in a 1% PPS solution, corresponding to approximately 10^9 CFU/ml. This suspension was the standardized bacterial suspension and was kept at room temperature and used for further experiments within 2 h. It was plated onto BHI agar plates (Oxoid Ltd., Basingstoke, England) using a spiral plating machine (Eddy Jet; IUL, Spain). Colonies were counted manually after incubation (for 24 h at 30°C). BHI broth was prepared and autoclaved according to the manufacturer's instructions and adjusted to the appropriate pH using sterile 0.5 M sulfuric acid (H_2SO_4) (Riedel-de Haën; Seelze, Germany).

Establishing experimental conditions

Initial estimates for the pH range for growth of *B. cereus* and the shape of its specific growth rate curve were obtained using the model of Presser *et al*. (30) (Equation 1):

$$\mu_{max} = \mu_{opt}(1-10^{pH_{min}-pH}) \quad (1)$$

where μ_{max} is the maximum specific growth rate (h^{-1}), μ_{opt} is the growth rate under optimal growth conditions (h^{-1}), pH_{min} is the minimum pH value required for growth, and pH is the pH value of the broth used for testing. The initial estimates from literature of pH_{min} and μ_{opt} were 4.6 (4) and 2 h^{-1}, respectively (38). Based on these parameter estimations and the resulting μ_{max} values of this curve, the pH values for the experiments were chosen in such a way that the increases in μ_{max} between consecutive pH values were of the same

order of magnitude. Three methods were applied to investigate the effect of pH on μ_{max} and, where possible, λ: the plate count method (8), the 2FD method (5), and the RRD method (20).

Estimating μ$_{max}$ and λ as a function of pH using the 2FD method

The 2FD method uses the time to reach a predefined OD level (reflecting visible growth) of 2-fold inoculum size variations to obtain μ_{max} and λ according to Equation 2 (5):

$$TTD_i = \lambda + \frac{1}{\mu_{max}} \ln\left(\frac{N_{turb}}{N_i}\right) \quad (2)$$

where TTD_i is time to detection (h) of the inoculum level (i), chosen as the time at which a well reaches an OD_{600} of 0.2 (20), λ is the duration of the lag phase (h), N_{turb} is the number of organisms per ml at which an OD_{600} of 0.2 is observed, N_i is the number of organisms per ml of the inoculum, and μ_{max} is the maximum specific growth rate (h^{-1}). N_{turb} was determined in a separate experiment where broth at nine different pH values was sampled as soon as some wells had reached an OD_{600} of 0.2, and the content was plated onto BHI agar to determine cell numbers.

Twenty target pH values were prepared, and the experiment was repeated twice, giving three data sets. For each experiment, 20 bottles containing 50 ml of BHI broth were pH adjusted, with values ranging from pH 4.4 to pH 7, using sulfuric acid. The liquids were filter sterilized (Steritop/Steriflip; Milipore Corporation, MA), and the standardized bacterial suspension was diluted 10,000-fold in pH-adjusted BHI broth using a new dilution series for every pH value and aiming for an initial cell concentration of approximately 10^4 CFU/ml. The pH 7 solution was spiral plated onto BHI agar plates in duplicate for enumeration. In both repetitions of the experiment, slight deviations of the target pH value occurred, resulting in a total number of 60 pH values for further data analysis.

All wells of the 100-well honeycomb plate (Oy Growth Curves AB Ltd; Helsinki, Finland) were filled with 150 µl of pH-adjusted BHI broth, with five wells filled per pH value. Every pH value was investigated in duplicate using a second honeycomb plate for the duplicate. Every first well of a pH series was inoculated with 150 µl of a particular target pH value-adjusted bacterial culture. Twofold dilutions were made up to the fifth

well for that pH value. Both honeycomb plates were incubated in the Bioscreen C (Oy Growth Curves AB Ltd; Helsinki, Finland) at 30°C for 3 days with continuous, medium shaking, and the OD_{600} was measured every 10 min. The OD_{600} data obtained from the Bioscreen were imported in Microsoft Excel for data capturing and processing. Rarely, wells showed an initial OD_{600} above the detection limit due to pipetting errors or air bubbles in the liquid; when this occurred, such wells were removed from the data set. For all other curves the TTD, defined as the time to reach an OD_{600} of 0.2, was determined. The OD values were not corrected for the background color of the broth (~0.1 at OD_{600}). For wells not reaching an OD_{600} of 0.2 within the time frame of the experiment, viability of bacteria was determined by plating the content of the well. In the event that plates did not show colonies, bacteria were considered dead, and the μ_{max} was set to 0 h^{-1}.

For processing of data regarding the 2FD method, wells of the same target pH were grouped, and μ_{max} and λ were calculated using Equation 2, Excel solver add-in, and a linear fit, minimizing the residual sum of squares (RSS). The mean square error (MSE) between the data and the fit was calculated using Equation 3:

$$\mathrm{MSE} = \frac{\mathrm{RSS}}{\mathrm{DF}} = \frac{\sum_{i=1}^{n}\left(\mathrm{TTD}^{i}_{\mathrm{observed}} - \mathrm{TTD}^{i}_{\mathrm{fitted}}\right)^2}{n - s} \tag{3}$$

where $TTD^{i}_{observed}$ (h) is the TTD when the well reaches OD_{600} 0.2, TTD^{i}_{fitted} (h) is the fitted TTD, and DF is the number of data points (n) minus the number of parameters (s). The lower the MSE value, the better the model describes the data.

The following rules were applied for data exclusion: MSE > 5, $\lambda < 0$, $\mu_{max} < 0$, and $\mu_{max} > 3.5$. If any of the parameters was out of range, both resulting parameters μ_{max} and λ for the same experimental condition were excluded from further data processing.

Estimating μ_{max} as a function of pH using the RRD method

The RRD method uses one well per target pH value with known, equal inoculum levels for all wells. The same data set was used as for evaluation of the 2FD method, and therefore the preparation of media, dilution series, and the filling of the plates are identical. The TTD, again defined as the time (h) until the OD_{600} of a well reaches 0.2, was determined for every test condition (TTD_i) and at optimal conditions (TTD_{opt}), in this case, at pH 7. The μ_{opt} value was estimated independently by plate counting and fitting of the Gompertz

model to the counts. Equation 4 was used to derive RRD values and to calculate μ_{max} values for various test conditions from RRD and μ_{opt}:

$$\mu_{max,i} = \mu_{opt}\,\mathrm{RRD}_i = \mu_{opt}\,\frac{\mathrm{TTD}_{opt(OD_{600}=0.2)}}{\mathrm{TTD}_{i(OD_{600}=0.2)}} \quad (4)$$

With respect to evaluating both OD methods, for the RRD method the well with the highest inoculum level for a particular target pH value was selected, and the RRD was calculated according to Equation 4, using the TTD of the well with pH 7 as TTD_{opt}.

Estimating μ$_{max}$ and λ as a function of pH using the plate count method

Erlenmeyer flasks (500 ml) containing 100 ml of BHI broth were adjusted to pH 5 or pH 7 using sulfuric acid and inoculated with the standardized bacterial culture to an initial level of ~10^4 CFU/ml. The experiment to test the effect of BHI broth adjusted to pH 7 was conducted five times, and the experiment to test the effect of BHI broth adjusted to pH 5 was conducted three times. The cultures were incubated at 200 rpm and 30°C, and the number of cells was enumerated in duplicate at regular time intervals. The growth data obtained were fitted using the Gompertz model (Equation 5) (39) to obtain values for μ_{max} and λ:

$$\ln\left(\frac{N_t}{N_0}\right) = A\,\exp\left\{-\exp\left[\frac{\mu_{max}\mathrm{e}}{A}(\lambda - t)+1\right]\right\} \quad (5)$$

where N_t is the number of microorganisms (CFU/ml) at time t (h), N_0 is the number of microorganisms at the time of inoculation, A is the dimensionless asymptotic value (39), μ_{max} is the maximum specific growth rate (h^{-1}), and λ is the lag time (h).

Results

Growth boundary

The lower limit for growth of *B. cereus* F4810/72 in BHI broth acidified with sulfuric acid was pH 4.8, which is 0.2 above the published estimated growth boundary for *B. cereus* NCIMB 11796 (4). The initial estimate of the shape of the growth-pH curve (the pH model of Presser *et al*. [30]) (Equation 1) is included in Figure 1 for illustration purposes. The

estimated μ_{max} values are higher than the μ_{max} values obtained using the 2FD method, but this is mainly caused by the difference in growth boundary, which caused a shift of the curve. The estimated μ_{max} values for optimal growth conditions (pH 7) are equal.

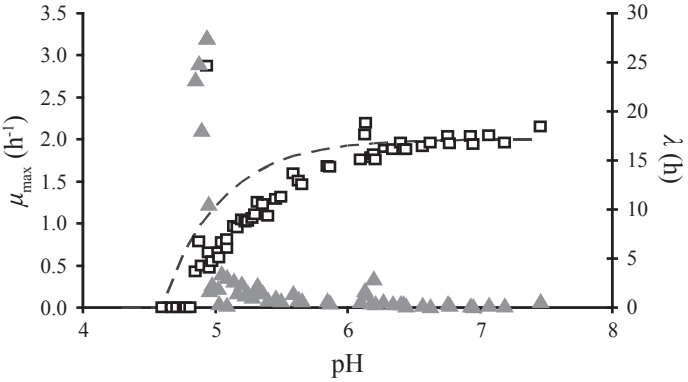

Figure 1. Values for μ_{max} (h^{-1}) (□) and λ (h) (▲) estimated by the 2FD method as a function of pH for *B. cereus* F 4810/72 cultured at 30°C in BHI broth acidified with sulfuric acid. The estimation growth curve (dashed line) using Equation 1 is based on the model of Presser *et al*. (30).

2FD method

Figure 2 shows for one pH value (6.93) how μ_{max} and λ were obtained using the 2FD method.

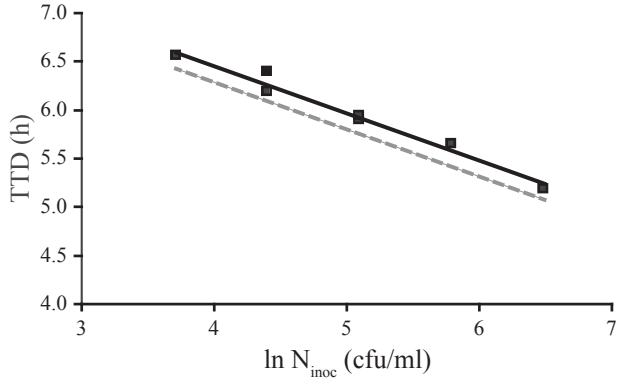

Figure 2. TTD as a function of the natural logarithm of the inoculum size (ln N_{inoc}) (■) in BHI broth at pH 6.93, linear fitting (solid line) of the data points to estimate μ_{max}, and estimation of λ using the theoretical TTD (dashed line) assuming λ = 0, according to the 2FD method of Cuppers and Smelt (5).

The negative reciprocal slope of the curve fitting the data points equals μ_{max}, 2.05 h^{-1}, whereas λ, which equals 0.80 h, is derived from the deviation from the theoretical TTD for a λ of 0. For every μ_{max} and λ data point obtained with this method, five wells were used, limiting the number of data points to 20 per honeycomb plate. Figure 1 shows μ_{max} and λ for 57 pH values out of the total of 60 pH values tested. All wells not showing growth (pH < 4.8) failed to generate colonies on the plate, indicating no surviving microorganisms. Two data points, pH 4.9 and pH 4.88, both close to the growth boundary, had to be excluded because the MSE was > 5. One data point (pH 4.83) had to be excluded because of an optical failure in the Bioscreen toward the end of the experiment.

Figure 3 shows that at pH 7, the OD_{600} threshold value of 0.2 (N_{turb}) was approximately equivalent to 7.5 log CFU/ml.

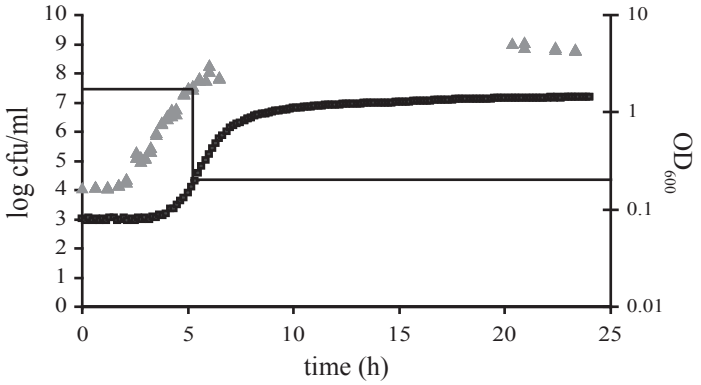

Figure 3. Numbers of *B. cereus* F4810/72 CFU in BHI broth at pH 7 cultured at 30°C, as monitored by plate count (▲) and OD_{600} measurement (■).

The exact value for N_{turb} is required for the 2FD method to calculate λ, and this value was determined for nine different target pH values by enumerating the number of microorganisms in each well when the OD was approximately 0.2 (Figure 4). The number of cells relative to the OD was different for every well, and no trend was visible. N_{turb} had an average value of 7.3 (±0.31) log CFU/ml. The 95% confidence interval of N_{turb} was calculated, and the highest and lowest values of the interval were used to determine the effect of various N_{turb} values on the calculated λ. Two pH values were selected, the highest tested pH value (~pH 7) and the lowest tested pH value (~pH 5) showing clear growth. The value of λ for *B. cereus* in BHI broth of pH 6.93 varied between -0.5 and 0.86,

whereas λ varied between -1.26 and 4.66 h for broth of pH 4.96, showing that λ cannot be estimated with reliability due to the variability in the microbial numbers at the TTD.

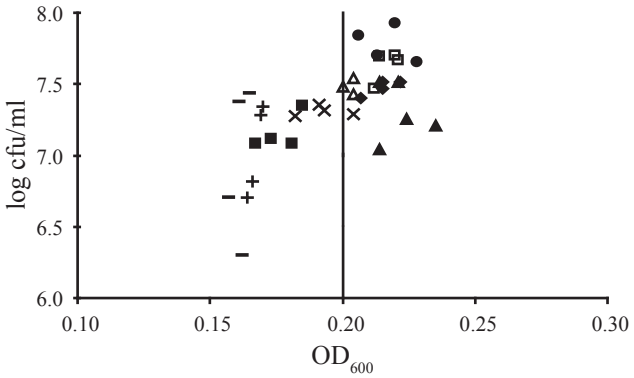

Figure 4. Relationship between cell numbers and an OD_{600} value of 0.2 (vertical line) of the Bioscreen C. The pH of BHI broth was set at the following values: 7 (◆), 6.75 (■), 6.5 (▲), 6.25 (×), 6 (□), 5.8 (●), 5.6 (+), 5.4 (△), and 5.2 (-).

RRD method

For each Bioscreen run, 100 data points could be obtained since no inoculum size variations were necessary. In this investigation the same data set was used for testing both the RRD method and the 2FD method. Only the wells with the highest inoculum levels were selected for further investigation, and therefore RRD values were calculated as a function of pH for 59 different pH values obtained from three separate Bioscreen runs. The RRD values were multiplied by μ_{opt} (2.42 h^{-1}) to obtain $\mu_{max,RRD}$ (Figure 5). Since the calculation of RRD does not require fitting of data points and therefore MSE values were not relevant, no data points needed to be excluded on the basis of MSE values. The data point at pH 4.83 was excluded because of equipment failure. The RRD data were transformed to μ_{max} values by multiplying RRD by μ_{opt}, which was estimated at pH 7 by plate count to be 2.42 h^{-1}. All calculated values for μ_{max} met the criterion of a μ_{max} of < 3.5 h^{-1}.

Plate count method

The μ_{max} values for the individual experiments are displayed in Figure 5. The mean μ_{max} value for growth of *B. cereus* F4810/72 in BHI broth adjusted to pH 7 was 2.42 h^{-1} (± 0.35). The best overall fit of the same data using the Gompertz equation was calculated

to be 2.39 h^{-1} (± 0.10). The mean μ_{max} value in BHI broth adjusted to pH 5 was 0.63 h^{-1} (± 0.08). The average value of λ for BHI broth of pH 7 was 2.41 h and varied between 1.87 h and 2.76 h. The average λ for cells cultured at pH 5 was found to be 7.62 h and varied between 7.02 h and 8.16 h. Values obtained by plate counting did not significantly differ from either of the other methods.

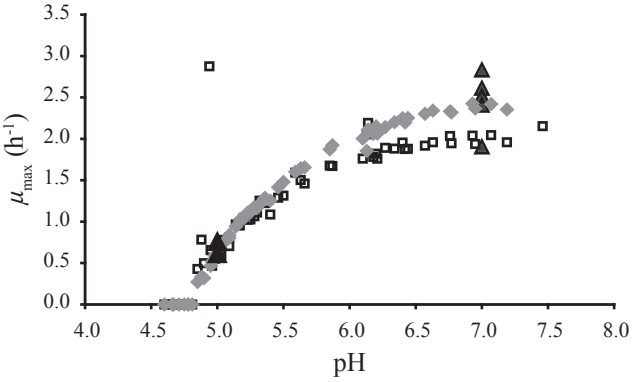

Figure 5. Values for μ_{max} (h^{-1}) as a function of pH for *B. cereus* F4810/72, as determined by the 2FD method (□) (57 target values), the RRD method (◆) (59 target values) and the plate count method (▲) (8 target values).

Discussion

Maximum specific growth rate determination

The classical method to determine μ_{max} is based on plate counting, where samples are taken in time and plated on agar. In this study the parameters μ_{max} and λ were obtained by fitting the experimental data using the Gompertz model (39). The model of Rosso (32) returned μ_{max} values which were 6% lower than the values obtained using the model of Gompertz when both models were fitted to the same data set. The Gompertz model was selected since it showed the lowest RSS value and also because of its smooth transition from the lag phase to the exponential phase. The choice for the Gompertz model is in line with a comparison made by other authors (39). The model of Presser *et al*. was used to predict the pH-growth rate curve and the range of pH values for the experiments to be performed. It proved to be useful to use a model and parameters from literature to design the experiment and select pH values to collect data points (Figure 1).

Figure 3 shows an example of a growth curve for growth at optimal conditions, namely, pH 7. The derived μ_{max} value (2.6 h^{-1}) fits within the range of 2.3 h^{-1} to 3.33 h^{-1}

from published data for growth in laboratory media (10, 19). Both OD methods tested, the RRD method and the 2FD method, derived similar μ_{max} values from the TTD data, so these alternative methods to classic plate counting could confidently be used. The variability between the TTD data for equal experimental conditions was minimal.

Various other studies showed that μ_{max} can be derived from turbidimetric measurements (2, 6, 7); Lindqvist (26) compared TTD methods and turbidimetric methods and considered the TTD methods best to estimate the growth rates. None of the above studies, however, considered the use of the RRD method (20).

When the RRD method is used, μ_{opt} has to be estimated in a separate experiment to obtain μ_{max}. If μ_{opt} is wrongly estimated, the resulting μ_{max} value will be heavily affected. Estimating μ_{opt} can be done by plate counting of a growing culture of a particular strain using optimal growth conditions or by using the 2FD method. Multiple repetitions of this experiment are necessary to establish a reliable value for μ_{opt}. Once established, this same value for μ_{opt} can be used for every experiment. The μ_{opt} value used to establish $\mu_{max,RRD}$ is the average of the five μ_{max} values obtained by plate count at pH 7. Since the plate count method at pH 7 shows a large variability in μ_{max} (Figure 5), the data points do not adequately reflect a best fit of the growth rate. Since the $\mu_{max,RRD}$ data are based on μ_{opt} obtained by plate count, these two methods are related, and both therefore show the same conservative estimate. Differences between the methods might be caused by the difference in aeration levels between the Erlenmeyer flask and the microtiter plate (9), although they were assumed to be equal. Since use of a Bioscreen and microtiter plates is a convenient method to allow high-throughput screening of different growth conditions, this assumption is unavoidable. Considering the difference in aeration between plate counts and Bioscreen experiments, the RRD method is favored over the 2FD method. For the RRD method the relative difference between two test conditions is determined, so possible oxygen effects are considered to be equal and do not contribute to the final RRD value. When μ_{opt} is determined using plate counts, without any negative growth effects due to low aeration, the μ_{max} value obtained with the RRD method is considered equal to the values obtained using plate counts.

More important for safety is the behavior of the methods under more growth-inhibiting conditions, and here the difference is significantly smaller than under optimal growth conditions. This difference is supported by the residuals, which showed a consistent difference and were not normally distributed. This difference may be explained

by the way the TTD data were analyzed. The inoculum level of the culture was 10^4 cells/ml, and the detection limit of the Bioscreen (OD_{600} = 0) is ~10^7 cells/ml. TTD is defined as the time until the threshold value of OD_{600} 0.2 is reached. This OD_{600} threshold value was chosen because it is well above the detection limit of the Bioscreen C, and such a threshold helps avoid false-positive growth samples due to fluctuations in optical density close to the detection limit of the Bioscreen C. Considering the inoculum level, the TTD consists of a lag time and the time necessary to reach the OD_{600} threshold value, while the bacterial culture is already exponentially growing. For this reason, the TTD method is not able to distinguish λ separately. The increase of λ around the growth boundary becomes significantly longer than under optimal conditions, as has been reported for *Listeria monocytogenes* (31) and *Pseudomonas fragi* (13). The increase of λ closer to the growth boundary is also seen for *B. cereus* (Figure 1). The use of the RRD method relies on the assumption that $TTD_{opt}/TTD_i = \mu_i/\mu_{opt}$. Since TTD does not distinguish between μ_{max} and λ, this assumption can only be made when the product of μ_{max} and λ is constant for all pH values. If this assumption is not valid, for example, when the RRD is calculated for data close to the growth boundary, the ratio between TTD_i and TTD_{opt} changes more than expected since λ contributes more to TTD_i than to TTD_{opt}, thereby underestimating μ_{max}. This difference between the two methods is, however, smaller than the variability in μ_{max} data obtained by plate counting, as can be seen in Figure 5. Additionally, the products of μ_{max} and λ are in the same order for different pH values, and no clear trend of increasing product ($\mu_{max} \times \lambda$) is visible with decreasing pH toward the growth boundary. It can be concluded that both methods are valid although their results are not identical.

Determining the lag time

Variability in λ is observed for replicates of plate count experiments using the same culture conditions. The values of λ range between 1.78 h and 2.73 h, with an average value of 2.41 h for *B. cereus* cultured in BHI broth at pH 7. As can be seen in Figure 1, such a wide variability is not observed when the 2FD method is used (λ = 0.09 to 0.23 h) for the same culture condition. This is in line with Wu *et al*. (36), who obtained accurate estimation of λ using the Bioscreen C. The λ value obtained using the 2FD method, however, depends on the number of cells estimated to be present at the time TTD is reached (N_{turb}). The value of N_{turb} was tested for nine different pH values, and it was shown that the number of cells in the wells varied, but there was no trend between pH and N_{turb}. For further analysis, the

average N_{turb} value (7.3 ± 0.31 log CFU/ml) was used, but ideally N_{turb} has to be determined for every test condition in order to have a good estimate of λ. To determine N_{turb} for every experiment requires extra time when the effect of a lot of different pH values on μ_{max} and λ is tested, and this is not, therefore, convenient.

The cause of the difference in N_{turb} for various pH values is unknown. Literature reveals that environmental conditions might influence the cell length, showing significant elongation of *Salmonella enterica* serovar Enteritidis when cells are exposed to low water activity (16) and elongation of *B. cereus* cells from 2 to 5 up to 15 to 40 µm when cells are exposed to a sublethal growth condition of pH 5.0 (14). An increase in cell length causes an increase in biomass and, for that reason, an increase in OD but no increase in cell numbers. Another explanation for this variation might be clustering of the microorganism at a lower pH value, which gives an underestimation of the number of microorganisms since a cluster is counted as one CFU even though it originated from more than one individual cell. Microscopic analysis of the cell culture when N_{turb} was reached did not show elongation or clustering of the cells. This suggests that something else is causing variation in N_{turb} values, for example, heterogeneity of the population. Due to heterogeneity of the population, only a small number of cells may actually start growing at low pH values. The dead or dormant cells hardly contribute to the OD compared to the total amount of cells, but they are counted when wells are sampled since dormant cells might recover on plate. This mechanism is not of importance under more favorable growth conditions, resulting in lower cell counts at an OD_{600} of 0.2 for higher pH values.

Efficiency and accuracy of the methods

With respect to the efficiency and accuracy of the different methods, a number of factors can be considered. These are summarized in Table 1 for all three methods in order of appearance in this discussion. First, the number of data points obtained per experiment for all three methods will be discussed. For the 2FD method the data of five 2-fold-diluted wells are necessary to calculate μ_{max} and λ, compared to one well using the RRD method. The RRD method therefore retrieves five times more data from one experiment than the 2FD method. Both methods are able to retrieve much more data in one experiment than the widely used plate count method. The use of the latter method enables a maximum of six conditions to be performed in one plate count run, assuming sampling of an Erlenmeyer flask every 20 min and a work load of approximately 3 min to dilute and

plate a sample. For this reason, the number of data points per condition is limited to three data points per hour, whereas the number of OD measurements per hour using the Bioscreen can be as high as 12 measurements per well per hour. The Bioscreen is also able to measure day and night for multiple days, which is not practical using the plate count method. Furthermore, plate counting needs additional labor such as pouring of the plates, plating, and counting. The labor required when the plate count method is used for a 3-day experiment is therefore estimated to be 4 days. Both OD methods are less labor-intensive than the plate count method. Filling of plates when the RRD method is used is less time-consuming than with the 2FD method, and the data analysis is quicker since no fitting of the data points, as shown in Figure 2, is necessary.

Compared to the plate count method, both the 2FD method and the RRD method are of equal, good reproducibility, as can be concluded by comparing the standard deviations of the mean μ_{max} (Table 1), which are considerably larger for the plate count method. Analysis of the standard deviation between the replicate experiments as a function of the pH proved that the within-experiment errors were evenly distributed. Plate counts generally have a limited precision, and the fitting performance of the growth models has influence on the estimation of growth parameters. Since the 2FD method is able to derive both μ_{max} and λ from the Bioscreen, this method seems for this reason more favorable for research purposes than the RRD method.

Considering inoculum levels, different initial cell numbers may cause different growth behaviors of a microorganism although the same experimental conditions are applied (18). Wells inoculated with assumed equal amounts of cells can consequently show variability in the detection times (11). However, this is only plausible when counts are high enough to allow cell-to-cell communication/quorum sensing. What may be a more plausible explanation is that low densities lead to a less reproducible response. If only a small fraction of the population is able to initiate growth rapidly at boundary conditions, a few more or a few less rapidly growing cells in the population may have a major effect on the outcome of the experiment. This is less likely to happen under optimal growth conditions than close to the growth boundary. The inoculum level of *B. cereus* at concentrations below the detection limit of the Bioscreen was deliberately chosen, and the time until the culture passed a preestablished OD value was measured. Any inoculum level can be chosen as long as it is equal for all wells, and it is better if the level is below the detection limit of the Bioscreen to determine the growth rate before the conditions

have changed due to growth. The inoculum size proved to have no effect on experimental outcomes when growth boundaries or MICs were determined (3).

Increase in variance of TTD values for equal experimental conditions is especially the case under more severe stress conditions, which in our study are low pH values close to the growth boundary. It becomes harder to fit a linear line through the data points due to the increase in the variability of the detection times, resulting in high MSE values and/or unrealistic values for μ_{max} and λ. The use of the 2FD method will therefore result in fewer data points around the growth boundary than with the RRD method. The effect of inoculum size on the behavior of cells around the growth boundary or under suboptimal conditions was previously studied by Pascual *et al*. (29), who showed that inoculum size has an effect on the estimated μ_{max} value and λ. Bidlas *et al*. (3) also discussed the effect of inoculum size on the MIC and the growth–no-growth interface for the 2FD method and the RRD method. Both studies concluded that the effect of a changing inoculum size can be modeled independently of any other factor, suggesting that simple, short experiments measuring the TTDs of various initial inocula can be used as an adjunct to currently available models. This suggestion favors the use of the RRD method, which does not require inoculum size variations. Moreover, apart from variability in inoculum level, variability in cell numbers at TTD (N_{turb}) is also possible, resulting in wrong estimates of λ for the tested conditions when the 2FD method is used.

Table 1. Characteristics for the three methods to estimate growth parameters

Characteristic(s)	Value for the indicated method		
	2FD method	RRD method	Plate count
Data points per run	20	100	6
Time interval between measurements (min)	5-10 (24h/day)	5-10 (24h/day)	20 (<24h/day)
Labor[a]	5 h	4 h	4 Days
Reproducibility (SD)	Good (0.085)	Good (0.032)	Less precise (0.346)
Parameter(s) obtained	μ_{max}, λ	μ_{max}	μ_{max}, λ
Criteria[b]	MSE < 5, λ > 0, 0 < μ_{max} < 3.5	0 < μ_{max} < 3.5	MSE < 5, λ > 0, 0 < μ_{max} < 3.5
Factors(s) affecting data	Inoculum levels, N_{turb} data	μ_{opt} obtained by plate counts	Choice of fitting model

[a] Required for a 3-day experiment.

[b] Criteria that were applied to the fitting process and the resulting parameters before parameters were included for further analysis.

The method used to make predictions to evaluate food safety risks depends on the scenario to be tested. For the study of growth boundaries, the RRD method is considered the best to use since it gives more data points at the growth boundary. Information about μ_{max} and λ is needed to make a prediction when studying growth kinetics, and in this case the 2FD method has to be used since it provides both parameters.

In summary, this research shows that OD measurements can be used to derive growth rates and lag times of bacterial cultures to investigate the effect of a large variety of pH values on growth parameters. Plate counting, however, will always remain a good method to locally investigate growth of cultures and to test the effect of specific growth conditions like modified atmospheres, which cannot be achieved in OD measurements, and will remain necessary for validation of new methods to establish parameters for growth. Notably, it was established that the use of the 2FD method or the RRD method is justified as the performances of both methods are comparable. The choice of one method over the other will depend mainly on the experimental setup, the particular objective of the research, and the growth parameters targeted. If μ_{max} has to be determined around the growth boundary, the RRD method will be most efficient. If information on λ is needed, the 2FD method is the better choice.

Acknowledgments

This work was financially supported by Nestlé Research Centre, Lausanne, Switzerland. Aneta Linka is gratefully acknowledged for skillful experimental work during the first stages of this research.

References

1. **Adams, M. R., and M. O. Moss.** 2000. Food Microbiology, 2 ed. The Royal Society of Chemistry.

2. **Baranyi, J., and C. Pin.** 1999. Estimating bacterial growth parameters by means of detection times. Appl. Environ. Microbiol. 65:732-736.

3. **Bidlas, E., T. Du, and R. J. W. Lambert.** 2008. An explanation for the effect of inoculum size on MIC and the growth/no growth interface. Int. J. Food Microbiol. 126:140-152.

4. **Browne, N., and B. C. A. Dowds.** 2002. Acid stress in the food pathogen *Bacillus cereus*. J. Appl. Microbiol. 92:404-414.

5. **Cuppers, H. G. A. M., and J. P. P. M. Smelt.** 1993. Time to turbidity measurement

as a tool for modeling spoilage by *Lactobacillus*. J. Ind. Microbiol. Biotechnol. 12:168-171.

6. **Dalgaard, P., and K. Koutsoumanis.** 2001. Comparison of maximum specific growth rates and lag times estimated from absorbance and viable count data by different mathematical models. J. Microbiol. Meth. 43:183-196.

7. **Dalgaard, P., T. Ross, L. Kamperman, K. Neumeyer, and T. A. McMeekin.** 1994. Estimation of bacterial growth rates from turbidimetric and viable count data. Int. J. Food Microbiol. 23:391-404.

8. **den Besten, H. M. W., M. Mataragas, R. Moezelaar, T. Abee, and M. H. Zwietering.** 2006. Quantification of the effects of salt stress and physiological state on thermotolerance of *Bacillus cereus* ATCC 10987 and ATCC 14579. Appl. Environ. Microbiol. 72:5884-5894.

9. **Duetz, W. A., and B. Witholt.** 2004. Oxygen transfer by orbital shaking of square vessels and deepwell microtiter plates of various dimensions. Biochem. Eng. J. 17:181-185.

10. **Enfors, S. O., and G. Molin.** 1980. Effect of high concentrations of carbon dioxide on growth rate of *Pseudomonas fragi, Bacillus cereus* and *Streptococcus cremoris*. J. Appl. Microbiol. 48:409-416.

11. **Francois, K., F. Devlieghere, A. R. Standaert, A. H. Geeraerd, I. Cools, J. F. Van Impe, and J. Debevere.** 2005. Environmental factors influencing the relationship between optical density and cell count for *Listeria monocytogenes*. J. Appl. Microbiol. 99:1503-1515.

12. **Gould, G. W.** 1996. Methods for preservation and extension of shelf life. Int. J. Food Microbiol. 33:51-64.

13. **Hudson, J. A., and S. J. Mott.** 1994. Comparison of lag times obtained from optical density and viable count data for a strain of *Pseudomonas fragi*. J. Food Saf. 14:329-339.

14. **Jobin, M.-P., T. Clavel, F. Carlin, and P. Schmitt.** 2002. Acid tolerance response is low-pH and late-stationary growth phase inducible in *Bacillus cereus* TZ415. Int. J. Food Microbiol. 79:65-73.

15. **Kandhai, M. C., M. W. Reij, C. Grognou, M. van Schothorst, L. G. M. Gorris, and M. H. Zwietering.** 2006. Effects of preculturing conditions on lag time and specific growth rate of *Enterobacter sakazakii* in reconstituted powdered infant formula. Appl. Environ. Microbiol. 72:2721-2729.

16. **Kieboom, J., H. D. Kusumaningrum, M. H. Tempelaars, W. C. Hazeleger, T. Abee, and R. R. Beumer.** 2006. Survival, elongation, and elevated tolerance of *Salmonella enterica* serovar Enteritidis at reduced water activity. J. Food Prot.

69:2681-2686.

17. **Kotiranta, A., K. Lounatmaa, and M. Haapasalo.** 2000. Epidemiology and pathogenesis of *Bacillus cereus* infections. Microb. Infect. 2:189-198.

18. **Koutsoumanis, K. P., and J. N. Sofos.** 2005. Effect of inoculum size on the combined temperature, pH and a_w limits for growth of *Listeria monocytogenes.* Int. J. Food Microbiol. 104:83-91.

19. **Kramer, J. M., and R. J. Gilbert.** 1989. *Bacillus cereus* and other *Bacillus* species. M. Dekker, New York (USA).

20. **Lambert, R. J. W., and E. Bidlas.** 2007. An investigation of the Gamma hypothesis: A predictive modelling study of the effect of combined inhibitors (salt, pH and weak acids) on the growth of *Aeromonas hydrophila*. Int. J. Food Microbiol. 115:12-28.

21. **Lambert, R. J. W., and E. Bidlas.** 2007. A study of the Gamma hypothesis: Predictive modelling of the growth and inhibition of *Enterobacter sakazakii*. Int. J. Food Microbiol. 115:204-213.

22. **Lanciotti, R., M. Sinigaglia, F. Gardini, L. Vannini, and M. E. Guerzoni.** 2001. Growth/no growth interfaces of *Bacillus cereus, Staphylococcus aureus* and *Salmonella enteritidis* in model systems based on water activity, pH, temperature and ethanol concentration. Food Microbiol. 18:659-668.

23. **Larsen, H. D., and K. Jørgensen.** 1999. Growth of *Bacillus cereus* in pasteurized milk products. Int. J. Food Microbiol. 46:173-176.

24. **Leistner, L., and L. G. M. Gorris.** 1995. Food preservation by hurdle technology. Trends Food Sci. Technol. 6:41-46.

25. **Liem, D. G., and C. de Graaf.** 2004. Sweet and sour preferences in young children and adults: role of repeated exposure. Physiol. Behav. 83:421-429.

26. **Lindqvist, R.** 2006. Estimation of *Staphylococcus aureus* growth parameters from turbidity data: characterization of strain variation and comparison of methods. Appl. Environ. Microbiol. 72:4862-4870.

27. **McClure, P. J., M. B. Cole, K. W. Davies, and W. A. Anderson.** 1993. The use of automated tubidimetric data for the construction of kinetic models. J. Ind. Microbiol. 12:277-285.

28. **McKellar, R. C., and K. Knight. 2000.** A combined discrete-continuous model describing the lag phase of *Listeria monocytogenes*. Int. J. Food Microbiol. 54:171-180.

29. **Pascual, C., T. P. Roberts, M. J. Ocio, O. O. Aboaba, and B. M. Mackey.** 2001. The effect of inoculum size and sublthal injury on the ability of *Listeria monocytogenes*

to initiate growth under suboptimal conditions. Lett. Appl. Microbiol. 33:357-361.

30. **Presser, K. A., D. A. Ratkowsky, and T. Ross.** 1997. Modelling the growth rate of *Escherichia coli* as a function of pH and lactic acid concentration. Appl. Environ. Microbiol. 63:2355-2360.

31. **Robinson, T. P., M. J. Ocio, A. Kaloti, and B. M. Mackey.** 1998. The effect of the growth environment on the lag phase of *Listeria monocytogenes*. Int. J. Food Microbiol. 44:83-92.

32. **Rosso, L., S. Bajard, J. P. Flandrois, T. C. Lahellec, J. Fournaud, and P. Veit.** 1996. Differential growth of *Listeria monocytogenes* at 4 and 8°C: consequences for the shelf life of chilled products. J. Food Prot. 59:944-949.

33. **Sutherland, J. P., A. Aherne, and A. L. Beaumont.** 1996. Preparation and validation of a growth model for *Bacillus cereus:* the effects of temperature, pH, sodium chloride and carbon dioxide. Int. J. Food Microbiol. 30:359-372.

34. **Taylor, A. J., and R. J. Gilbert.** 1975. *Bacillus cereus* food poisoning: a provisional serotyping scheme. J. Med. Microbiol. 8:543-550.

35. **Wijnands, L. M., J. B. Dufrenne, and F. M. van Leusden.** 2005. *Bacillus cereus:* characteristics, behaviour in the gastro-intestinal tract, and interaction with Caco-2 cells. RIVM. 250912003.

36. **Wu, Y., M. W. Griffiths, and R. C. McKellar.** 2000. A comparison of the Bioscreen method and microscopy for the determination of lag times of individual cells of *Listeria monocytogenes*. Lett. Appl. Microbiol. 30:468-472.

37. **Zhao, L., T. J. Montville, and D. W. Schaffner.** 2002. Time-to-detection, percent-growth-positive and maximum growth rate models for *Clostridium botulinum* 56A at multiple temperatures. Int. J. Food Microbiol. 77:187-197.

38. **Zwietering, M. H., J. C. de Wit, and S. Notermans.** 1996. Application of predictive microbiology to estimate the numbers of *Bacillus cereus* in pasteurised milk at the point of consumption. Int. J. Food Microbiol. 30:55-70.

39. **Zwietering, M. H., I. Jongenburger, F. M. Rombouts, and K. van 't Riet.** 1990. Modeling the bacterial growth curve. Appl. Environ. Microbiol. 56:1875-1881.

Chapter 3

Physiological parameters of *Bacillus cereus* marking the end of acid-induced lag phases

Elisabeth G. Biesta-Peters, Maarten Mols, Martine W. Reij, Tjakko Abee

Published in International Journal of Food Microbiology (2011), Vol. 148, No. 1, p. 42-47

3

Abstract

During lag phases microbial cells adapt to their environment and prepare to proliferate. Physiological parameters of B. cereus *cells upon exposure to near-growth-boundary acid stress were investigated and markers for the transition between lag phase and growth were identified using fluorescent probes combined with flow cytometry. Determination of cell counts and optical density revealed lag phases of 1 h, 2 h and 5 h, in cultures shifted to pH 7, pH 5.3 (set with lactic acid) and pH 4.9 (set with sulfuric acid), respectively. The obtained lag phases fitted the trends in ATP levels, which were constant during the lag phase and increased after the onset of growth. Both the percentage of PI-stained cells and cells with a significant membrane potential decreased during the lag phase. This points to repair of membrane damage and the loss of membrane potential. However, both trends extended in the growth phase, thus not suitable to mark the onset of growth. The activity of the electron transfer chain and esterases did allow for assessment of transition between lag phase and growth phase. These activities were generally low during the lag phase and increased after the onset of growth. Our results show that, independent of the duration of the lag phase, for different conditions the same physiological trends could be observed. The change in signal of selected probes can be used as a marker for transition from lag phase to the growth phase and may aid in identification of novel targets interfering with bacterial exit from lag phase.*

Introduction

Bacillus cereus is a food-borne organism and is associated with food spoilage and intoxication (1, 19). It is a Gram positive, facultative anaerobic, spore-forming rod (13) that can be found in for example soil, food, and the human gastrointestinal tract (14). The spores formed by *B. cereus* may resist thermal pasteurisation treatments used to prolong the shelf life of food. Viable spores present in a food product may germinate and the vegetative cells can subsequently grow if conditions are favorable; leading to spoilage of the food product and possible production of toxins in the food or in the host (8). In order to delay or prevent spoilage and toxin production, one or more hurdles are applied to hamper germination and/or outgrowth in the food or food environment. Therefore, food is often acidified and organic acids are frequently added as food preservatives (11).

The maximum specific growth rate (μ_{max}) decreases and the lag phase (λ) increases when microorganisms are exposed to stresses such as low pH and organic acids (4). The lag phase is typically observed as a delay in growth of the microbial population as a result of a (sudden) change in the environment (20). The delay in growth is most prominent when the stress is applied at levels close to the level that completely inhibits the growth of microorganisms, the so-called growth boundary (4). The definition of the lag phase is however solely mathematic; λ is the time point a horizontal line starting at the data point t_0 crosses an extrapolated linear line fitted through the exponential part of the curve (3, 23). Various models can be used to estimate the lag phase, however the lack of understanding of the physiological parameters of cells when they are in a lag phase contributes to difficulties in assessing if the model predictions are correct (3).

A delay of growth is a phenomenon which is typically observed as response of the microbial population to changes in the environment. The duration of the lag phase is influenced by (changes in) environmental conditions, the bacterial species, the growth stage, physiological history of the cells, and the inoculum level at the moment of the environmental change (20). It is however convincible that an apparent “lag phase” may also be caused by a partial inactivation of the culture and simultaneous growth of another population, resulting in a stable bacterial cell count. Changes in bacterial cell size may also affect the observed lag phase of a growing culture when using optical density to determine growth.

Several studies have investigated the physiological state of bacterial cells before and after exposure of a culture to stress (2, 5, 9, 12, 17). This study compares the

physiological state of cells while in lag phase and when the lag phase has elapsed. The behaviour and corresponding physiological parameters of *B. cereus* upon exposure to acid conditions, i.e., low pH and/or the presence of organic acids such as lactic acid, is of importance for the food industry. Therefore, the objective of this research is to investigate physiological parameters during the lag phase and onset of growth of *B. cereus* upon exposure to near growth boundary acid stress for both strong and weak organic acids, and to identify markers for the transition between lag and growth phase on population and/or single cell level.

Materials and methods

Bacterial strain and culture conditions

Bacillus cereus F4810/72, an emetic toxin producing strain, was originally isolated from human vomit (21). The culture was stored frozen at -80°C in cryovials (Greiner Bio-one GmbH; Frickenhausen, Germany) containing 0.3 ml glycerol (87%, Fluka-Chemica GmbH; Buchs, Switzerland) and 0.7 ml overnight culture in Brain Heart Infusion (BHI) broth (Becton Dickinson and Company; Le Pont de Claix, France). For every experiment, a pre-culture was prepared by adding a droplet of the frozen stock culture to BHI broth, and incubated for 16 h at 30°C while shaking at 200 rpm (Julabo SW20; Julabo Labortechnik GmbH, Germany).

Three batches of 100 ml BHI broth of different pH values were prepared; pH 7.0 using sulfuric acid (H_2SO_4) (stock solution of 2.5 M, Riedel-de Haën, Seelze, Germany), pH 5.3 using lactic acid (HLa) (stock solution of 2.7 M, Sigma-Aldrich Chemie GmbH, Steinheim, Germany) and pH 4.9 using H_2SO_4. The pH values were selected based on the growth boundaries of the two acids for the organism, and were set 0.1 ± 0.05 above the boundary pH for growth of *B. cereus* F4810/72 (4). BHI broth of pH 7.0 is close to the normal pH of BHI broth, but is standardized to be used as a reference condition for optimal growth. The BHI broth was prepared and autoclaved according to the manufacturer's instructions, acidified, filter sterilized (Steritop/Steriflip; Millipore Corporation, MA) and 100 ml was transferred to 500 ml sterile Erlenmeyer flasks. To obtain an initial cell concentration of 10^6 cfu/ml (lower limit for flow cytometer), 100 µl pre-culture was added to the 100 ml BHI in the Erlenmeyer flasks, and incubated while shaking (30°C, 200 rpm). The experiments were all performed in triplicate.

Cell counts, pH, absorbance and ATP experiments

The cultures (pH 7.0, pH 5.3 or pH 4.9) were incubated for 24 hours, and sampled hourly for 12 hours and after 24 h. The samples were plated in duplicate onto BHI agar plates (Becton Dickinson BHI broth supplemented with 1.5% bacteriological agar, Oxoid, Basingstoke, Hampshire, England), incubated at 30°C for 24 h and finally enumerated. The lag phase (λ) and maximum specific growth rate (μ_{max}) were determined for every condition by fitting the growth curves using the reparameterised model of Gompertz (Equation 1).

$$\ln\left(\frac{N_t}{N_0}\right) = A\,\exp\left\{-\exp\left[\frac{\mu_{max}e}{A}(\lambda - t)+1\right]\right\} \quad (1)$$

N_t is the number of microorganisms (CFU/ml) at time t (h), N_0 is the number of microorganisms at the time of inoculation, A is the dimensionless asymptotic value of the maximal numbers of microorganisms, μ_{max} is the maximum specific growth rate (h^{-1}), and λ is the lag phase (h) (24).

The pH (WTW pH 525, 8120 Weilheim, Germany) and optical density at a wavelength of 600 nm (OD_{600}) (Novaspec® II, Pharmacia LKB, England) were determined for 24 h.

ATP levels of the cultures were measured every hour for 8 h using an ATP Bioluminescence Assay Kit HS II (Roche Diagnostics GmbH, Mannheim, Germany) and a Biocounter (Biocounter M2500, Luminac b.v., Landgraaf, The Netherlands) according to manufacturer's instructions. Hourly, two samples (400 µl and 500 µl) of every condition were taken. The largest volume was centrifuged (1 min, 10°C, 10,000 × *g*) and 400 µl of the supernatant was transferred to a new tube. 400 µl cell lysis reagent of the ATP Bioluminescence Assay Kit HS II was added to the 400 µl culture and the 400 µl supernatant and subsequently incubated for five minutes at room temperature. The samples were stored frozen (-20°C) until further analysis. Before analysis, the samples were thawed by incubation in a water bath at room temperature until the samples had reached the water temperature. The pH of every sample was measured using a micro pH electrode (pH C3359, Radiometer, Denmark) and adjusted to a pH value ranging from pH 7.6 to pH 8.0 using concentrated hydrochloric acid (HCl). The bioluminescence of every sample was measured in triplicate. When the measured bioluminescence was above 100,000 rlu, the

upper measuring boundary of the Biocounter, the sample was diluted in dilution buffer (from the kit) and measured again. The amount of ATP per ml culture was calculated by extracting the ATP level of the dilution buffer (background) and of the supernatant, of the total ATP level measured.

Flow cytometry experiments

Flow cytometry in combination with various commercially available fluorescent probes (Invitrogen, The Netherlands) was used to study the heterogeneity in physiological parameters of cells during the lag phase and the transition to growth in the three culture conditions described above. Esterase activity was detected using the fluorescent probe carboxyfluorescein diacetate (cFDA). Propidium iodide (PI) was used to stain cells with compromised membranes. The fluoresecent probe C_{12} resazurin (C_{12}) was used to measure electron transfer chain activity and (3,3'-diethyloxacarbocyanine iodide ($DiOC_2(3)$) was used to study the bacterial membrane potential.

The cultures were inoculated and samples were obtained at designated time points (t=0, 1, 2, 3, 4, 5, 6, 7, 8 h) by centrifuging 1 ml of culture (15,000 × *g*, 1 min). The supernatant was discarded and the pellet was resuspended in 1 ml filter sterilized phosphate buffered saline (PBS). Subsequently, cFDA, PI, C_{12} and $DiOC_2(3)$ were added individually at a final concentration of 10 µM (cFDA, C_{12}) or 3 µM (PI, $DiOC_2(3)$) and incubated at 30°C, shielded from light, for 30 min (cFDA, PI) or 15 min (C_{12}, $DiOC_2(3)$). The probes were all used according to manufacturer's instructions. The samples were analyzed on a flowcytometer (FACSCalibur, BD Biosciences, San Jose, California, USA) with the following voltage settings: E00 (FSC), 400 (SSC), 700 (FL1) and 650 (FL3) for both cFDA and PI and 600 (FL1) and 600 (FL3) for C_{12} and $DiOC_2(3)$. The voltage settings of the flow cytometer were determined using control cells and total fluorescence in separate experiments. The intensity of the fluorescent signal of 10,000 events (cells) at high flow rate using Cellquest Pro (version 4.0.2) was recorded. The data were analyzed using Cyflogic (version 1.2.1), where the distribution of the single cell intensity was plotted. When one population was displayed (cFDA and C_{12}-resazurin) the shifts of the geometric mean of the distribution of the signal intensity were used to evaluate the esterase activity and electron transfer in time. A shift towards higher mean values indicated increased fluorescence of the cells and thus higher esterase and electron transfer chain activities. In case of two apparent populations (PI and $DioC_2(3)$, the number of cells in both populations

was determined and the percentage of cells showing membrane damage or membrane potential was calculated as a function of the total population measured.

To measure the size of the cells the flowcytometer was calibrated using polystyrene microspheres of 1.1, 2.0, 4.2, 5.9, and 9.9 µm (Flow Cytometry Size Calibration Kit, Invitrogen, Germany). A mixture of these beads was analyzed on the flowcytometer for 100,000 events. The data were plotted in a forward scatter (FSC) histogram, the five peaks belonging to the different sizes of the microspheres were selected, and the mean FSC-value of each peak was calculated. To obtain a reference curve, the polystyrene microsphere diameter was plotted against the mean FSC-value of the beads. Cells were obtained from every culture as previously described and the FSC-values of 10,000 events were measured. From every sample the mean FSC was determined and the cell size was obtained by comparing the mean FSC of the sample to the mean FSC-values of the polystyrene microspheres.

Results

Growth

The growth of *B. cereus* F4810/74 in BHI at pH 7.0, pH 5.3 (set with lactic acid) and pH 4.9 (set with H_2SO_4) was investigated by measuring viable counts, pH and absorbance for 24 h (Figure 1). To compare the growth for the different conditions, Equation 1 was fitted to the growth curve, resulting in parameter estimates for growth in BHI of pH 7.0 and pH 4.9 (Table 1). It was not possible to reliably estimate μ_{max} and λ for cultures in BHI at pH 5.3 by plate counting due to the decrease in cell counts in the culture at t=3 h and t=4 h. The maximum specific growth rate was 2.90 h^{-1} for growth in BHI of pH 7.0 and 0.71 h^{-1} for growth in BHI of pH 4.9, a 4-fold reduction of growth rate when the pH decreased to a value close to the boundary pH. The lag phases were 2.13 h and 5.84 h respectively, a 2.5-fold increase when the pH decreased to a value close to the boundary pH.

Optical density of the cultures was measured in time (Figure 1B). Since the OD curve for cultures at pH 5.3 showed no decrease in measured values after onset of growth, a reliable estimate for λ, which could be compared to the other test conditions, could be made using absorbance measurements. To determine the length of the lag phase, λ was defined as the time (h) needed for the OD to increase to 0.03. The value of 0.03 was appropriately chosen because at this value growth clearly occurred; i. the measured OD values remained increasing once above 0.03, and ii. at this point, plate counts increased

for cultures at pH 7 and pH 4.9 as fitted by the reparameterised model of Gompertz. The measured lag phases were 1 h, 2 h and 5 h for pH 7.0, pH 5.3 (HLa) and pH 4.9 (H_2SO_4) respectively (Table 1). OD estimated λ values were lower than the growth curve estimated values, but allowed estimating of λ also for cultures which showed a decrease in culturable cells on BHI plates, which made estimation of parameters for growth using CFU's impossible. These OD estimated λ values were the reference values used for further experiments.

The pH of the three broths was followed in time to compare the different cultures and to determine the onset of pH change (Figure 1A). Notably, in all cases, alterations in growth medium pH were only noted long after growth had commenced. The pH started to increase after 5 hours (pH 7.0), 6 hours (pH 5.3), and 15 hours (pH 4.9) in the different conditions.

The cells were occasionally observed microscopically, and no consistent clustering of cells was seen. Most of the cells were single cells, but the presence of sporadic duplo-cells could not be excluded.

The first 7 hours of the growth curve was studied in more detail because it covers the lag phase and onset to growth for the three tested conditions (Figure 1C). In this period the physiological processes in the cell upon exposure to near growth boundary acid stress were investigated and markers for the transition between lag phase and growth were identified.

Table 1: Parameter estimates based on the growth curve and OD curve using the Gompertz model and increase in OD_{600}

pH	Growth curve		OD curve
	μ_{max} (h^{-1})	λ (h)	λ (h)
7	2.9	2.13	1
5.3	ND[a]	ND[a]	2
4.9	0.71	5.84	5

[a] ND, not determined due to the unculturable state of the cells at 3 and 4 hours incubation of cultures in BHI at pH 5.3 set with HLa.

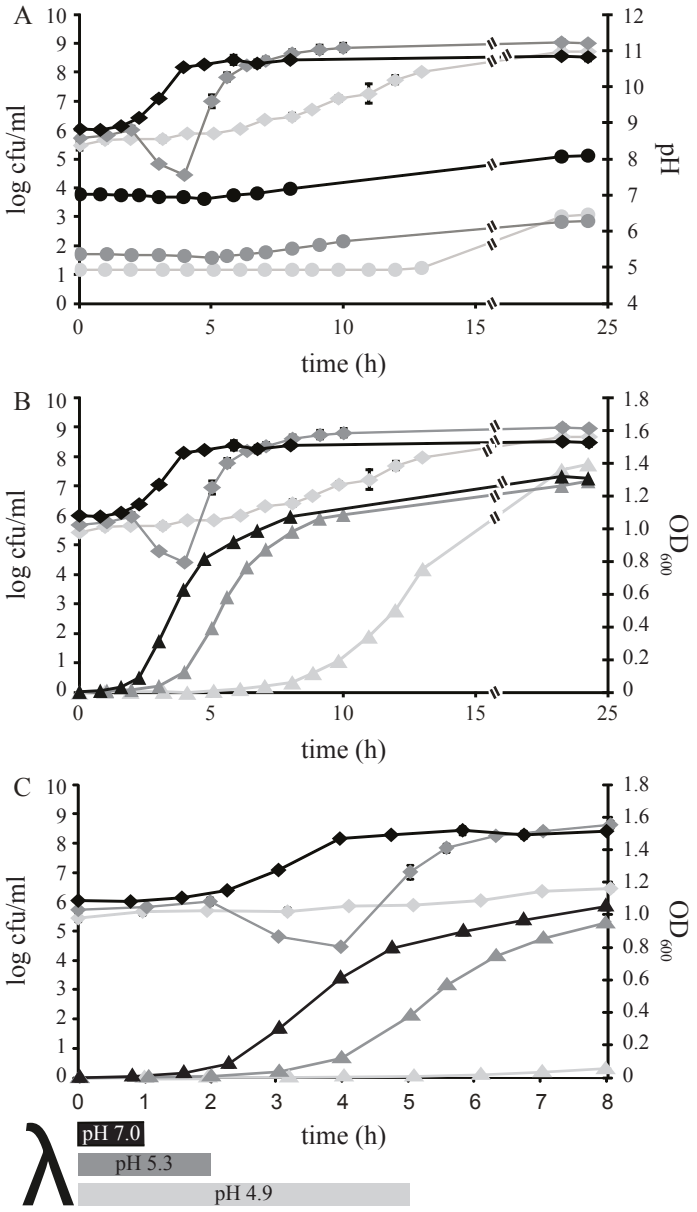

Figure 1. Growth of *B. cereus* F4810/72 at pH 7.0, pH 5.3 (HLa), and pH 4.9 (H_2SO_4). A: Cell counts (◇) and pH (○) in time for 24 h. B: Cell counts (◇) and OD_{600} (Δ) in time for 24 h; and C: Cell counts (◇) and OD_{600} (Δ) in time for 7 h, the time frame used for further experiments. Cultures at pH 7.0 are depicted by black symbols, pH 5.3 by dark gray symbols and pH 4.9 by light gray symbols.

Physiological parameters during lag phase and onset to growth

The ATP levels for all three cultures was around 1×10^{18} molecules ATP per ml culture just after inoculation at t=0 (Figure 2A, B, C). The ATP levels remained stable for 1 h at pH 7.0 (Figure 2A), 2 h at pH 5.3 (Figure 2B) and 5 h at pH 4.9 (Figure 2C), herewith reflecting the duration of the lag phase. After the lag phase had elapsed, the ATP levels increased to maximum levels of around 1×10^{19}, 1×10^{20} and 7×10^{19} molecules ATP per ml culture for pH 4.9, pH 5.3 and pH 7.0 respectively. This increase in ATP levels is partly caused by an increase in the total number of cells. The ATP level was not expressed per cell, because at pH 5.3 the amount of cells determined by plate counts decreased while the OD already increased. This disturbed a good estimation of the cell numbers and the amount of ATP per cell.

The average cell size in the pH 7.0 culture increased between 0 and 1 hour from 2 µm to 2.5 µm and decreased gradually afterwards to values just below 2 µm (Figure 2A). For pH 5.3 a decrease in cell size after 2 hours was observed from 2 µm to 1.5 µm and no apparent increase was measured (Figure 2B). For pH 4.9 the cell size increased up to 5 hours from 2 µm to 2.5 µm and a gradual decrease back to 2.0 µm was observed when growth commenced (Figure 2C). However, these trends are not significant, since the data point all fall within the standard deviations of their previous or subsequent time points.

The esterase activity was measured as cFDA-derived green fluorescent signal for all three conditions. The majority of cells became green fluorescent during the first hour of incubation of cultures at pH 7.0 with a change in signal intensity from around 40 to values close to 500 (arbitrary units) (Figure 2D). Afterwards the intensity of the signal increased to levels as high as 3600. For pH 5.3 as well as for pH 4.9 the trend of the fluorescent signal was similar (Figure 2E and 2F, respectively). A low green fluorescent signal, below 100, was detected during the lag phase and the signal increased to levels of 3400 and just above 100 for pH 5.3 and pH 4.9 respectively during the growth phase. A higher growth rate was associated with a faster increase in green fluorescent signal. cFDA is often used as live/dead indicator, that gives green fluorescent staining in live cells with esterase activity and an intact membrane, allowing for the accumulation of cF. The absence of a signal during the lag phase is therefore supposed to indicate that most cells are not alive at t=0 up until growth starts. However, cF fluorescence is also pH dependent with highest signals at alkaline pH, and low fluorescence signals may also be attributed to low intracellular pH values.

The percentage of cells with a compromised membrane as measured by PI staining (often used as indicator for dead cells) at t=0 was 15 % for pH 7.0 (Figure 2D), 20 % for pH 5.3 (Figure 2E) and 25 % for pH 4.9 (Figure 2F), indicating that approximately 80 % of the cells did have intact membranes. The percentage of cells with compromised membranes decreased during the lag phase for all three conditions, indicating that the cells were able to repair membrane damage. When growth starts, the percentage of cells with a compromised membrane reduced further to levels below 3%, due to an increase

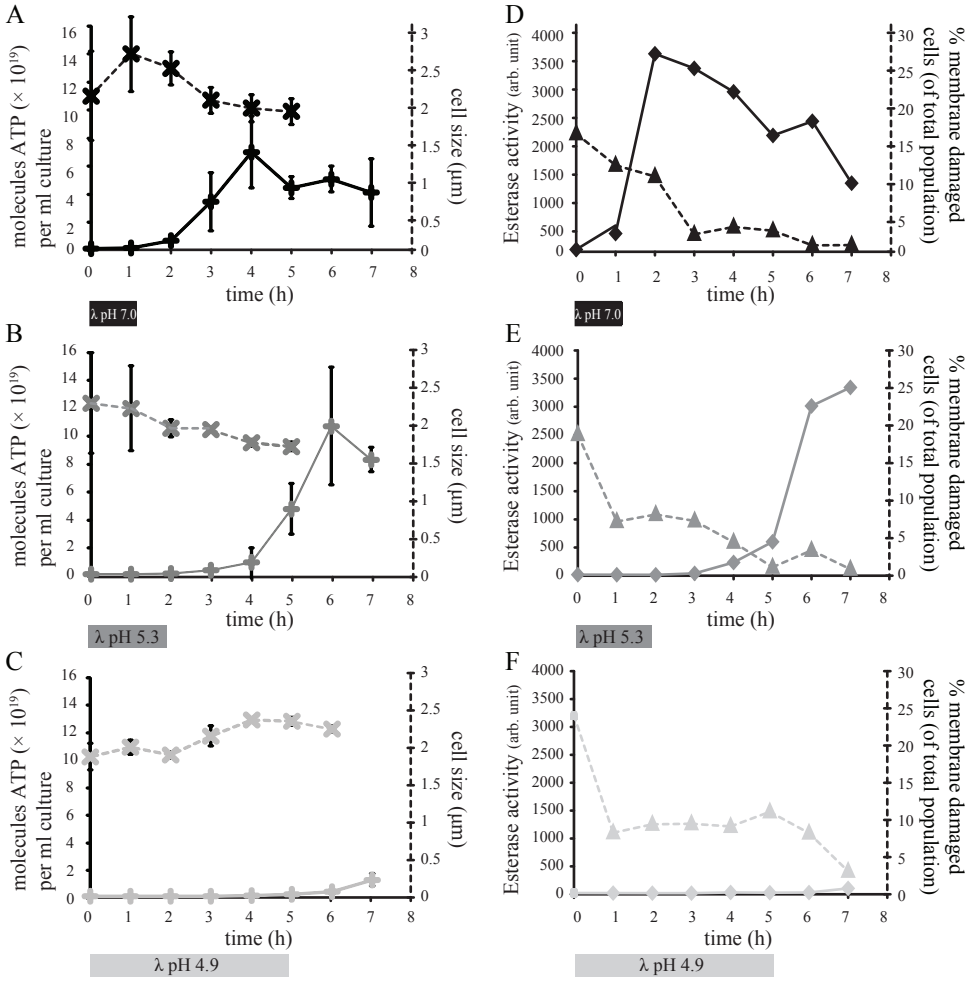

Figure 2. Physiological parameters of *B. cereus* F4810/72 during the lag phase and transition to growth for pH 7.0 (black symbols), pH 5.3 (HLa) (dark gray symbols) and pH 4.9 (H_2SO_4) (light gray symbols). A, B, C: molecules ATP per ml culture (**+**) and average size of the cells (**x**), D, E, F: esterase activity (◇) and membrane damaged population (Δ).

of total cells in the culture.

The electron transport chain activity, indicated by the change in red fluorescent signal, was also investigated. For pH 7.0 the red fluorescent signal, indicating the level of electron transfer chain activity, was stable during the lag phase and increased slightly during the growth phase (Figure 2G). The same trend was observed for pH 5.3 (Figure 2H) and pH 4.9 (Figure 2I). Overall the electron transfer chain activity was only slightly influenced by growth, since the change in red fluorescent signal was small.

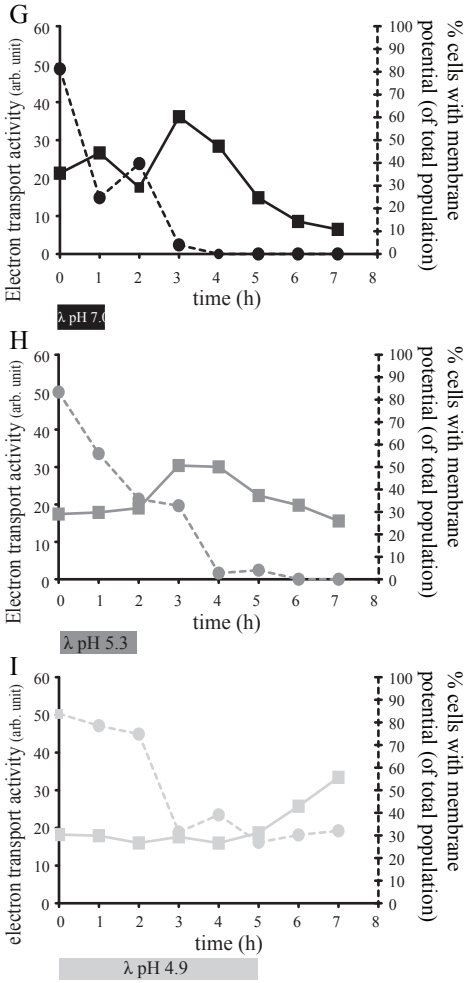

Figure 2. Physiological parameters of *B. cereus* F4810/72 during the lag phase and transition to growth for pH 7.0 (black symbols), pH 5.3 (HLa) (dark gray symbols) and pH 4.9 (H_2SO_4) (light gray symbols). G, H, I: electron transfer chain activity (□) and membrane potential (○).

The membrane potential, the difference in interior and exterior charge of a cell, was also measured for the three different conditions. The percentage of cells with high membrane potential was very high at inoculation for pH 7.0, 80 %, and started to decrease from that point. Four hours after inoculation the membrane potential had disappeared (Figure 2G). For pH 5.3 just after inoculation also 80 % of the cells had a membrane potential and this potential was lost 6 hours after inoculation (Figure 2H). In the case of pH 4.9 also 80 % of the cells had a membrane potential just after inoculation but at the end of the experiment, after 7 hours, only 30 % of the cells still had a membrane potential (Figure 2I). For all conditions it was shown that at the lag phase/growth transition point, approximately half of the cells had no measureable membrane potential, with this number further decreasing during growth.

Discussion

The current work, using *B. cereus* F4810/72 as a model, has provided insight in the microbiological lag phase phenomenon and parameters affecting this biological state under non-stressed and acid-stressed conditions. The analysis of selected physiological parameters during the lag phase of *B. cereus* upon exposure to near-growth-boundary acid stress allowed for the identification of markers for the transition between the lag phase and growth. The lactic acid-stressed culture at pH 5.3 displayed a short, transient viable, but non-culturable state on agar plates just after onset of growth. Bacteria in the viable but nonculturable state fail to grow on the routine bacteriological media on which they would normally grow and develop into colonies, but are still alive, and they are again culturable upon resuscitation (16). The apparent recovery of transient non-culturable cells is reflected in a large increase in plate counts, that by assuming growth, resulted in a μ_{max}-value of 3.85 h^{-1}, thereby exceeding the μ_{max} previously determined for *B. cereus* growth under optimal conditions (2.42 h^{-1}) (4). The time to onset of increase in OD was used as an alternative method to reliably estimate the transition of the cells to the growth phase (4). Although cell counts remained similar in the lag phase of the pH 7 and pH 4.9 cultures, the OD slightly increased during the lag phase, with an accelerated increase during the growth phase. The increase in OD might be caused by the increase in cell size, as observed during the lag phase, resulting in more biomass but not in cell numbers. For lactic acid-stressed cells at pH 5.3 this increase in cell size during the lag phase was not observed and the cell size even decreased to 1.5 µm, followed by an

increase during growth. This might be linked to the decrease in viable counts three to four hours after inoculation. At this time point, the cell size is smaller than for the other two conditions and the ATP levels are higher. The time point marking the decrease in culturable cells is also the time point were the pH increased again after a small drop in pH, putatively marking the transition from glucose to amino acid metabolism. This transition of metabolism, high ATP levels and small cell sizes, at this time point might be indicative of this viable, but non-culturable state. The decrease in cell numbers when plating the cells, which were originally cultured in broth of pH 5.3, did not allow for the representation of the amount of ATP per cell. For that reason the ATP levels were expressed per ml of culture. Independent of the pH of the medium, the defined lag phases fitted with the trends in ATP levels in the different cultures.

Using fluorescent probes in combination with flow cytometry revealed membrane damage and membrane potential to be affected in the lag phase. The percentage PI-stained cells decreased, pointing to repair of membrane damage, and the percentage of cells with a significant membrane potential decreased. Both trends extended in the growth phase, thus not allowing for detection of the lag phase. The membrane potential together with the pH difference between the inside and the outside of the cell (ΔpH), constitutes the proton motive force (15, 18). Analysis of the overnight culture used for inoculation showed that almost all cells maintained a membrane potential. It is conceivable that the ΔpH was small, allowing the low intracellular pH to contribute to the extension of the lag phase in the acid-stressed cultures. Already during the lag phase the contribution of membrane potential decreased, conceivably pointing to conversion of the membrane potential to a pH gradient, resulting in higher values of intracellular pH, allowing resumption of growth. Unfortunately, in this research measuring of intracellular pH was not possible, as discussed further below.

Esterase and electron transfer activities were generally low in the lag phase and increased after the onset of growth. The low cF signal in the lag phase was supposed to indicate that hardly any cells were alive, but simultaneous experiments with PI showed that only approximately 25 % of the cells had a compromised membrane, indicating that most cells were actually alive. A plausible explanation for the lack of green fluorescent signal is the pH dependency of the cF probe, which shows high fluorescence at internal pH values of 7 and up. During the lag phase cellular metabolism and ATP levels are low and, especially combined with the low pH in the acid-stressed cultures, the intracellular

pH will decrease (7). The induced acid stress may trigger activation of pH homeostasis mechanisms that result in an increase of the intracellular pH (10), finally leading to increased esterase activity, i.e., cF fluorescence. Unfortunately, the internal pH could not be measured since this requires loading of the initial culture to follow the cells in time (6, 22), which was not possible for dividing cells. The observed decrease in cF fluorescence at later stages of growth may be explained by the fact that *B. cereus*, like a wide range of bacteria can actively pump cF out of the cell (6).

The physiological parameters of the cell behavior were summarized in a conceptual figure (Figure 3), describing the trend of the parameters during the lag phase and the growth phase. The trends reflected in this conceptual figure allow for the identification of markers for the lag and growth transition phase.

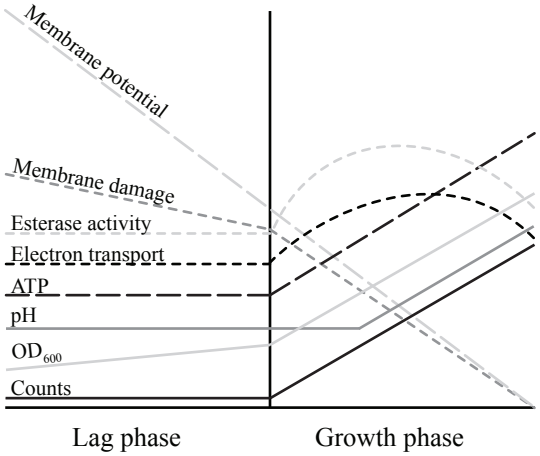

Figure 3. Trends of the physiological parameters during the lag phase and the onset of growth.

It can be concluded that both the induction of cF fluorescence indicating esterase activity and the electron transport chain activity are good markers. It is also apparent that the markers act independently of the culture conditions used in this research, and that they are effective in different time frames, i.e., short and extended, stress-induced lag phases. Although some physiological parameters are stable during the lag phase, there are indeed already physiological changes in the cell while the cells are not multiplying, such as a decrease in membrane potential and repair of membrane damage. Our observations and the physiological parameters identified may contribute to a better understanding

of the lag phase and can be of added value for food industry, where transition of microorganisms from lag to growth phase should be avoided. Therefore, this research aids in the identification of novel targets interfering with bacterial exit from lag phase.

Acknowledgments

This work was financially supported by Nestlé Research Centre, Lausanne, Switzerland. The authors acknowledge Maarten Overes for experimental assistance.

References

1. **Adams, M. R., and M. O. Moss.** 2000. Food Microbiology. 2 ed. The Royal Society of Chemistry.
2. **Baatout, S., P. de Boever, and M. Mergeay.** 2005. Temperature-induced changes in bacterial physiology as determined by flow cytometry. Ann. Microbiol. 55:73-80.
3. **Baty, F., and M.-L. Delignette-Muller**. 2004. Estimating the bacterial lag time: which model, which precision? Int. J. Food Microbiol. 91:261-277.
4. **Biesta-Peters, E. G., M. W. Reij, H. Joosten, L. G. M. Gorris, and M. H. Zwietering.** 2010. Comparison of two optical density methods and a plate count method for estimation of growth parameters of *Bacillus cereus*. Appl. Environ. Microbiol. 76: 1399-1405.
5. **Braga, P. C., C. Bovio, M. Culici, and M. Dal Sasso.** 2003. Flow cytometric assessment of susceptibilities of *Streptococcus pyogenes* to erythromycin and rokitamycin. Antimicrob. Agents Chemother. 47:408-412.
6. **Breeuwer, P., J. Drocourt, F. M. Rombouts, and T. Abee.** 1996. A novel method for continuous determination of the intracellular pH in bacteria with the internally conjugated fluorescent probe 5 (and 6-)-carboxyfluorescein succinimidyl ester. Appl. Environ. Microbiol. 62:178-183.
7. **Browne, N., and B. C. A. Dowds.** 2002. Acid stress in the food pathogen *Bacillus cereus*. J. Appl. Microbiol. 92:404-414.
8. **Choma, C., T. Clavel, H. Dominguez, N. Razafindramboa, H. Soumille, C. Nguyen-The, and P. Schmitt.** 2000. Effect of temperature on growth characteristics of *Bacillus cereus* TZ415. Int. J. Food Microbiol. 55:73-77.
9. **Cronin, U. P., and M. G. Wilkinson.** 2008. Physiological response of *Bacillus cereus* vegetative cells to simulated food processing treatments. J. Food Prot. 71:2168-2176.
10. **Foster, J. W.** 1995. Low pH adaptation and the acid tolerance response of

Salmonella typhimurium. Crit. Rev. Microbiol. 21:215-237.

11. **Gould, G. W.** 1996. Methods for preservation and extension of shelf life. Int. J. Food Microbiol. 33:51-64.

12. **Hewitt, C., J., G. Nebe-Von Caron, A. W. Nienow, and C. M. McFarlane.** 1999. Use of multi-staining flow cytometry to characterise the physiological state of *Escherichia coli* W3110 in high cell density fed-batch cultures. Biotechnol. Bioeng. 63:705-711.

13. **Kotiranta, A., K. Lounatmaa, and M. Haapasalo.** 2000. Epidemiology and pathogenesis of *Bacillus cereus* infections. Microbes Infect. 2:189-198.

14. **Larsen, H. D., and K. Jørgensen.** 1999. Growth of *Bacillus cereus* in pasteurized milk products. Int. J. Food Microbiol. 46:173-176.

15. **Michels, M., and E. P. Bakker.** 1985. Generation of a large, protonophore-sensitive proton motive force and pH difference in the acidophilic bacteria *Thermoplasma acidophilum* and *Bacillus acidocaldarius*. J. Bacteriol. 161:231-237.

16. **Oliver, J. D.** 2005. The viable but nonculturable state in bacteria. J. Microbiol. 43:93-100.

17. **Papadimitriou, K., H. Pratsinis, G. Nebe-von-Caron, D. Kletsas, and E. Tsakalidou.** 2006. Rapid assessment of the physiological status of *Streptococcus macedonicus* by flow cytometry and fluorescence probes. Int. J. Food Microbiol. 111:197-205.

18. **Richard, H., and J. W. Foster.** 2004. *Escherichia coli* glutamate- and arginine-dependent acid resistance systems increase internal pH and reverse transmembrane potential. J. Bacteriol. 186:6032-6041.

19. **Stenfors Arnesen, L. P., A. Fagerlund, and P. E Granum.** 2008. From soil to gut: *Bacillus cereus* and its food poisoning toxins. FEMS Microbiol. Rev. 32:579-606.

20. **Swinnen, I. A. M., K. Bernaerts, E. J. J. Dens, A. H. Geeraerd, and J. F. van Impe.** 2004. Predictive modelling of the microbial lag phase: a review. Int. J. Food Microbiol. 94:137-159.

21. **Taylor, A. J., and R. J. Gilbert.** 1975. *Bacillus cereus* food poisoning: a provisional serotyping scheme. J. Med. Microbiol. 8:543-550.

22. **Valli, M., M. Sauer, P. Branduardi, N. Borth, D. Porro, and D. Mattanovich.** 2005. Intracellular pH distribution in *Saccharomyces cerevisiae* cell populations, analyzed by flow cytometry. Appl. Environ. Microbiol. 71:1515-1521.

23. **Zwietering, M. H., F. M. Rombouts, and K. van 't Riet.** 1992. Comparison of definitions of the lag phase and the exponential phase in bacterial growth. J. Appl. Microbiol. 72:139-145.

24. **Zwietering, M. H., I. Jongenburger, F. M. Rombouts, and K. van 't Riet.** 1990. Modeling the bacterial growth curve. Appl. Environ. Microbiol. 56:1875-1881.

Chapter 4

Comparing nonsynergistic gamma models with interaction models to predict growth of emetic *Bacillus cereus* when using combinations of pH and individual undissociated acids as growth-limiting factors

Elisabeth G. Biesta-Peters, Martine W. Reij, Leon G.M. Gorris, Marcel H. Zwietering

Published in Applied and Environmental Microbiology (2010), Vol. 76, No. 17, p. 5791-5801

4

Abstract

A combination of multiple hurdles to limit microbial growth is frequently applied in foods to achieve an overall level of protection. Quantification of hurdle technology aims at identifying synergistic or multiplicative effects and is still being developed. The gamma hypothesis states that inhibitory environmental factors aiming at limiting microbial growth rates combine in a multiplicative manner rather than synergistically. Its validity is tested here with respect to the use of pH and various concentrations of undissociated acids, i.e. acetic-, lactic-, propionic- and formic acid, to control growth of Bacillus cereus *in brain heart infusion broth. The key growth parameter considered was the maximum specific growth rate, μ_{max}, as observed by optical density. A variety of models from literature describing the effect of various pH values and undissociated acid concentrations on μ_{max} were fitted to experimental datasets, compared based on a predefined set of selection criteria and the best models were selected. The cardinal model developed by Rosso (for pH dependency) and the model developed by Luong (for undissociated acid) were found to provide the best fit and were combined in a gamma model with good predictive performance. The introduction of synergy factors into the models was not able to improve the quality of the prediction. On the contrary, including synergy factors led to an overestimation of the growth boundary with the inherent risk of leading to underestimation of the risk under the conditions tested in this research.*

Introduction

Consumers expect safe and sufficiently stable food within the given shelf life of a food product or component. Several growth-limiting factors, collectively referred to as hurdles, can be used to ensure food stability and safety. Examples of such hurdles are low pH, low water activity, or low temperature (12). Combining hurdles to achieve food stability and safety, known as hurdle technology, can be used to achieve an overall level of protection in food while minimizing impacts on food quality (20). When a combination of hurdles is used, generally, the intensity of the hurdles may be lower, to exert a comparable preservative effect, than the intensity of those hurdles when used individually (20). Three classes of interaction can be defined when applying hurdle technology: "no interaction," in which the effect of a combination is as expected from the response of the separate factors; "synergy," in which the effect is greater than expected; and "antagonism," in which the effect is less than expected (6).

Though the concept of hurdle technology is rather well established, the quantification of the combined impact of hurdles on growth of microorganisms is still being developed. One significant problem is that there are two opposite views of how antimicrobial factors combine. One view states that there are interactive effects between hurdles; when they are applied together, they give a protection significantly greater than that expected on the basis of the application of the individual hurdles (synergy). The alternative view considers that the combined effect may be complex but that there are no interactive effects culminating in synergy. The latter view is called the gamma hypothesis (41) and states that inhibitory environmental factors combine in a multiplicative manner to produce the observed overall microbial inhibition. A major benefit of models based on the gamma hypothesis is a reduction in experimental work, since growth rates and, as a result, growth boundaries can be estimated upon evaluating single hurdles rather than their various combinations. This benefit can only be realized, however, when the gamma hypothesis is valid for the combination of hurdles considered. If the hypothesis is not valid and interactive effects are present, growth boundaries are estimated wrongly, which might result in fail-safe predictions.

Over the years, the gamma hypothesis has been confirmed by several studies (16, 17, 26, 34, 38) that concluded that the combined effect of hurdles on growth rates is multiplicative rather than synergistic. Contrarily, Rödel and Scheuer (30) concluded that interaction occurs when various hurdles are combined, stressing the occurrence of synergy.

Both Le Marc *et al.* (21) and Augustin and Carlier (5) developed a synergy model to take account of synergy occurring when hurdles are combined. It is prudent to conclude that the effect of combinations of hurdles is best evaluated on a case-by-case basis in order to ensure appropriate utility of hurdle technology approaches in establishing food designs that are stable and safe.

This research aimed to validate or falsify the gamma hypothesis for two closely related hurdles often used in the food industry: the pH level and the undissociated acid concentration ([HA]). The approach chosen was to establish an overview of models for pH and undissociated acid from the literature. Based on pre-defined criteria, models were then selected to construct a new gamma model without synergy factors for the various hurdle combinations. The criteria were meant to enable evaluation of the fitting performance of all individual models to select the best-performing models for inclusion in the new gamma models. Finally, the validity of the gamma hypothesis was judged by comparing the predictive performance of the newly constructed gamma models with two gamma models including a synergy factor reported in the literature. *Bacillus cereus* F4810/72, relevant for both food spoilage and poisoning (14, 19), was used as the model microorganism. Maximum specific growth rates were determined by optical density measurements combined with time to detection. This method was selected after thorough investigation of three different methods to obtain parameters for growth, as recently published (8).

Materials and methods

Bacterial strain and culture conditions

B. cereus F4810/72, an emetic toxin producer, was originally isolated from human vomit (33). This strain is also known as *B. cereus* NCTC 11143, DSM 4312 and PAL 25 (36) (Health Protection Agency Culture Collections [www.nctc.org.uk]).

Preparation of the strain and the culture conditions were as previously described (8). In short, a loopful of microorganisms was inoculated in a 500-ml Erlenmeyer flask containing 100 ml brain heart infusion (BHI) broth, and incubated for 16 h at 30˚C with shaking at 200 rpm. The overnight culture was standardized by resuspending the concentrated bacterial suspension in 1 ml of 1% (wt/vol) peptone physiological salt solution (PPS). The cell suspension was diluted to an optical density at 600 nm (OD_{600}) of 0.5 in a 1% PPS solution, corresponding to approximately 10^9 CFU/ml. This suspension was the standardized bacterial suspension used for further experiments.

BHI broth was prepared and autoclaved according to the manufacturer's instructions and adjusted to the appropriate pH (7 or 5.5) using sterile 0.5 M sulfuric acid (H_2SO_4) (Riedel-de Haën, Seelze, Germany).

Experimental design

The maximum specific growth rate, μ_{max} (h^{-1}), was determined using the relative rate to detection (RRD) method by measuring time to detection (TTD) using the Bioscreen C analysis system (Oy Growth Curves AB Ltd, Helsinki, Finland) (8). This method was chosen since previous research showed that compared to other methods, it resulted in more data points close to the growth boundary where possible interactive effects are expected to be present (8).

The experiments were divided into three groups: 1, testing of the pH effect using strong acids (pKa < 1); 2, testing of the undissociated acid effect using weak acids (pKa > 1) in a buffer solution at a fixed pH of 5.5; and 3, testing of both pH and undissociated acid effects using weak acids. Table 1 provides an overview of the three groups of experiments, including the acids used (acetic acid [HAc], lactic acid [HLa], propionic acid, [HPr], and formic acid, [HFo]), and the ranges of pH values and undissociated acid concentrations ([HA]) tested.

Table 1. Acids (solutes) used for experiments and key experimental data obtained

Exptl group(s)	Acid	Chemical formula	Acid supplier	pK_a	Tested pH range	No. of bins	No. of data points (no. excluded[a])
1	Sulfuric acid	H_2SO_4	Riedel-de Haën, Seelze, Germany	< 1	4.60-7.46	56	598 (2; 0)
2, 3	Acetic acid (HAc)	$C_2H_4O_2$	Merck KGaA; Darmstadt, Germany	4.75	5.11-7.0	36	399 (0; 1)
2, 3	Lactic acid (HLa)	$C_3H_6O_3$	Sigma-Aldrich Chemie GmbH, Steinheim, Germany	3.85	4.86-7.11	49	496 (7; 0)
2, 3	Propionic acid (HPr)	$C_3H_6O_2$	Merck KGaA; Darmstadt, Germany	4.88	4.67-7.02	54	599 (0; 1)
2, 3	Formic acid (HFo)	CH_2O_2	Acros organics, New Jersey, USA	3.75	4.49-7.00	39	399 (1; 0)

[a] The first number is the number of data points excluded since at t = 0 the optical density (OD) values were above the detection limit of OD = 0.2. The second number is the number of data points excluded according to the criteria in Material en Methods.

To test the effect of the undissociated acid concentration on μ_{max}, the pH of the BHI broth was set to 5.5 using sulfuric acid. This value was chosen for being approximately half a pH unit higher than the minimal pH, to be able to observe either an increase or a decrease in the μ_{max}. The ratio between the dissociated and undissociated forms at the set pH was calculated using the Henderson-Hasselbalch equation (Equation 1):

$$\mathrm{pH} = \mathrm{p}K_a + \log\frac{[\mathrm{A}^-]}{[\mathrm{HA}]} \quad (1)$$

where pH is the pre-set pH of the medium using sulfuric acid, pK_a is the acid dissociation constant (acid dependent, see Table 1), [A^-] is the concentration of anions, and [HA] is the concentration of the undissociated acid, which at a fixed pH has a fixed ratio. For each type of weak acid, a stock solution was prepared at pH 5.5 by adding the acid and its conjugated salt ion in the correct ratio (Table 1).

Table 1 - *Continued*

Tested conc range (mM)	No. of bins	No. of data points (no. excluded[a])	Conjugated salt	Salt supplier
0-10	16	596 (3; 1)	Potassium acetate (KAc)	Merck KGaA; Darmstadt, Germany
0-5	16	400 (0; 0)	Potassium lactate (KLa)	PURAC biochem, Gorinchem, Netherlands
0-10	17	558 (0; 2)	Calcium propionate (CaPr)	Riedel-de Haën, Seelze, Germany
0-8	21	599 (0; 1)	Potassium formate (KFo)	Sigma-Aldrich Chemie GmbH, Steinheim, Germany

[a] The first number is the number of data points excluded since at t = 0 the optical density (OD) values were above the detection limit of OD = 0.2. The second number is the number of data points excluded according to the criteria in Material en Methods.

Effect of pH and undissociated acid concentrations on μ_{max}

For every experiment of groups 1 and 3, 20 bottles containing 50 ml BHI broth (pH 7) were pH adjusted with the selected acid, either H_2SO_4, HAc, HLa, HPr, or HFo. After the pH of the BHI had been set, the liquids were filter sterilized (Steritop/Steriflip; Milipore Corporation, Massachusetts, USA). The standardized bacterial suspension was diluted 10,000 fold in pH-adjusted BHI, using a new dilution series for every pH value, aiming at an initial cell concentration of approximately 10^4 CFU/ml. This resulted in 20 inoculated test tubes, 1 for every pH value to be tested. The content of the tube of pH 7 was spiral plated on BHI agar plates for enumeration.

Honeycomb plates were filled and incubated as previously described (8). In short, wells were filled with 150 µl of pH-adjusted BHI, filling five wells per pH value. Every pH value was investigated in a duplicate plate. Every first well of a pH series was inoculated with 150 µl of a particular target pH-value adjusted bacterial culture, and, after mixing, half of the content was transferred to the nearest well of the same pH, continuing in this manner up to the fifth well. Both honeycomb plates were incubated in a Bioscreen C system at 30˚C for 3 days with continuous shaking at the medium setting. The OD_{600} was measured every 10 min. The OD_{600} data obtained from the Bioscreen system were imported into the Microsoft Excel software program for data capturing. Wells with an initial OD_{600} above 0.2 were removed from the data set since they were likely to have an incidental too-high inoculum level (8). For all relevant data series, the time to detection (TTD), defined as the time (h) to reach an OD_{600} of 0.2, was determined. For wells not reaching an OD_{600} of 0.2 within the time frame of the experiment, viability of bacteria was determined and if no viable bacteria were detected, the μ_{max} value was set to 0 h^{-1}. For all acids to be tested, the experiment was repeated at least once. In case two experiments did not give enough information about the exact growth boundary, the experiment was repeated once more.

The TTD determined for every test condition (TTD_i) was related to the TTD under optimal conditions (TTD_{opt}), in this case at pH 7. Subsequently, the specific growth rate ($\mu_{max,i}$) was calculated according to Equation 2:

$$\mu_{\max,i} = \mu_{opt}\,\mathrm{RRD}_i = \mu_{opt}\,\frac{\mathrm{TTD}_{opt}}{\mathrm{TTD}_i} \qquad (2)$$

The μ_{opt} value was estimated independently by plate counting and subsequent fitting of the Gompertz model to the counts (8). In assessing TTD_{opt} and TTD_i for use in Equation 2, care was taken to always start with equal inoculum levels.

To test the effect of the undissociated acid concentration for the weak acids (experiments of group 2), a buffer solution was prepared. Ten bottles containing 50 ml of standardized BHI were adjusted to pH 5.5 using sulfuric acid. The acid and the conjugated salt were added to the pH-adjusted BHI in the right ratio according to Equation 1, hereupon the medium was filter sterilized. The concentration ranges of the acids tested are presented in Table 1. The standardized bacterial suspension was diluted 10,000-fold in adjusted BHI, one for every undissociated acid concentration condition to be tested. The dilution with no undissociated acid present was spiral plated on BHI agar plates in duplicate for enumeration. Filling of the plates, running of the Bioscreen system and capturing and processing of data were as described for the experiments of groups 1 and 3, except for the number of replicates within the experiments, which was four instead of two. Every experiment was repeated at least once and twice in cases where the growth boundary could not be determined from the previous experiments. To determine μ_{max}, Equation 2 was used. TTD_{opt} was defined as the test condition with no undissociated acid present.

For the three groups of experiments, the growth rate curves were studied in more detail. Generally, the μ_{max} values per replicate of tested pH value or undissociated acid concentration were in the same order of magnitude, but sometimes no growth was measured for some of the replicates, while the other points showed considerable μ_{max} values. For these cases the data points per test conditions were divided into two groups: growth and no growth. The number of data points per group was determined, and the ratio between the numbers in the smallest and largest group was calculated. In cases where the number of data points in the smallest group was more than 10 %, the values in this group were considered to be representative for the experimental condition and were included for further analysis. In cases where the contribution was less than 10 %, the 99% confidence interval of the μ_{max} values of the largest group was calculated. If the μ_{max} values of the smallest group were within the 99% confidence interval, the values were also included for further research; otherwise, they were excluded from further data analysis.

Model selection and performance

Three criteria were used to select the best-fitting models: (i) the mean square error (MSE) value for the model fit should be below 0.01 to ensure a high level of fit; (ii) the standard deviations for individual model parameters should be smaller than the parameter estimates themselves, since standard deviations greater than the respective parameter estimate indicate large variation; and (iii) the model parameters should preferably have biological significance.

Secondary models for growth rate, which actually included or could be amended to include a pH term or an undissociated acid term, were selected from the literature. The pH models are summarized in Table 2 and the undissociated acid models are summarized in Table 3. The names of the parameters were standardized to improve transparency and comparability throughout this research. All outcomes of the models were expressed as μ_{max} values. The pH models were fitted to the μ_{max} data of group 1, and the undissociated acid models were fitted to the μ_{max} data of group 2. Model performance (MSE values) and parameter estimates for the two types of models are included in Tables 2 and 3, respectively.

The models for pH and undissociated acid concentration that were selected on the basis of the three criteria stated above were tested against the best performing model with one parameter less, using an *F* test to evaluate if the reduction of one parameter was still statistically acceptable (10). The experimental *f* value was tested against the 95 % confidence *F* table value (F_{∞}^{1} = 3.84). If the *f* value was smaller than the *F* table value, the *F* test was accepted and the model with the least number of parameters was accepted.

Evaluating gamma hypothesis validity

The selected best-fitting models for pH and undissociated acid concentration were combined in a gamma model according to Equation 3 (41):

$$\mu_{\max} = \mu_{\text{opt}}\ \gamma(\text{pH})\ \gamma([\text{HA}]) \tag{3A}$$

with $$\gamma(\text{pH}) = \frac{\mu_{\max,\text{pH}}}{\mu_{\text{opt},\text{pH}}} \tag{3B}$$

and $$\gamma([\text{HA}]) = \frac{\mu_{\max,[\text{HA}]}}{\mu_{\text{opt},[\text{HA}]}} \tag{3C}$$

where μ_{max} is the maximum specific growth rate at the tested condition, μ_{opt} and $\mu_{opt,pH}$ are the maximum specific growth rates in medium with pH 7 as determined by a plate count (2.42 h^{-1}) and $\mu_{opt,[HA]}$ is the maximum specific growth rate when no undissociated acid is present in buffer solution with pH 5.5, as determined from the pH-growth rate curve for H_2SO_4 fitted with the model of Rosso *et al*. (31) (1.51 h^{-1}); all maximum growth rates were obtained from the pH-growth rate curve and the best-fitting model of this curve. Parameter estimates derived by fitting of single models were incorporated into the gamma model, and predictions were made using the optimal fit of the growth rate curves for the combined effect of pH and undissociated acid. In total, four sets of predictions were made, one for each acid tested. These predictions were compared to the experimental data of the acids of group 3, where both pH and undissociated acid effects were present. The ratio between the dissociated and undissociated forms of the acid could be calculated from Equation 1, since the pH of the broth was measured while adding the acid. The concentrations of the dissociated and undissociated acids could be calculated, since the amount and concentration of the acid added to the broth were known. The differences between predictions and experimental data were expressed as MSE values, to be able to compare between the acids and, if necessary, between models.

Two gamma models, including a synergy factor, were found in the literature and compared with the newly composed gamma models combining pH and undissociated acid effects. The first synergy model was described by Le Marc *et al*. (21) (Equation 4):

$$\mu_{max} = \mu_{opt}\,\gamma(\mathrm{pH})\,\gamma([\mathrm{HA}])\,\xi(\mathrm{pH},[\mathrm{HA}]) \quad (4)$$

in which "ξ" is the synergy factor. The second synergy model was the model of Augustin and Carlier (4, 5). This model does not include a synergy factor, but the different inhibitory factors were corrected independently for synergy by estimating new minimal growth values, which were again used in the nonsynergistic gamma model according to Equations 5A, B and C:

$$\mu_{max} = \mu_{opt}\ \gamma_{new}(pH)\ \gamma_{new}([HA]) \quad (5A)$$

$$\text{with} \quad pH_{min,new} = pH_{opt,\,fit} - (pH_{opt,\,fit} - pH_{min,\,fit})\left(1 - \frac{[HA]}{[HA]_{max,\,fit}}\right)^{1/3} \quad (5B)$$

$$\text{and} \quad [HA]_{max,new} = [HA]_{max}\left(1 - \left(\frac{pH_{opt,\,fit} - pH}{pH_{opt,\,fit} - pH_{min,\,fit}}\right)^{3}\right) \quad (5C)$$

Results

Effect of pH and undissociated acid concentrations on μ_{max}

Three groups of experiments were conducted to investigate the effect of pH (group 1), the effect of undissociated acid (group 2), and the combined effect of pH and undissociated acid (group 3). For every group of experiments and for every acid evaluated, Table 1 shows the pH range tested, the number of pH groups (bins), the number of data points in the data set generated and the number of data points removed from the initial data set (for reasons described Material and Methods).

Using H_2SO_4 to set the pH, the lower pH boundary was pH 4.8. The experimental data for this first group of experiments are displayed in Figure 1A. The results for the undissociated effect of HAc, HLa, HPr and HFo in a pH 5.5 buffer solution are shown in Figure 1B to E. For these, the measured growth boundaries were 8, 2.5, 4.7, and 0.80 mM undissociated acid, respectively.

Selection of the best-fitting model to describe growth rate as a function of pH

Eleven pH models, as displayed in Table 2, were fitted to the pH-growth rate curve of *B. cereus* F4810/72 cultured in BHI adjusted for pH by the addition of H_2SO_4. The fitting performance (expressed as MSE values) and the parameter estimates with their standard deviations are represented in Table 2, as well. Five models, namely, models 3, 4, 6, 7, and 9 were rejected, since at least one of the standard deviations of their estimated parameters was larger than the parameter estimate itself. Models 1 and 5 were not considered further, since the MSE values exceeded 0.01. Models 2 and 11 were rejected based on the inclusion of parameters without an evident biological relevance, while,

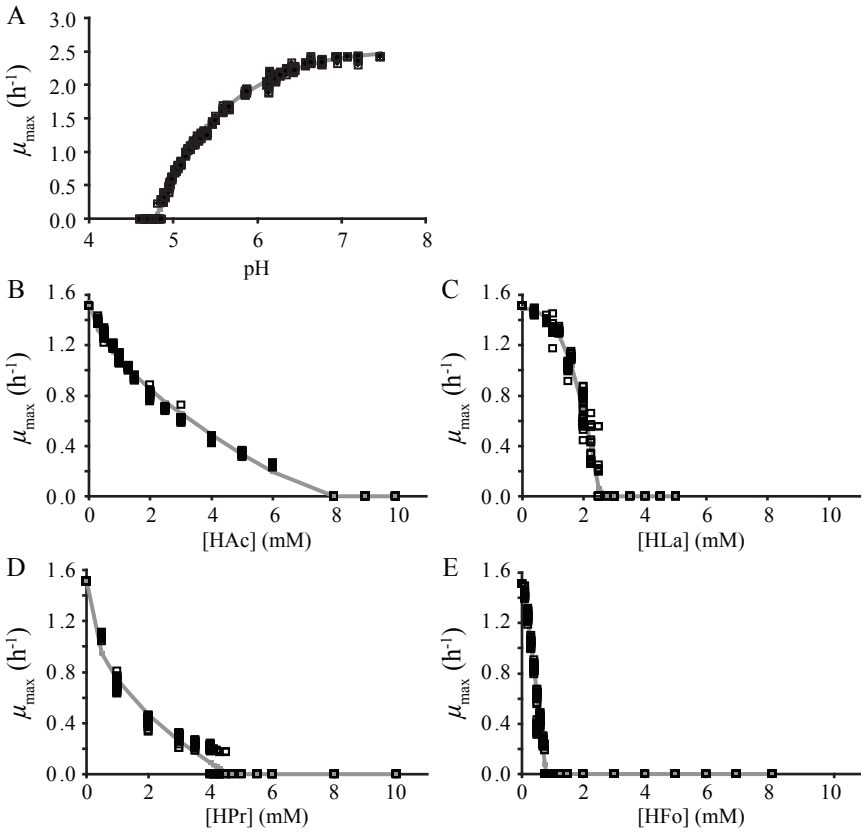

Figure 1. Experimental data (□) for the effect on μ_{max} of pH, set using H_2SO_4 (A), and of the undissociated acid concentration ([HA]), using HAc (B), HLa (C), HPr (D) and HFo (E); the solid gray line shows the fit of the best fitting model for pH (model 8) and [HA] (model 18) to the data-sets.

additionally, model 11 was not able to fit the growth boundary since it is an asymptotic model. Of the two remaining models, models 8 and 10, model 8 of Rosso *et al.* (31) was considered the best model, since it had the best fitting performance (MSE = 0.0023) and included parameters that were biological relevant. Model 10 of Zwietering *et al.* (40), with one parameter less, met al criteria but had a slightly lower fitting performance (MSE = 0.0074). The *F* test was applied to investigate if the difference in MSE-values between model 8 and model 10 was significant. Since f = 1,364.68 exceeds F_{∞}^{1} = 3.84, model 8 with four parameters was judged to be the best model to describe the behavior of *B. cereus* cultured in BHI acidified by H_2SO_4.

Selection of the best-fitting model to describe growth in the presence of undissociated acid

Twelve undissociated acid models (Table 3) were fitted to the undissociated acid-growth rate curves of *B. cereus* F4810/72 cultured in pH 5.5 buffered BHI with various concentrations of undissociated acid. The models were fitted to all four datasets: HAc, HLa, HPr and HFo. Table 3 shows the MSE values and the parameter estimates and their standard deviations for the various models applied to all four acids. Models 12, 14, 15, 16, and 22 were rejected since the standard deviation of one or more parameters exceeded the estimated value of that parameter for at least one acid. Models 13, 17, 19, 20 and 21 were rejected since for at least one acid the MSE value exceeded the MSE-value criterion of 0.01. Model 18 of Luong (MSE = 0.0132) (24) and Model 23 of Lambert and Bidlas (MSE = 0.0175) (16) were the models remaining, although both include a parameter with no evident biological significance. Both models include three parameters. Model 18 of Luong was selected as the best-fitting model since it had the lowest MSE value. Although model 16 of Pasos *et al.* (27), had been rejected, the criteria for rejection were tested by comparing model 18 to model 16, which had a lower MSE value (MSE = 0.0119) than model 18 but a standard deviation exceeding the parameter estimate for HFo. Model 16 also contains one more parameter than model 18. The two models were tested for all four acid data sets with the *F* test ($F_{\infty}^{1} = 3.84$). The *f* values for the HAc, HLa, HPr, and HFo data sets were 424, 1, 8, and -35, respectively. This indicates that for the HLa and HFo datasets, model 18 fits best, whereas for HAc and HPr, model 16 is the best to use. Model 18 of Luong was also compared with an *F* test to model 17 of Ghose and Tyagi (11), which was the best model with two parameters for all data sets. The sum of the MSE values for model 17 was the lowest of the two parameter models tested, but this model was initially rejected, since the MSE values exceeded the criterion of 0.01. The *f* values were 494, 330, 445, and 79 for the respective acids, indicating that the reduced model with two parameters would not be the best choice for fitting the data, as was already concluded from the high MSE values.

Evaluating the gamma hypothesis validity

Models 8 and 18 were combined in a gamma model according to Equation 3 to form the models 24A, 25A, 26A, and 27A, as presented in Table 4. In addition, the synergy models of Le Marc *et al*. (Equation 4, Table 4, models B (21)) and Augustin and Carlier (Equation 5, Table 4 models C, (4, 5)), were combined into predictive models. With these three Equations, the growth of *B. cereus* in BHI broth in the presence of weak acid was predicted, as was the growth boundary. Figure 2A, B, C, and D show the predictions of the three models for HAc, HLa, HPr, and HFo, respectively, next to the experimental data. For acetic acid and formic acid, the shape of the curves and the growth boundaries were predicted very well by the gamma model. For all four acids, the predictions of the models of μ_{max} were lower than the experimental data for the whole curve. For lactic acid, however, the growth boundary was underestimated by 0.25 pH units, while the data points at pH 5.5 or higher were predicted correctly by the gamma model. The model of Le Marc *et al*. underestimated the boundary by 0.15 pH unit, and the model of Augustin and Carlier overestimated the boundary by 0.15. For all acids, the predictions by Le Marc *et al*. were very close to those of the gamma model, while the model of Augustin and Carlier consequently underestimated growth rates in the lower half of the pH range.

As shown in Table 4 and Figure 2, the addition of a synergy factor according to the model of Le Marc *et al*. does not reduce the MSE values between predictions and experiments. On the contrary, in most cases the MSE values increased compared to those for the gamma model. For lactic acid, however, the MSE value decreased due to the addition of the synergy factors, and the growth boundary was more closely approached. The proposed model of Augustin and Carlier was also able to reduce the MSE-value between predictions and experiments for the HLa data, but on the other hand the growth boundary was overestimated. For the other three acids, both synergy models lead to overestimation of the minimal growth boundaries and an increase in MSE values as compared to the gamma model.

Table 2. Singular models, describing the maximum specific growth rate (h^{-1}) as a function of pH, their fitting performance (indicated by the MSE value) and the optimal parameter estimates with standard deviations when fitted to the experimental data set obtained with *B. cereus* F4810/72

Model no.[a]	Model	Reference
1	$\mu_{max} = a^2 (pH - pH_{min})$	1
2	$\mu_{max} = a(pH - pH_{min})(pH - pH_{max})$	37
3	$\mu_{max} = a(pH - pH_{min})\{1 - e^{b(pH - pH_{max})}\}$	37
4	$\mu_{max} = [a(pH - pH_{min})\{1 - e^{b(pH - pH_{max})}\}]^2$	29
5	$\mu_{max} = a(1 - 10^{pH_{min} - pH})$	28
6	$\mu_{max} = a(1 - 10^{pH_{min} - pH})(1 - 10^{pH - pH_{max}})$	28
7	$\mu_{max} = \mu_{opt} \frac{(pH - pH_{max})(pH - pH_{min})^2}{(pH_{opt} - pH_{min})[(pH_{opt} - pH_{min})(pH - pH_{opt}) - (pH_{opt} - pH_{max})(pH_{opt} + pH_{min} - 2pH)]}$	32
8	$\mu_{max} = \mu_{opt} \frac{(pH - pH_{max})(pH - pH_{min})}{(pH - pH_{min})(pH - pH_{max}) - (pH - pH_{opt})^2}$	23, 31
9	$\mu_{max} = \mu_{opt} \frac{(pH - pH_{min})(pH_{max} - pH)}{(pH_{opt} - pH_{min})(pH_{max} - pH_{opt})}$	40
10	$\mu_{max} = \mu_{opt} \frac{(pH - pH_{min})(2pH_{opt} - pH_{min} - pH)}{(pH_{opt} - pH_{min})^2}$	40
11	$\mu_{max} = \mu_{opt} \exp\left[-\left(\frac{[H^+]}{10^{-a}}\right)^b\right]$	16

[a] Boldface indicates model selected for further analysis.

Table 2 - *Continued*

Model no.[a]	No. of parameters	MSE	μ_{opt} (SE)	a (SE)	b (SE)	pH_{min} (SE)	pH_{max} (SE)	pH_{opt} (SE)
1	2	0.0765		1.03 (0.007)		4.39 (0.020)		
2	3	0.0074		-0.52 (0.007)		4.72 (0.004)	9.02 (0.031)	
3	4	0.0075		79.73 (446.78)	0.01 (0.038)	4.71 (0.005)	9.00 (0.107)	
4	4	0.0257		152.59 (5381)	0.002 (0.060)	4.29 (0.027)	9.23 (0.172)	
5	2	0.0208	2.21 (0.009)			4.86 (0.003)		
6	3	0.0208	2.21 (0.013)			4.86 (0.00)	16.11 (4.2×10^6)	
7	4	0.0075	2.41 (0.007)			4.73 (27.384)	9.01 (0.033)	6.87 (0.015)
8	4	0.0023	2.49 (0.018)			4.79 (0.002)	19.16 (1.252)	8.00 (0.135)
9	4	0.0074	2.38 (71884)			4.72 (0.004)	9.02 (0.031)	7.10 (298016)
10	3	0.0074	2.41 (0.007)			4.72 (0.004)		6.87 (0.015)
11	3	0.0097	2.35 (0.010)	5.15 (0.004)	1.08 (0.016)			

[a] Boldface indicates model selected for further analysis.

Table 3. Singular models describing the effect of undissociated acid on the maximum specific growt rate (h^{-1}), fitting performance (indicated by MSE value), and optimal parameter estimates with their standard deviations when fitted to the experimental data set obtained with *B. cereus* F4810/72

Model no.[a]	Model	Reference	No. of parameters	Acids	MSE	MSE total, 4 acids
12	$\mu_{max} = a\left(1 - \frac{[HA]}{[HA]_{max}\left(1 + 10^{pH - pK_a}\right)}\right)$	28	2	Hac HLa HPr HFo	0.0732 0.0657 0.0579 0.0652	0.2620
13	$\mu_{max} = \mu_{opt}\left(1 - \sqrt{\frac{[HA]}{[HA]_{max}}}\right)$	20	2	Hac HLa HPr HFo	0.0028 0.0840 0.0040 0.0235	0.1143
14	$\mu_{max} = \mu_{opt}\left(\frac{a([HA]_{max} - [HA])}{[HA]_{max}(a - [HA])}\right)$	13	3	Hac HLa HPr HFo	0.0006 0.0058 0.0034 0.0212	0.0310
15	$\mu_{max} = \mu_{opt}\left(1 - \frac{[HA]}{[HA]_{max}}\right)^{\alpha}$	22	3	Hac HLa HPr HFo	0.0014 0.0066 0.0045 0.0036	0.0161
16	$\mu_{max} = \mu_{opt}\left(1 + \frac{a[HA]}{b + [HA]}\right)\left(1 - \frac{[HA]}{[HA]_{max}}\right)$	27	4	Hac HLa HPr HFo	0.0004 0.0050 0.0030 0.0035	0.0119
17	$\mu_{max} = \mu_{opt}\left(1 - \frac{[HA]}{[HA]_{max}}\right)$	11	2	Hac HLa HPr HFo	0.0083 0.0291 0.0175 0.0038	0.0587
18	$\mu_{max} = \mu_{opt}\left[1 - \left(\frac{[HA]}{[HA]_{max}}\right)^{\alpha}\right]$	24	3	Hac HLa HPr HFo	0.0014 0.0050 0.0035 0.0033	0.0132
19	$\mu_{max} = \mu_{opt}\exp(-a[HA])$	2	2	Hac HLa HPr HFo	0.0022 0.0803 0.0046 0.0219	0.1090
20	$\mu_{max} = \mu_{opt}\left(\frac{a}{a + [HA]}\right)$	27	2	Hac HLa HPr HFo	0.0179 0.1359 0.0173 0.0538	0.2249
21	$\mu_{max} = \mu_{opt}\left(\frac{a}{a + [HA]} - b[HA]\right)$	27	3	Hac HLa HPr HFo	0.0011 0.0638 0.0071 0.0506	0.1226
22	$\mu_{max} = \mu_{opt}\exp(-a([HA] - [HA]_{max}))$	39	3	Hac HLa HPr HFo	0.0003 0.0207 0.1280 0.0090	0.1580
23	$\mu_{max} = \mu_{opt}\exp\left[-\left(\frac{[HA]}{10^{-a}}\right)^{b}\right]$	16	3	Hac HLa HPr HFo	0.0019 0.0071 0.0044 0.0041	0.0175

[a] Boldface indicates model selected for further analysis.

Table 3 - *Continued*

Model no.[a]	μ_{opt} (SE)	$[HA]_{max}$ (SE)	*a* value (SE)	*b* value (SE)	*α* value (SE)
12		4.00 (1.139) 2.00 (4.370) 2.00 (0.517) 0.40 (1.052)	1.00 (0.021) 1.06 (0.032) 1.04 (0.030) 1.06 (0.029)		
13	1.62 (0.005) 1.91 (0.038) 1.48 (0.007) 1.73 (0.017)	8.24 (0.049) 3.89 (0.110) 8.89 (0.054) 1.02 (0.014)			
14	1.51 (0.003) 1.55 (0.009) 1.51 (0.007) 1.59 (0.017)	8.65 (0.051) 2.52 (0.006) 10.17 (0.128) 0.95 (0.015)	-4.93 (0.067) 3.56 (0.048) -3.32 (0.091) 19.73 (23.760)		
15	1.48 (0.004) 1.56 (0.010) 1.50 (0.008) 1.55 (0.007)	15.68 (0.693) 2.28 (0.007) 2.78×10^{8} (2.5×10^{8}) 0.77 (0.005)			4.24 (0.223) 0.34 (0.010) 9.40×10^{7} (2.5×10^{8}) 0.87 (0.017)
16	1.52 (0.003) 1.50 (0.011) 1.51 (0.007) 1.54 (0.008)	8.20 (0.037) 2.53 (0.007) 9.39 (0.097) 0.78 (0.006)	-0.70 (0.016) -2.38 (0.405) -0.70 (0.030) 67.38 (12797)	2.95 (0.112) -5.98 (0.756) 0.84 (0.084) 275.97 (52475)	
17	1.36 (0.006) 1.75 (0.020) 1.33 (0.014) 1.57 (0.006)	6.45 (0.050) 2.99 (0.035) 6.46 (0.087) 0.81 (0.003)			
18	1.54 (0.005) 1.49 (0.008) 1.51 (0.008) 1.53 (0.007)	7.46 (0.045) 2.58 (0.055) 4.59 (0.034) 0.79 (0.004)			0.61 (0.006) 2.54 (0.007) 0.44 (0.007) 1.16 (0.018)
19	1.52 (0.004) 1.79 (0.039) 1.50 (0.008) 1.66 (0.017)		0.32 (0.002) 0.59 (0.020) 0.34 (0.004) 2.37 (0.043)		
20	1.62 (0.015) 1.72 (0.056) 1.55 (0.017) 1.64 (0.029)		1.63 (0.044) 0.99 (0.076) 1.20 (0.037) 0.22 (0.010)		
21	1.53 (0.004) 1.69 (0.036) 1.53 (0.011) 1.63 (0.028)		2.80 (0.029) 3.13 (0.414) 1.75 (0.043) 0.24 (0.011)	0.03 (0.000) 0.12 (0.010) 0.01 (0.000) 0.01 (0.002)	
22	0.13 (3016) 0.95 1.48 (3.7×10^{6}) 0.37		0.31 (0.001) 0.25 (0.011) 0.07 (2.2×10^{6}) 1.96 (0.028)		
23	1.49 (0.005) 1.44 (0.009) 1.51 (0.009) 1.49 (0.007)		-0.50 (0.003) -0.32 (0.002) -0.47 (0.005) 0.30 (0.002)	1.08 (0.010) 4.67 (0.127) 0.98 (0.015) 2.16 (0.035)	

[a] Boldface indicates model selected for further analysis.

Table 4. MSE values for predictions obtained with the nonsynergistic gamma model, model of Le Marc *et al.*, and model of Augustin and Carlier for HAc, HLa, HPr, and HFo

Model ID.[a]	Acid	Model	MSE	Boundary pH
24				
A	HAc	$\mu_{max} = 2.42 \frac{(pH - 19.16)(pH - 4.79)}{(pH - 4.79)(pH - 19.16) - (pH - 8.00)^2} \left[1 - \left(\frac{[HA]}{7.46}\right)^{0.61}\right]$	0.0181	5.19
B	HAc	$\mu_{max} = 2.42 \frac{(pH - 19.16)(pH - 4.79)}{(pH - 4.79)(pH - 19.16) - (pH - 8.00)^2} \left[1 - \left(\frac{[HA]}{7.46}\right)^{0.61}\right] \xi(pH, [HA])$	0.0226	5.30
C	HAc	$\mu_{max} = 2.42 \frac{(pH - 19.16)(pH - pH_{min,new})}{(pH - pH_{min,new})(pH - 19.16) - (pH - 8.00)^2} \left[1 - \left(\frac{[HA]}{[HA]_{max,new}}\right)^{0.61}\right]$	0.0609	5.54
25				
A	HLa	$\mu_{max} = 2.42 \frac{(pH - 19.16)(pH - 4.79)}{(pH - 4.79)(pH - 19.16) - (pH - 8.00)^2} \left[1 - \left(\frac{[HA]}{2.58}\right)^{2.54}\right]$	0.0925	4.95
B	HLa	$\mu_{max} = 2.42 \frac{(pH - 19.16)(pH - 4.79)}{(pH - 4.79)(pH - 19.16) - (pH - 8.00)^2} \left[1 - \left(\frac{[HA]}{2.58}\right)^{2.54}\right] \xi(pH, [HA])$	0.0889	5.02
C	HLa	$\mu_{max} = 2.42 \frac{(pH - 19.16)(pH - pH_{min,new})}{(pH - pH_{min,new})(pH - 19.16) - (pH - 8.00)^2} \left[1 - \left(\frac{[HA]}{[HA]_{max,new}}\right)^{2.54}\right]$	0.0745	5.31
26				
A	HPr	$\mu_{max} = 2.42 \frac{(pH - 19.16)(pH - 4.79)}{(pH - 4.79)(pH - 19.16) - (pH - 8.00)^2} \left[1 - \left(\frac{[HA]}{4.59}\right)^{0.44}\right]$	0.0355	5.50
B	HPr	$\mu_{max} = 2.42 \frac{(pH - 19.16)(pH - 4.79)}{(pH - 4.79)(pH - 19.16) - (pH - 8.00)^2} \left[1 - \left(\frac{[HA]}{4.59}\right)^{0.44}\right] \xi(pH, [HA])$	0.0384	5.56
C	HPr	$\mu_{max} = 2.42 \frac{(pH - 19.16)(pH - pH_{min,new})}{(pH - pH_{min,new})(pH - 19.16) - (pH - 8.00)^2} \left[1 - \left(\frac{[HA]}{[HA]_{max,new}}\right)^{0.44}\right]$	0.0814	5.66
27				
A	HFo	$\mu_{max} = 2.42 \frac{(pH - 19.16)(pH - 4.79)}{(pH - 4.79)(pH - 19.16) - (pH - 8.00)^2} \left[1 - \left(\frac{[HA]}{0.79}\right)^{1.16}\right]$	0.0127	5.25
B	HFo	$\mu_{max} = 2.42 \frac{(pH - 19.16)(pH - 4.79)}{(pH - 4.79)(pH - 19.16) - (pH - 8.00)^2} \left[1 - \left(\frac{[HA]}{0.79}\right)^{1.16}\right] \xi(pH, [HA])$	0.0149	5.30
C	HFo	$\mu_{max} = 2.42 \frac{(pH - 19.16)(pH - pH_{min,new})}{(pH - pH_{min,new})(pH - 19.16) - (pH - 8.00)^2} \left[1 - \left(\frac{[HA]}{[HA]_{max,new}}\right)^{1.16}\right]$	0.0919	5.46

[a] The nonsynergistic gamma model (A), the model of Le Marc *et al.* (21) (B), and the model of Augustin and Carlier (C) (4,5) were used. MSE_{tot}: 0.1588 (A), 0.1648 (B), or 0.3087 (C).

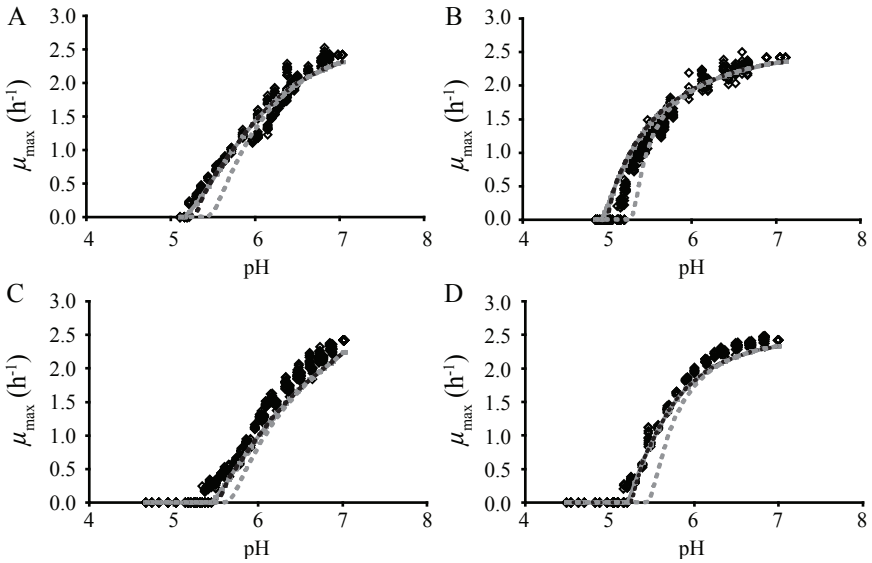

Figure 2. Experimental data (◇) and predictions using model 8 and model 18 for the combined effect of pH and undissociated acid concentration on μ_{max} without (solid gray line) and with (dashed black line) interaction factor and predictions using the model of Augustin (dashed gray line) for HAc (A), HLa (B), HPr (C) and HFo (D).

Discussion

Model criteria and selection

The model selection applied started by reviewing literature for pH models and undissociated acid models. This resulted in a selection of 11 pH models and 12 undissociated acid models. Few articles present an extended overview of available models (27, 35) and for this reason, this review and the selection procedure might be of value for predictive microbiology studies.

For all models, the parameters were standardized and all models were expressed in the form $\mu_{max} = \mu_{opt}\ \gamma(\text{pH})$ or $\mu_{max} = \mu_{opt}\ \gamma([\text{HA}])$. Also, the RRD models (model 11 and model 23) of Lambert and Bidlas (16) were expressed as such to be able to compare MSE values between experiments and to allow fitting performance to be expressed on the same scale.

Three selection criteria were proposed for model selection. First, MSE values should be below 0.01. This value was proposed on the basis of multiple visual inspections of the fitting performance of different models with respect to the experimental data.

Moreover, the MSE value of 0.01 allowed some difference between experiments and model fitting performance while significantly reducing the number of models to be considered in gamma hypothesis validation. Second, standard deviations for any parameter had to be smaller than the parameter estimates. A large standard deviation indicates that a large variation in the estimated parameter is possible, meaning that parameter estimates can be zero, which indicates overparameterization of the model. The third criterion was the inclusion of parameters without biological significance; this should be kept to a minimum. A set of criteria should be preferred over a single criterion since several aspects of model fit can be considered. The proposed criterion for the MSE value eliminated, for example linear models, like model 1, which did not fit the experimental data well, whereas the model would not be eliminated based only on the standard deviations of parameter estimates.

The criteria were further evaluated for relevance by comparing the undissociated acid concentration selected model 18 (MSE_{tot} = 0.0132) with three parameters, to model 17 (MSE_{tot} = 0.0587) with two parameters, which just exceeded the sum total MSE value of 0.04. Comparison by an *F* test showed that for all four acids model 17 was not to be selected as fitting best, meaning that the proposed criteria (MSE = 0.01) are adequate selection criteria and do not need to be less stringent. Concerning the criterion that standard deviations should not exceed parameter estimates, this was tested by comparing model 18 to model 16, with four parameters, where the standard deviation exceeded the parameter estimate for model 16. Model 16 was found to not be acceptable for HAc and HPr, while it was acceptable for HLa and HFo. However, in the case of HFo, the standard deviations exceeded the parameter estimates and two parameters without evident biological significance are included. Consequently, it was concluded that model 16 was not the best choice. The third criterion, that parameters preferably have biological meaning, is in principle met for the chosen model 8. However, although the maximum pH parameter (pH_{max}) has biological meaning, the estimated value is unrealistic, caused by the fact that no experiments were performed at pH values above 7.5. Fixing pH_{max} in model 8 at a pH of 11 resulted in a fit of the data with an MSE value of 0.0033. Exclusion of this parameter by choosing model 10 with a slightly higher MSE value also solved the problem of an unrealistic pH_{max}, but model 8 still had better performance, as shown in Results. Apparently the pH_{max} value is a valuable shape parameter, necessary to make a good fit of the data.

Undoubtedly, proper and thorough selection of models for describing combined pH and undissociated acid effects needs to rely on selection of the models that are best able to accurately describe the individual hurdles correctly or most optimally, since the model choice may well impact on conclusions drawn about possible synergy between the hurdles.

Evaluation of the gamma hypothesis validity

To falsify the hypothesis that no interaction between the two hurdles occurs at the growth boundary, as suggested by Bidlas and Lambert (7), two models assuming synergy between factors were compared to the newly constructed gamma models for the four acids combined with pH effect. Considering the acids HAc, HPr, and HFo, the synergy models of Le Marc *et al*. and Augustin and Carlier did not reduce the MSE values, so the predictions were not better than those obtained with the gamma model without an interaction factor. For HPr, all three models underestimated growth, suggesting that pH and the concentration of undissociated propionic acid exhibit a slight antagonistic effect when applied in combination. The growth boundary, however, was predicted relatively well by the gamma model, and the inclusion of a synergy factor did not improve the quality of the prediction. It has to be noted that both synergy models are developed to study growth kinetics of *Listeria*. The use of the synergy models to study growth kinetics of *B. cereus* might therefore lead to nonoptimal predictions of growth behavior.

For the lactic acid data set as shown in Figure 2B, the gamma model performed less well than for the other acids, mainly because the growth boundary was not properly estimated. New parameter estimates for the effect of undissociated lactic acid were made based on a data set with different concentrations of undissociated acid in a buffered BHI solution at pH 5.7 (data not shown). These new parameter estimates (and standard deviations) (μ_{opt} = 1.7 [0.011], $[HA]_{max}$ = 2.57 [0.016], α = 2.21 [0.068] were incorporated in the gamma model, and a new prediction of the HLa experiment for the two hurdles was made. The MSE value between the prediction and the experiment was 0.0790, somewhat lower than that for model performance using the original parameter estimates at pH 5.5 (MSE = 0.0925), but the growth boundary was still underestimated by 0.2 pH unit with the new parameter estimates. The observed improvement in model performance as judged from the decreased MSE, may be due mainly to better predictability of experimental data generated at somewhat higher pH values rather than by a shift in the growth boundary.

For lactic acid, the use of model 16 in the combined gamma model (which had been rejected based on an *F* test), did not result in a better estimate of the growth boundary (MSE = 0.1367) either. As a consequence, it cannot be ruled out that for HLa, interaction between hurdles might play a role close to the growth boundary. For the HLa data, the synergy models gave slightly lower MSE values than the non-interaction models, but visual inspection of the relevant pH-growth rate curves showed that the growth boundary was not predicted correctly. The model of Augustin and Carlier predicted more interaction than did the model of Le Marc *et al*.

According to Augustin and Carlier (5), their interaction model improves the fail-safe growth predicted by 1.4% and the fail-dangerous no-growth by 9%. There may be more than one reason why different studies draw different conclusions regarding synergy. While the current study would not support a synergistic effect with the factors investigated, Augustin and Carlier (4) set up a model to specifically take into account interactive effects, based on a large quantity of growth data retrieved from the literature (4). It may be that due to the particular origin of their data set, in which there is more likely spreading of the data, especially around the growth boundary, the results are not comparable to the data set generated in the investigation described here. Conceivably, in a situation of data spreading, assuming interaction between factors and use of a synergistic model may improve the prediction of growth data and of the growth boundary.

The possibility of predicting growth behavior of microorganisms with multiple inhibitory factors by the use of models without interaction was found to be applicable for several microorganisms for different combined hurdles (16, 17, 26, 34, 38). Other studies concluded there is indeed synergy when using a mixture of nisin and lactates, salts, or lysozyme and nisin for different bacteria and yeast (3, 9, 25). This synergy is supposed to occur due to metal cations, which have an effect on intracellular ATP levels, which results in higher sensitivity of cells to other hurdles (25). Importantly, as stressed by Lambert and Lambert (18), when investigating the effect of combinations of antimicrobial factors on microorganisms, it is important to understand whether or not the individual factors exert the same inhibitory impact at the same concentration, i.e., whether the factors have an identical response. Mixing antimicrobials with different dose responses relationships may result in apparently synergistic impacts without actually being based on synergistic interactions. Next to insight into the response effects of individual inhibitory factors that are to be applied in combination, it is important to understand the mechanisms of action

of the individual factors (6). Lambert and Stratford (15) studied mechanisms of microbial inhibition and responses for weak-acid preservatives and concluded that inhibition depends more on the degree to which individual preservatives are concentrated within the cell rather than on the undissociated acid concentration. Physiological experiments exploring the mechanism of action of HLa on the *B. cereus* strain investigated in our current study may provide insight into why, with this acid only there was a notable difference between predictions and experimental data, in particular an overestimation of the growth boundary. As suggested in the literature and tested for *Listeria monocytogenes*, this synergistic effect for combinations including lactate might be due to metal cations, which have an effect on intracellular ATP levels, which results in higher sensitivity of cells to other hurdles (25). It is interesting to investigate if this hypothesis is also valid for *B. cereus*, which might explain why, with this acid only, there is an overestimation of the growth boundary.

In conclusion, the nonsynergistic gamma model built in this study with the two best-fitting models for individual factors was sufficiently capable of describing the combined effect of these factors, pH and undissociated acid concentration, on the growth rate of the test microorganism. Synergy between these two factors thus could not be proven, except maybe for the use of lactic acid. This investigation also established an extensive overview of models for predicting effects of either pH or undissociated acid on growth of microorganisms as reported in the literature. The model selection criteria used were found to be practical to identify those models that best fit the data sets. For describing the effects of pH and of the undissociated acid concentration, the models of Rosso *et al*. and of Luong, respectively (24, 31) were found to be the best-fitting models. The model of Luong could be used for all four acids investigated (i.e., acetic, lactic, propionic, and formic) regardless of the shape of the undissociated acid curve. When using these models in a gamma model for predicting the combined effect of pH and the undissociated acid concentration, it was found to be unnecessary to include a synergy factor in the model, since in three out of four cases, addition of this factor to the nonsynergistic model did not reduce MSE values between predictions and experiments. For lactic acid, the MSE value was reduced by the use of a synergistic model, but the growth boundary was still not estimated correctly. In general, both synergy models that were investigated were found to shift the growth boundary to a higher pH due to assumed interaction between the factors. Users of predictive models, notably those in the food industry that use them

in establishing safe product and process designs, should be cautioned against the use of synergistic models in situations where there is no synergy. Evidently, when models erroneously predict an upward shift of a growth boundary to a higher pH, for instance, their use may possibly lead to unsafe food designs or other situations compromising food safety.

Acknowledgments

This work was financially supported by Nestlé Research Centre, Lausanne, Switzerland. Fan Wang and Linlin Fan are gratefully acknowledged for skillful experimental work during this research.

References

1. **Adams, M. R., C. L. Little, and M. C. Easter.** 1991. Modelling the effect of pH, acidulant and temperature on the growth rate of *Yersinia enterocolitica*. J. Appl. Bacteriol. 71:65-71.

2. **Aiba, S., M. Shoda, and M. Nagatani.** 1968. Kinetics of product inhibition in alcohol fermentation. Biotechnol. Bioeng. 10:845-864.

3. **Almagro, A., C. Prista, S. Castro, C. Quintas, A. Madeira-Lopes, J. Ramos, and M. C. Loureiro-Dias.** 2000. Effects of salts on *Debaryomyces hansenii* and *Saccharomyces cerevisiae* under stress conditions. Int. J. Food Microbiol. 56:191-197.

4. **Augustin, J.-C., and V. Carlier.** 2000. Mathematical modelling of the growth rate and lag time for *Listeria monocytogenes*. Int. J. Food Microbiol. 56:29-51.

5. **Augustin, J.-C., and V. Carlier.** 2000. Modelling the growth rate of *Listeria monocytogenes* with a multiplicative type model including interactions between environmental factors. Int. J. Food Microbiol. 56:53-70.

6. **Berenbaum, M. C.** 1989. What is synergy? Pharmacol. Rev. 41:93-141.

7. **Bidlas, E., and R. J. W. Lambert.** 2008. Quantification of hurdles: Predicting the combination of effects - Interaction vs. non-interaction. Int. J. Food Microbiol. 128:78-88.

8. **Biesta-Peters, E. G., M. W. Reij, H. Joosten, L. G. M. Gorris, and M. H. Zwietering.** 2010. Comparison of two optical density methods and a plate count method for estimation of growth parameters of *Bacillus cereus*. Appl. Environ. Microbiol. 76:1399-1405.

9. **Chung, W., and R. E. W. Hancock.** 2000. Action of lysozyme and nisin mixtures

against lactic acid bacteria. Int. J. Food Microbiol. 60:25-32.

10. **Den Besten, H. M. W., M. Mataragas, R. Moezelaar, T. Abee, and M. H. Zwietering.** 2006. Quantification of the effects of salt stress and physiological state on thermotolerance of *Bacillus cereus* ATCC 10987 and ATCC 14579. Appl. Environ. Microbiol. 72:5884-5894.

11. **Ghose, T. K., and R. D. Tyagi.** 1979. Rapid ethanol fermentation of cellulose hydrolysate. I. Batch versus continuous systems. Biotechnol. Bioeng. 21:1387-1400.

12. **Gould, G. W.** 1996. Methods for preservation and extension of shelf life. Int. J. Food Microbiol. 33:51-64.

13. **Houtsma, P. C., B. J. M. Kusters, J. C. de Wit, F. M. Rombouts, and M. H. Zwietering.** 1994. Modelling growth rates of *Listeria innocua* as a function of lactate concentration. Int. J. Food Microbiol. 24:113-123.

14. **Kotiranta, A., K. Lounatmaa, and M. Haapasalo.** 2000. Epidemiology and pathogenesis of *Bacillus cereus* infections. Microb. Infect. 2:189-198.

15. **Lambert, R. J., and M. Stratford.** 1999. Weak-acid preservatives: modelling microbial inhibition and response. J. Appl. Microbiol. 86:157-164.

16. **Lambert, R. J. W., and E. Bidlas.** 2007. An investigation of the Gamma hypothesis: A predictive modelling study of the effect of combined inhibitors (salt, pH and weak acids) on the growth of *Aeromonas hydrophila*. Int. J. Food Microbiol. 115:12-28.

17. **Lambert, R. J. W., and E. Bidlas.** 2007. A study of the Gamma hypothesis: Predictive modelling of the growth and inhibition of *Enterobacter sakazakii*. Int. J. Food Microbiol. 115:204-213.

18. **Lambert, R. J. W., and R. Lambert.** 2003. A model for the efficacy of combined inhibitors. J. Appl. Microbiol. 95:734-743.

19. **Larsen, H. D., and K. Jørgensen.** 1999. Growth of *Bacillus cereus* in pasteurized milk products. Int. J. Food Microbiol. 46:173-176.

20. **Leistner, L., and L. G. M. Gorris.** 1995. Food preservation by hurdle technology. Trends Food Sci. Technol. 6:41-46.

21. **Le Marc, Y., V. Huchet, C. M. Bourgeois, J. P. Guyonnet, P. Mafart, and D. Thuault.** 2002. Modelling the growth kinetics of *Listeria* as a function of temperature, pH and organic acid concentration. Int. J. Food Microbiol. 73:219-237.

22. **Levenspiel, O.** 1980. The Monod equation: a revisit and a generalization to product inhibition situations. Biotechnol. Bioeng. 22:1671-1688.

23. **Lobry, J. R., L. Rosso, and J. P. Flandrois.** 1991. A FORTRAN subroutine for the

determination of parameter confidence limits in non-linear models. Binary 3:86-93.

24. **Luong, J. H. T.** 1985. Kinetics of ethanol inhibition in alcohol fermentation. Biotechnol. Bioeng. 27:280-285.

25. **McEntire, J. C., T. J. Montville, and M. L. Chikindas.** 2003. Synergy between nisin and select lactates against *Listeria monocytogenes* is due to the metal cations. J. Food Prot. 66:1631-1636.

26. **McMeekin, T. A., K. Presser, D. A. Ratkowsky, T. Ross, M. Salter, and S. Tienungoon.** 2000. Quantifying the hurdle concept by modelling the bacterial growth/no growth interface. Int. J. Food Microbiol. 55:93-98.

27. **Pasos, F. V., H. P. Fleming, D. F. Ollis, D. F. Hassan, and R. M. Felder.** 1993. Modeling the specific growth rate of *Lactobacillus plantarum* in cucumber extract. Appl. Microbiol. Biotechnol. 40:143-150.

28. **Presser, K. A., D. A. Ratkowsky, and T. Ross.** 1997. Modelling the growth rate of *Escherichia coli* as a function of pH and lactic acid concentration. Appl. Environ. Microbiol. 63:2355-2360.

29. **Ratkowsky, D. A., R. K. Lowry, T. A. McMeekin, A. N. Stokes, and R. E. Chandler.** 1983. Model for bacterial culture growth rate throughout the entire biokinetic temperature range. J. Bacteriol. 154:1222-1226.

30. **Rödel, W., and R. Scheuer.** 2007. Recent results on the hurdle technology - measuring of combined hurdles. Mitteilungsblatt der Fleischforschung Kulmbach 46:3-10.

31. **Rosso, L., J. R. Lobry, S. Bajard, and J. P. Flandrois.** 1995. Convenient model to describe the combined effects of temperature and pH on microbial growth. Appl. Environ. Microbiol. 61:610-616.

32. **Rosso, L., J. R. Lobry, and J. P. Flandrois.** 1993. An unexpected correlation between cardinal temperatures of microbial growth highlighted by a new model. J. Theor. Biol. 162:447-463.

33. **Taylor, A. J., and R. J. Gilbert.** 1975. *Bacillus cereus* food poisoning: a provisional serotyping scheme. J. Med. Microbiol. 8:543-550.

34. **Te Giffel, M. C., and M. H. Zwietering.** 1999. Validation of predictive models describing the growth of *Listeria monocytogenes*. Int. J. Food Microbiol. 46:135-149.

35. **Vereecken, K. M., F. Devlieghere, A. Bockstaele, J. Debevere, and J. F. van Impe.** 2003. A model for lactic acid-induced inhibition of *Yersinia enterocolitica* in mono- and coculture with *Lactobacillus sakei*. Food Microbiol. 20:701-713.

36. **Wijnands, L. M., J. B. Dufrenne, and F. M. van Leusden.** 2005. *Bacillus cereus:* characteristics, behaviour in the gastro-intestinal tract, and interaction with Caco-2 cells. RIVM report 250912003.

37. **Wijtzes, T., J. C. de Wit, J. H. J. Huis in 't Veld, K. van 't Riet, and M. H. Zwietering.** 1995. Modelling bacterial growth of *Lactobacillus curvatus* as a function of acidity and temperature. Appl. Environ. Microbiol. 61:2533-2539.

38. **Wijtzes, T., F. M. Rombouts, M. L. T. Kant-Muermans, K. van 't Riet, and M. H. Zwietering.** 2001. Development and validation of a combined temperature, water activity, pH model for bacterial growth rate of *Lactobacillus curvatus*. Int. J. Food Microbiol. 63:57-64.

39. **Yeh, P. L.-H., R. K. Bajpai, and E. L. Iannotti.** 1991. An improved kinetic model for lactic acid fermentation. J. Ferment. Bioeng. 71:75-77.

40. **Zwietering, M. H., J. C. de Wit, and S. Notermans.** 1996. Application of predictive microbiology to estimate the numbers of *Bacillus cereus* in pasteurised milk at the point of consumption. Int. J. Food Microbiol. 30:55-70.

41. **Zwietering, M. H., T. Wijtzes, J. C. de Wit, and K. van 't Riet.** 1992. A decision support system for prediction of the microbial spoilage in foods. J. Food Prot. 55:973-979.

Chapter 5

Comparing non-synergy gamma models and interaction models to predict growth of emetic *Bacillus cereus* for combinations of pH and water activity lowering solutes

Elisabeth G. Biesta-Peters, Martine W. Reij, Marcel H. Zwietering, Leon G.M. Gorris

Published in Applied and Environmental Microbiology (2011), Vol. 77, No. 16

5

Abstract

This research aims to test the absence (gamma hypothesis) or occurrence of synergy between two growth limiting factors, i.e. pH and a_w*, using a systematic approach for model selection. In this approach, pre-set criteria were used to evaluate the performance of models. Such a systematic approach is required to be confident in the correctness of the individual components of the combined (synergy) models. With* Bacillus cereus *F4810/72 as the test organism, estimated growth boundaries for the* a_w *lowering solutes NaCl, KCl, and glucose were 1.13 M, 1.13 M, and 1.68 M, respectively. The accompanying* a_w*-values were 0.954, 0.956, and 0.961, indicating that equal* a_w*-values result in similar effects on growth. Following a structured procedure and pre-set criteria, out of 12 models evaluated the best model was selected and combined with the previously selected pH model into a gamma model and into two synergy models. None of the three models was able to describe the combined pH and* a_w *conditions sufficiently well to satisfy the pre-set criteria. The best matches between predicted and experimental data were obtained with the gamma model, followed by the Le Marc synergy model. No combination of models could be found that was able to predict the impact of both individual and combined hurdles correctly. Consequently, in this case we could not prove the existence of synergy, nor falsify the gamma hypothesis.*

Introduction

The microorganism *Bacillus cereus* is associated with food spoilage as well as food poisoning (1, 34). The spores formed by *B. cereus* generally will resist treatments used to prolong the shelf life of food. Viable spores present in a food product may germinate and the vegetative cells can subsequently grow if conditions are favorable; leading to spoilage of the food product (9, 14, 18). Several growth limiting factors, collectively referred to as hurdles, can be used to ensure food stability and safety. Examples of such hurdles are low pH, low water activity (a_w) and low temperature (12). Combining hurdles to achieve food stability and safety, known as hurdle technology, can be used to achieve an overall level of protection in food while minimizing detrimental impacts on food quality (20).

Improved quantification of the combined impact of hurdles on growth of microorganisms is an ongoing endeavor, but there are different views of how antimicrobial factors combine. One view is that there are interactive effects between hurdles. When combinations of hurdles are used they might give a significantly greater protection than expected on the basis of the application of the individual hurdles, so called synergy (20). The other view follows the gamma hypothesis (39) in which there is no synergy, but inhibitory environmental factors combine in a multiplicative manner to produce the observed overall microbial inhibition. Evidently, it is important in the selection of hurdles to know whether either the gamma hypothesis is valid or synergy occurs between factors. Assuming synergy where this does not occur can lead to wrong estimations of growth boundaries, which in turn can lead to unsafe food products.

Our previous study of testing the combined effect of pH and undissociated acid concentration did not confirm that there were synergistic effects between these two hurdles, which by definition are closely related (6). This finding was in line with several other studies (15, 16, 24, 36, 38). However, there have been as well studies showing that interaction occurs when various hurdles are combined, and for these interactions gamma models including a synergy factor were developed (4, 19, 29).

It is evident that quite different conclusions have been drawn in the studies in the field of quantification of microbial growth impact of combined hurdles. The underlying variation in test organisms and preservative factors as well as the different experimental approaches employed may have well contributed to the different conclusions. In our previous study we advocated a systematic approach for model selection. This approach was based on using a set of predetermined criteria to more objectively judge the

performance of individual models. In the current study, we used this systematic approach for another combination of hurdles, i.e. pH and a_w lowering solutes. The validity of the gamma hypothesis for the hurdles pH and a_w lowering solutes was judged by comparing the predictive performance of the newly constructed gamma model with two gamma models including a synergy factor reported in literature.

Material and methods

Bacterial strain, pre culturing conditions and growth rate determination

B. cereus F4810/72, an emetic toxin producer, was originally isolated from human vomit (35). A pre-culture of the strain was prepared by adding a loop full from a frozen (-80°C) culture of microorganisms to a 500 ml Erlenmeyer flask containing 100 ml Brain Heart Infusion (BHI) broth (Becton Dickinson and Company; Le Pont de Claix, France). The flask was incubated for 16 h at 30°C while shaking at 200 rpm , this way affording an overnight culture of approximately 10^9 cells/ml, which was used for further experiments.

The maximum specific growth rate for the different test conditions, μ_{max} (h^{-1}), was determined using the relative rate to detection (RRD) method by measuring time to detection (TTD) (6, 7) using the Bioscreen C (Oy Growth Curves AB Ltd, Helsinki, Finland).

Effect of pH, a_w lowering solutes, and combinations of both on μ_{max}

The experiments were divided into three groups: 1) testing the pH effect (tested in our previous research (6)), 2) testing the effect of different concentrations of selected a_w lowering solutes, and 3) testing the combined effect of pH and different concentrations of selected a_w lowering solutes. The solutes tested for the a_w effect were sodium chloride (NaCl, VWR International, Leuven, Belgium), potassium chloride (KCl, Sigma-Aldrich Chemie GmbH, Steinheim, Germany) and glucose (Merck KGaA, Darmstad, Germany).

The data for the pH experiments (group 1) were copied from our previous research. For the experiments of group 2 and 3, the selected a_w lowering solute was added in the desired amount to the BHI broth, whereupon the bottles were autoclaved. For the experiments of group 3 the pH was subsequently adjusted to the desired value (being either pH 7, 6.5, 6, 5.5 or 5) after autoclaving, and the broth was filter sterilized thereafter. For every individual test condition dilution tubes of the overnight culture were prepared with the adjusted corresponding broths, and the overnight bacterial suspension was diluted aiming at an initial cell concentration of approximately 10^4 cfu/ml. The

content of the tube of pH 7 without additional solute was spiral plated on BHI agar plates for determination of the exact start level of microorganisms.

Two honeycomb wells plates were filled per experiment, as previously described (7), and the experiment was repeated at least once. The honeycomb plates were incubated in a Bioscreen C at 30°C for three days while continuously shaking at the medium setting. The optical density at 600 nm (OD_{600}) was measured every ten minutes. The OD_{600} data obtained from the Bioscreen were imported in Microsoft Excel for data capturing. Wells with an initial OD_{600} above 0.2 (<1% of all wells measured), were removed from the data set as they were likely to have an, incidental, too high inoculum level. For all relevant data series, the time to detection (TTD), defined as the time (h) to reach OD_{600} 0.2, was determined. For wells not reaching OD_{600} 0.2 within the timeframe of the experiment, viability of bacteria was determined and if no viable bacteria were detected, μ_{max} was set to 0 h^{-1}. In case viable bacteria were detected the data point was removed from the data set, since no μ_{max} was determined but μ_{max} could also not be considered 0 h^{-1}.

The a_w experiments of group 2 were repeated once and the pH experiments of group 1 and combined pH and a_w experiments of group 3 were repeated twice.

The TTD determined for every test condition (TTD_i) was related to the TTD at optimal condition (TTD_{opt}), with TTD_{opt} being pH 7 with no additional a_w lowering solutes The specific growth rate ($\mu_{max,i}$) was calculated according to Equation 1.

$$\mu_{\max,i} = \mu_{opt}\ RRD_i = \mu_{opt}\ \frac{TTD_{opt}}{TTD_i} \quad (1)$$

The μ_{opt} value was estimated independently by plate counting and subsequent fitting of the Gompertz model to the counts (7). In assessing TTD_{opt} and TTD_i for use in Equation 2, care was taken to always start with equal inoculum levels. The obtained μ_{max} values were studied in more detail and in case outliers in replicate experiments were observed (e.g. one replicate showed no growth while the others showed considerable growth) these were evaluated based on criteria as previously described (6), and if not applying with the criteria the points were removed from the dataset.

To assess whether an incubation time of three days would be long enough to detect all possible growth in the wells, inoculated incubation experiments were conducted under near growth boundary conditions. BHI broths adapted to pH 6 with

additional NaCl in the range of 0.8 to 1.3 M or additional glucose in the range of 1.5 to 2.2 M were selected for this experiment. The cultures, with an initial cell level of 10^4 cells/ml, were incubated at 30°C while shaking at 200 rpm for 40 days. Growth of cells was determined by visually inspecting the turbidity of the broth.

The water activity of BHI with additional a_w lowering solute was measured using a water activity measuring device (Labmaster a_w, Novasina, Lachen, Switzerland). The samples were pre-warmed to 30°C prior to measuring, and also measured at 30°C, the same temperature as used for the growth experiments. The a_w-value was determined in triplicate.

Model selection and performance

Three criteria were used to select the best fitting models: 1) the Mean Square Error (MSE) value for the model fit should be below 0.01, ensuring a high level of fit, 2) the standard deviations for individual model parameters should be smaller than the parameter estimates themselves, since standard deviations greater than the respective parameter estimate indicate large variation, and 3) the model parameters should preferably have biological significance or be interpretable.

Secondary models for growth rate, which actually included or could be amended to include a pH term, were previously selected from literature (6). Equation 2 has been proven to be the best fitting model to describe the pH effect on μ_{max} and to predict gamma factors.

$$\mu_{max} = \mu_{opt} \frac{(pH - pH_{max})(pH - pH_{min})}{(pH - pH_{min})(pH - pH_{max}) - (pH - pH_{opt})^2} \quad (2)$$

Where μ_{opt} is the maximum specific growth rate under optimal conditions, pH_{max} is the maximum pH just not allowing growth, pH_{min} is the minimum pH just not allowing growth and pH_{opt} is the optimum pH for growth.

Secondary models for growth rate, which actually included or could be amended to include a term for a_w lowering solute concentration, were selected from literature and summarized in Table 1. The names of the parameters of all models were standardized to improve transparency and comparability throughout this research, and the models were made relative, if possible, and converted to a gamma model. All outcomes of the

models were expressed as μ_{max} values. Originally a_w-based models were transferred to solute concentration models, which was expected to give equal results since a_w and solute concentration were linearly related in the range tested (8). Whether this transfer was valid was assessed by testing model 1 of Table 1 both as an a_w model and as a concentration model. This was done by transferring the concentration data to a_w data using the linear transformation as proposed by Buchanan and Bagi (8).

The solute models were fitted to the μ_{max} data of group 2. Model performance (MSE-values) and parameter estimates are included in Table 1. The model selected on the basis of the three criteria stated above was tested against the best performing model with one parameter less, using an *F* test to evaluate whether the reduction of one parameter was still statistically acceptable (11). The *f* value was tested against the 95% confidence *F* table value ($F_{\infty}^{1} = 3.84$). If the *f* value was smaller than the *F* table value, the *F* test was accepted and the model with the smallest number of parameters was accepted.

Evaluating the gamma hypothesis

The selected models for pH and solute concentration were combined in a gamma model according to Equation 3 (39):

$$\mu_{max} = \mu_{opt}\ \gamma(\mathrm{pH})\ \gamma([\mathrm{solute}]) \quad (3A)$$

$$\text{with} \quad \gamma = \frac{\mu_{max}(\mathrm{pH},[\mathrm{solute}])}{\mu_{opt}(7,0)} \quad (3B)$$

Where μ_{max} is the maximum specific growth rate at the tested condition and μ_{opt} is the maximum specific growth rate as determined by plate count (2.42 h^{-1}) in medium of pH 7 when no a_w lowering solute is present. Parameter estimates derived by fitting single models were incorporated into the gamma model and predictions about the combined effect were made. These predictions were compared to the experimental data of group 3, which included both acid effects and a_w lowering solute effects. The differences between predictions and experimental data were expressed as MSE-values.

Two gamma models including a synergy factor from literature were compared with the newly composed gamma models combining pH and a_w lowering solute concentration. The first synergy model was that described by Le Marc *et al*. (19) (Equation 4).

$$\mu_{max} = \mu_{opt}\,\gamma(\mathrm{pH})\,\gamma([\mathrm{solute}])\,\xi(\mathrm{pH},[\mathrm{solute}]) \quad (4)$$

In which ξ is the synergy factor, calculated according to the model of Le Marc *et al*. (19). The second synergy model was that of Augustin and Carlier (3, 4). This model does not include a synergy factor but the different inhibitory factors were corrected independently for synergy by estimating new minimal growth values, which were then used in the non-synergistic gamma model according to Equation 5 A, B and C.

$$\mu_{max} = \mu_{opt}\,\gamma_{new}(\mathrm{pH})\,\gamma_{new}([\mathrm{solute}]) \quad (5A)$$

$$\text{with} \quad \mathrm{pH}_{min,new} = \mathrm{pH}_{opt,fit} - (\mathrm{pH}_{opt,fit} - \mathrm{pH}_{min,fit})\left(1 - \frac{[\mathrm{solute}]}{[\mathrm{solute}]_{max,fit}}\right)^{1/3} \quad (5B)$$

$$\text{and} \quad [\mathrm{solute}]_{max,new} = [\mathrm{solute}]_{max}\left(1 - \left(\frac{\mathrm{pH}_{opt,fit} - \mathrm{pH}}{\mathrm{pH}_{opt,fit} - \mathrm{pH}_{min,fit}}\right)^3\right) \quad (5C)$$

Apart from the MSE-values determined also the bias and accuracy factors of models were determined, which can be used as well for performance evaluation of predictive models (25, 30).

Results

Effect of a_w *lowering solute concentrations on* μ_{max} *and growth boundary*

The effects of the concentration of a_w lowering solutes NaCl, KCl, and glucose on μ_{max} and growth boundary are shown in Figure 1. The increase of solute concentration resulted in a decrease of the growth rate. The visually determined boundaries were 1.2 M, 1.2 M, and 1.7 M of solute for NaCl, KCl, and glucose respectively.

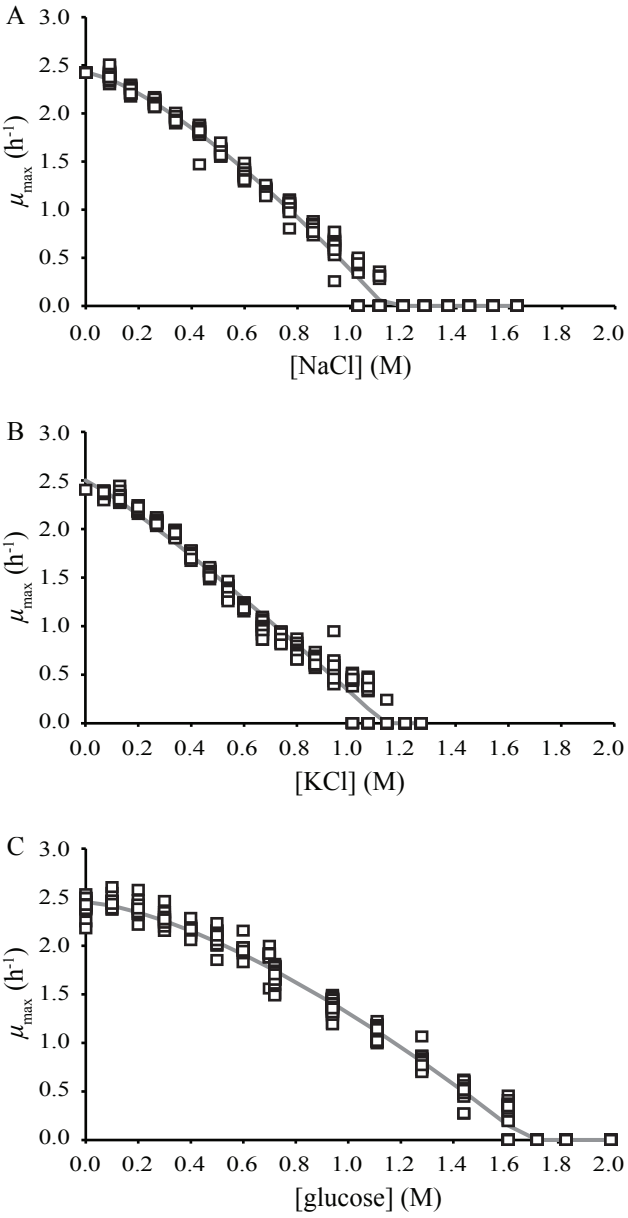

Figure 1. Maximum specific growth rate of emetic *B. cereus* as a function of a_w lowering solute concentration for NaCl (A), KCl (B), and glucose (C); □ represent experimental data and the solid gray lines show the fit of the most optimal solute concentration model (Model 9, see main text) to the data-sets.

Selection of the best-fitting model to describe growth in the presence of* a_w *lowering solutes

Twelve a_w lowering solute models (Table 1) were fitted to the growth rate curves of *B. cereus* F4810/72 cultured in BHI with various concentrations of NaCl, KCl or glucose. Table 1 reports the fitting performance of all models by means of MSE-values and their standard deviations. Fitting model 1 to the NaCl data resulted in an MSE-value of 0.0124. When this model was fitted as an a_w-based model to the a_w data of NaCl, the MSE-value was almost identical at 0.0125. Identical results were also obtained when fitting model 1 as solute concentration model and as a_w model to the KCl and glucose data. It is therefore considered valid to transfer the a_w models to concentration models, since a linear relationship between a_w-values and solute concentrations appears to be present (8).

Based on the criterion that the MSE-value between the datapoints and the fit should be below 0.01 for every solute tested, only model 9 (with three parameters) remained for further analysis. Using a slightly different approach, in which the MSE-value selection criterion was not taken as the first step, the best fitting model was assessed based firstly on the criterion that the standard deviation should not exceed the parameter estimate. Nine models were identified as meeting the criterion, i.e. model 1, 2, 3, 4, 6, 8, 9, 10, and 11. Model 9 with the lowest MSE value was compared to models 1, 4, 10 and 11 with less parameters than model 9, using an *F* test to see if the difference in MSE-value between each of the four models individually and model 9 was significant. The *f* test values ranged between 43 and 12562 (data not shown), all considerably exceeding the *F* table value, which indicated significant improvement of model 9 with three parameters over any of the two parameter models. Therefore, also following this approach, model 9 with three parameters was considered the best fitting model.

The growth boundaries were estimated using model 9. They were found to be 1.13 M, 1.13 and 1.68 M for NaCl, KCl, and glucose, respectively. The a_w-values determined experimentally (n=3) for the three solutes were 0.954 (±0.001), 0.956 (±0.001), and 0.961 (±0.000), respectively. The a_w-value of 1.13M glucose in BHI had been separately determined to be 0.972 (0.001) (n=3).

Table 1. Singular models describing the effect of a_w lowering solutes [*s*] on the maximum specific growth rate (h^{-1}), the fitting performance (indicated by the MSE-value), and optimal parameter estimates with standard deviations when fitted to the experimental data set obtained with *B. cereus* F4810/72

Model no.[1]	Model	Ref.	No. of parameters	Solutes	MSE
1	$\mu_{max} = \mu_{opt}\left(\frac{[s]_{max} - [s]}{[s]_{max}}\right)$	28	2	NaCl KCl glucose	0.0124 0.0101 0.0202
2	$\mu_{max} = \mu_{opt}\left(\frac{([s]_{max} - [s])^a \ ([s]_{min} - [s])}{([s]_{max} - [s]_{opt})^{a-1}\{([s]_{max} - [s]_{opt})([s]_{opt} - [s]) + ([s]_{min} - [s]_{opt})[(a-1)[s]_{opt} + [s]_{max} - a[s]]\}}\right)$ [2] $[s]_{min} = -0.322$ [3] $a = 2$	32	3	NaCl KCl glucose	0.0120 0.0088 0.0136
3	$\mu_{max} = a + b\sqrt{[s]} + c[s]$	10	3	NaCl KCl glucose	0.0468 0.0320 0.0518
4	$\mu_{max} = \mu_{opt}\left(1 - \sqrt{\frac{[s]}{[s]_{max}}}\right)$	19	2	NaCl KCl glucose	0.0791 0.0690 0.1256
5	$\mu_{max} = \mu_{opt}\left(\frac{a([s]_{max} - [s])}{[s]_{max}(a - [s])}\right)$	13	3	NaCl KCl glucose	0.0125 0.0102 0.0206
6	$\mu_{max} = \mu_{opt}\left(1 - \frac{[s]}{[s]_{max}}\right)^a$	21	3	NaCl KCl glucose	0.0062 0.0100 0.0103
7	$\mu_{max} = \mu_{opt}\left(1 + \frac{a[s]}{b + [s]}\right)\left(1 - \frac{[s]}{[s]_{max}}\right)$	27	4	NaCl KCl glucose	0.0064 0.0122 0.0064
8	$\mu_{max} = \mu_{opt}\exp\left[-\left(\frac{[s]}{10^{-a}}\right)^b\right]$	15	3	NaCl KCl glucose	0.0132 0.0110 0.0124
9	$\mu_{max} = \mu_{opt}\left[1 - \left(\frac{[s]}{[s]_{max}}\right)^a\right]$	22	3	NaCl KCl glucose	0.0063 0.0091 0.0062
10	$\mu_{max} = \mu_{opt}\exp(-a[s])$	2	2	NaCl KCl glucose	0.0889 0.0656 0.1551
11	$\mu_{max} = \mu_{opt}\exp(-a[s])$	27	2	NaCl KCl glucose	0.2108 0.1532 0.2141
12	$\mu_{max} = \mu_{opt}\left(\frac{a}{a + [s]} - b[s]\right)$	27	3	NaCl KCl glucose	0.0394 0.0127 0.0240

[1] Boldface indicates model selected for further analysis.
[2] $[s]_{min}$ is the minimum solute concentration at parameter $a_{w\,max}$= 1 as set by Rosso and Robinson (32). $a_{w\,max}$ is converted to $[s]_{min}$ using $a_{w\,min}$=0.955 and a_w (BHI) = 0.990.
[3] *a* is a shape parameters set for a_w in the original model of Rosso and Robinson (32).

Table 1 - *Continued*

Model no.[1]	MSE_{tot}	μ_{opt} (h^{-1}) (SE)	$[s]_{max}$ (M) (SE)	$[s]_{opt}$ (M) (SE)	*a* value (SE)	*b* value (SE)	*c* value (SE)
1	0.0427	2.63 (0.012) 2.58 (0.010) 2.64 (0.014)	1.20 (0.006) 1.15 (0.005) 1.81 (0.009)				
2	0.0344	2.37 (0.013) 2.39 (0.013) 2.51 (0.011)	1.41 (0.012) 1.39 (0.010) 2.12 (0.015)	0.08 (0.006) 0.04 (0.005) 0.16 (0.005)			
3	0.1306				0.80 (0.021) 0.80 (0.017) 0.84 (0.014)	1.47 (0.088) 1.36 (0.074) 1.30 (0.060)	-2.97 (0.093) -2.95 (0.078) -2.07 (0.057)
4	0.2737	3.18 (0.040) 3.16 (0.035) 2.93 (0.041)	1.46 (0.023) 1.39 (0.021) 2.30 (0.045)				
5	0.0433	2.63 (0.014) 2.57 (0.011) 2.61 (0.015)	1.19 (0.007) 1.16 (0.005) 1.83 (0.010)		-2.11×10^{20} (8.89×10^{27}) -2.98×10^{20} (1.49×10^{28}) -8.07×10^{18} (5.12×10^{26})		
6	0.0265	2.50 (0.011) 2.56 (0.013) 2.50 (0.012)	1.05 (0.004) 1.13 (0.011) 1.54 (0.011)		0.67 (0.010) 0.94 (0.022) 0.61 (0.014)		
7	0.0250	2.47 (0.012) 2.54 (0.016) 2.46 (0.011)	1.12 (0.004) 1.13 (0.009) 1.67 (0.007)		-3.27×10^{-6} 9.75×10^{6} (2.05×10^{14}) -4.71×10^{5} (5.34×10^{10})	-8.11×10^{-6} 2.16×10^{9} (4.53×10^{16}) -1.41×10^{6} (1.59×10^{11})	
8	0.0366	2.32 (0.015) 2.37 (0.002) 2.37 (0.012)			0.10 (0.003) 0.14 (0.003) -0.07 (0.002)	2.51 (0.053) 2.11 (0.037) 2.67 (0.044)	
9	0.0216	2.43 (0.013) 2.50 (0.016) 2.45 (0.100)	1.13 (0.004) 1.13 (0.006) 1.68 (0.006)		1.38 (0.022) 1.13 (0.021) 1.47 (0.019)		
10	0.3096	2.90 (0.045) 2.84 (0.036) 2.74 (0.040)			1.62 (0.040) 1.63 (0.034) 0.99 (0.024)		
11	0.5781	2.94 (0.087) 2.90 (0.069) 2.68 (0.061)			0.33 (0.022) 0.35 (0.020) 0.60 (0.034)		
12	0.0761	2.65 (0.032) 2.57 (0.016) 2.61 (0.018)			1.45 (0.141) 5.24 (1.97) 5.24×10^{3} (5.65×10^{8})	0.37 (0.020) 0.69 (0.050) 0.54 (20.58)	

[1] Boldface indicates model selected for further analysis.

[2] $[s]_{min}$ is the minimum solute concentration at parameter $a_{w\ max}$= 1 as set by Rosso and Robinson (32). $a_{w\ max}$ is converted to $[s]_{min}$ using $a_{w\ min}$=0.955 and a_w (BHI) = 0.990.

[3] *a* is a shape parameters set for a_w in the original model of Rosso and Robinson (32).

Evaluating the gamma hypothesis

The pH model and model 9 were combined into a gamma model as per Equation 3, resulting in the models displayed in Table 2, describing the combined effect of pH and either NaCl, KCl or glucose. In addition, the pH model and model 9 were combined into the synergy models of Le Marc *et al*. (Equation 4, Table 2; (19)) and Augustin and Carlier (Equation 5, Table 2; (3, 4)).

Table 2. MSE-values for predictions obtained with (A) the non-synergistic gamma model, (B) the model of Le Marc *et al*. (19), and (C) the model of Augustin and Carlier (3, 4), for NaCl, KCl, and glucose

Model ID.	Solute	Model
A[1]	NaCl	$\mu_{max} = 2.42\ \frac{(pH-19.16)(pH-4.79)}{(pH-4.79)(pH-19.16)-(pH-8.00)^2}\left[1-\left(\frac{[s]}{1.13}\right)^{1.38}\right]$
B[2]	NaCl	$\mu_{max} = 2.42\ \frac{(pH-19.16)(pH-4.79)}{(pH-4.79)(pH-19.16)-(pH-8.00)^2}\left[1-\left(\frac{[s]}{1.13}\right)^{1.38}\right]\xi(pH,[s])$
C[3]	NaCl	$\mu_{max} = 2.42\ \frac{(pH-19.16)(pH-pH_{min,new})}{(pH-pH_{min,new})(pH-19.16)-(pH-8.00)^2}\left[1-\left(\frac{[s]}{[s]_{max,new}}\right)^{1.38}\right]$
A[1]	KCl	$\mu_{max} = 2.42\ \frac{(pH-19.16)(pH-4.79)}{(pH-4.79)(pH-19.16)-(pH-8.00)^2}\left[1-\left(\frac{[s]}{1.13}\right)^{1.13}\right]$
B[2]	KCl	$\mu_{max} = 2.42\ \frac{(pH-19.16)(pH-4.79)}{(pH-4.79)(pH-19.16)-(pH-8.00)^2}\left[1-\left(\frac{[s]}{1.13}\right)^{1.13}\right]\xi(pH,[s])$
C[3]	KCl	$\mu_{max} = 2.42\ \frac{(pH-19.16)(pH-pH_{min,new})}{(pH-pH_{min,new})(pH-19.16)-(pH-8.00)^2}\left[1-\left(\frac{[s]}{[s]_{max,new}}\right)^{1.13}\right]$
A[1]	glucose	$\mu_{max} = 2.42\ \frac{(pH-19.16)(pH-4.79)}{(pH-4.79)(pH-19.16)-(pH-8.00)^2}\left[1-\left(\frac{[s]}{1.68}\right)^{1.47}\right]$
B[2]	glucose	$\mu_{max} = 2.42\ \frac{(pH-19.16)(pH-4.79)}{(pH-4.79)(pH-19.16)-(pH-8.00)^2}\left[1-\left(\frac{[s]}{1.68}\right)^{1.47}\right]\xi(pH,[s])$
C[3]	glucose	$\mu_{max} = 2.42\ \frac{(pH-19.16)(pH-pH_{min,new})}{(pH-pH_{min,new})(pH-19.16)-(pH-8.00)^2}\left[1-\left(\frac{[s]}{[s]_{max,new}}\right)^{1.47}\right]$

[1] MSEsum A: 1.3977
[2] MSEsum B: 1.7652
[3] MSEsum C: 3.7578

Using these three equations, the growth rates and the growth boundaries of *B. cereus* in BHI broth were predicted for combinations of the two hurdles pH and solute concentration. Figure 2 I, II, and III shows the predictions of the three models for various combinations of concentrations of NaCl, KCl, and glucose and pH values, respectively, next to the experimental data.

Table 2 - *Continued*

Model ID.	Solute	MSE-value				
		pH 5.0	pH 5.5	pH 6.0	pH 6.5	pH 7.0
A[1]	NaCl	0.0625 (n=105)	0.0716 (n=119)	0.0797 (n=118)	0.1096 (n=119)	0.0760 (n=128)
B[2]	NaCl	0.0531	0.0700	0.0793	0.1096	0.0760
C[3]	NaCl	0.1531	0.2032	0.1303	0.0835	0.0642
A[1]	KCl	0.0477 (n=106)	0.0496 (n=119)	0.0369 (n=120)	0.0294 (n=118)	0.0350 (n=130)
B[2]	KCl	0.0372	0.0457	0.0369	0.0297	0.0350
C[3]	KCl	0.1397	0.2282	0.2260	0.0968	0.0460
A[1]	glucose	0.1874 (n=103)	0.1796 (n=116)	0.2230 (n=150)	0.1937 (n=140)	0.0920 (n=132)
B[2]	glucose	0.2207	0.1907	0.2283	0.1937	0.0920
C[3]	glucose	0.5264	0.7750	0.7223	0.2365	0.1266

[1] MSEsum A: 1.3977
[2] MSEsum B: 1.7652
[3] MSEsum C: 3.7578

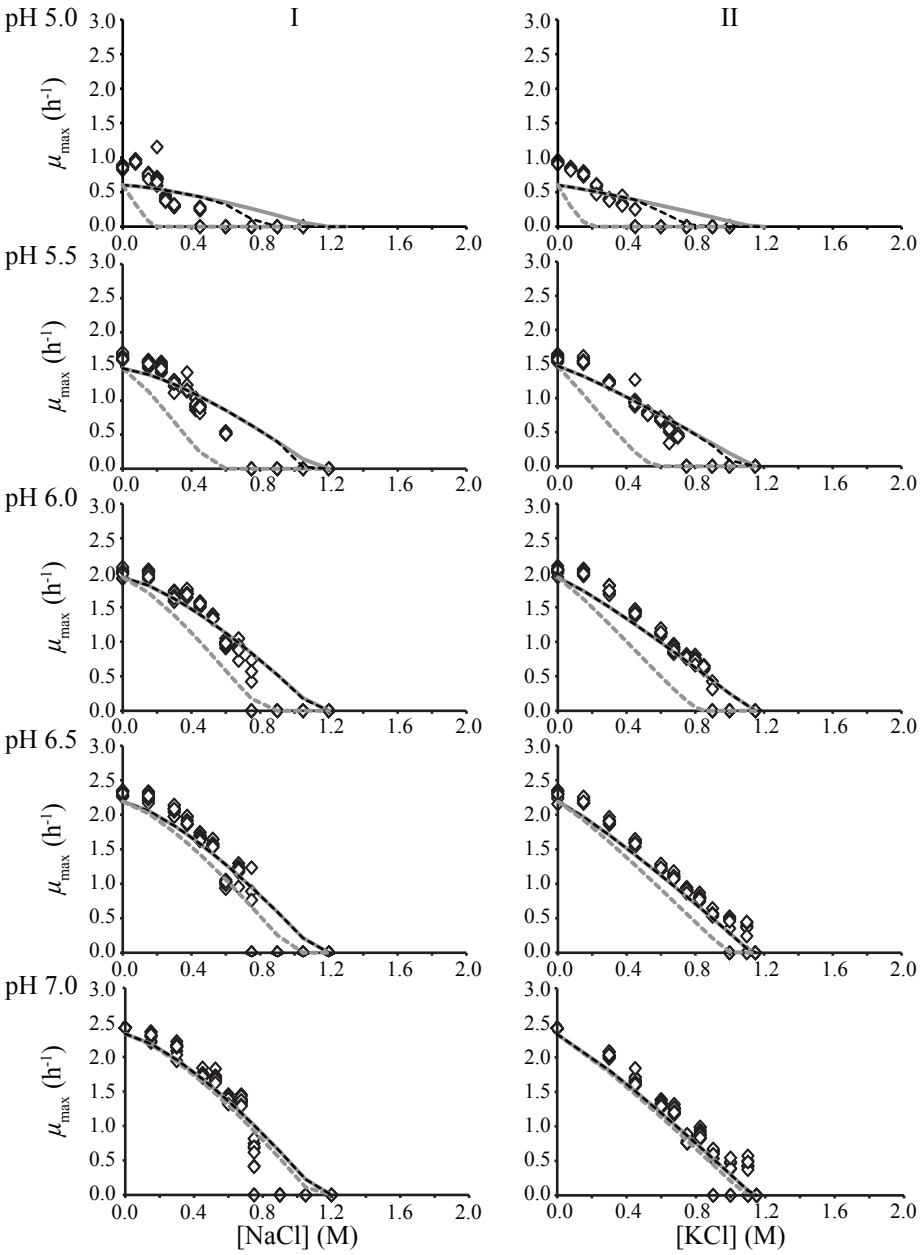

Figure 2 I, II. Experimental data (◇) and predictions using Equation 2 and Model 9 for the combined effect of pH and a_w lowering solute concentrations on μ_{max}, without (solid gray line) and with (dashed black line) interaction factor according to the model of Le Marc *et al.*, and predictions using the model of Augustin (dashed gray line) for NaCl (column I), and KCl (column II) at pH 5.0, 5.5, 6.0, 6.5, and 7.0 respectively.

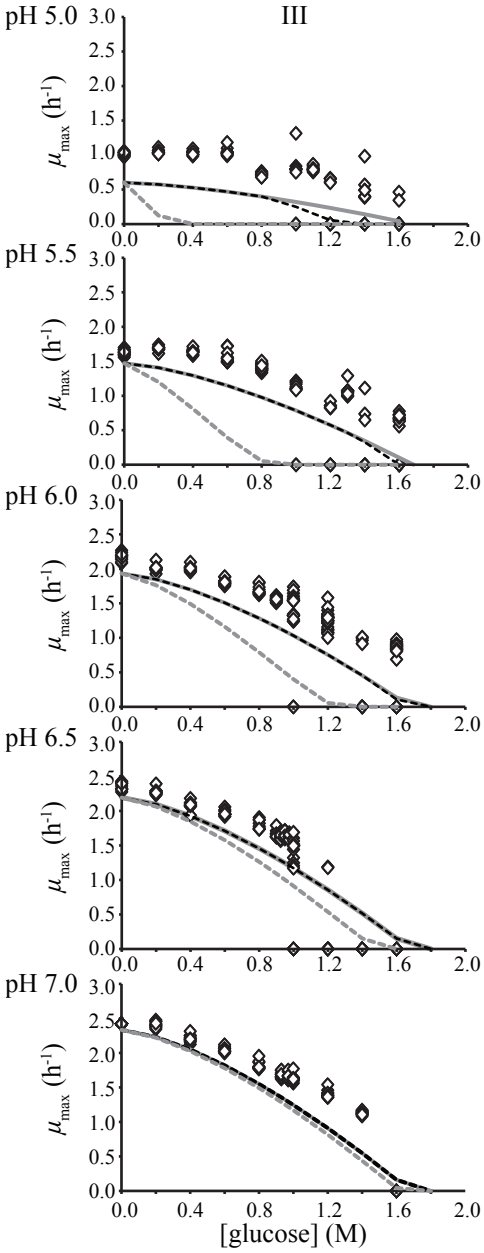

Figure 2 III. Experimental data (◇) and predictions using Equation 2 and Model 9 for the combined effect of pH and a_w lowering solute concentrations on μ_{max}, without (solid gray line) and with (dashed black line) interaction factor according to the model of Le Marc *et al.*, and predictions using the model of Augustin (dashed gray line) for glucose (column III) at pH 5.0, 5.5, 6.0, 6.5, and 7.0 respectively.

Overall, the MSE-values between prediction and experiments were found to be the lowest for the gamma model not assuming a synergy factor, which had MSE_{sum} A = 1.3977. The synergy model of Le Marc *et al*. was considered the next best model, having MSE_{sum} B = 1.7652, followed by the model of Augustin and Carlier, with MSE_{sum} C = 3.7578. All accuracy factors (data not shown) were higher than the accepted factor of 1.2 (10 % per number of environmental parameters in the model), indicating that for all models the estimate is not very accurate. In general the accuracy factors for the gamma model and the model of Le Marc *et al*. were the lowest ones, ranging from 1.226 to 2.337. The accuracy factors for the model of Augustin and Carlier were higher and ranged from 1.269 to 3.852, with most factors in the high range. The bias factors for the models of Augustin and Carlier were all indicating that the estimates were unacceptable and that the predictions were fail-dangerous. The gamma model and the model of Le Marc *et al*. had bias factors mainly ranging from good to acceptable, and no preference for one or the other model could be made based on the bias factors.

For most combinations of a_w lowering solutes in combination with pH, and especially in the case of low pH conditions, the data points were higher than the values predicted by the gamma model. This resulted in increased MSE-values for model fit and a poorer performance of the gamma model as compared to our previous study, in which pH and undissociated acid concentrations were combined (6). For NaCl and KCl, the growth boundary at pH 5 was also considerably overestimated by the gamma model, which also contributed to an increase of the MSE-values. The model of Le Marc *et al*. had lower MSE-values for these conditions, which is likely due to its assumed synergy which shifts the growth boundary to lower concentrations of a_w lowering solute. The reduction in MSE-values actually was from 0.0625 to 0.0531 for NaCl, and from 0.0477 to 0.0372 for KCl. For the other conditions evaluated, i.e. at higher pH, and for glucose, this reduction in MSE-values was not observed. For glucose, the growth boundary is underestimated by the model of Le Marc *et al*., therefore not reducing the difference between prediction and data. The model of Augustin and Carlier also assumed synergy, but this model underestimated the growth boundary considerably at pH values of 5 and 5.5, causing the MSE-values to increase to 0.1531 for pH 5 (NaCl) and 0.1397 (KCl).

Re-testing of the growth boundary to check whether three days of incubation was enough to determine the growth boundary, revealed that if cultures did not show growth within 3 days, growth was also not commencing in the 37 days following. This

indicates that the boundary found after three days of incubation corresponds well to the real growth boundary of the tested *B. cereus* strain.

Discussion

Model criteria and selection

This research aimed to test the gamma hypothesis for two independent hurdles, i.e. pH and various a_w lowering solutes. As part of the systematic approach deployed for testing of the gamma hypothesis for pH and various concentrations of undissociated acids (6), the most optimal model to predict the effect of the solute on the growth rate was selected. Relatively few models are available in the literature that incorporate the parameter a_w, or concentration of a_w lowering solutes. Where this was the case, predominantly model 1 was used (17, 23, 26, 28, 31, 38). However, many undissociated acid concentration models could be interpreted as a_w lowering solute models and were of equal performance as their original a_w models. The model selected as best fitting the data on the basis of having the lowest MSE-value and the least number of parameters, model 9, was not amongst the original a_w lowering solute models. Model 9 was adapted from a model describing the effect of undissociated acid on bacterial growth (22). The previously established selection procedures for model selection were also applied for selection of the best performing a_w lowering solute model, and allowed a considerable reduction in models to be used whilst not eliminating all.

Solute specific versus a_w *effect for single hurdles*

The differences found in the accuracy of the prediction of the boundary between the two salts and glucose may have two reasons. Firstly interactive effects may occur between the salts and the acid, which do not occur between glucose and the acids. Secondly, certain a_w specific effects of the solutes may exist. NaCl and KCl have almost equal a_w-values (0.954 and 0.956, respectively) at equal concentrations (1.13 M) of the solute. These values correspond to previously reported a_w-values for various concentration of NaCl and KCl in water by Samapundo *et al.* (33) and confirm the conclusion of Bidlas and Lambert (5) that NaCl and KCl have equal antimicrobial effects when calculated on a molar basis. This would encourage the view that these solutes have an a_w effect and not a solute specific effect. In our study we found that glucose had a much higher a_w-value (0.972) at a solute concentration of 1.13 M, whereas the a_w-value at the growth boundary

concentration for glucose (1.68 M) was found to be 0.961. The latter is in the same range as the growth boundary a_w-values of NaCl and KCl. Although NaCl and KCl have identical growth boundaries, for the NaCl and KCl graphs at pH 6.5 and pH 7 (Figure 2 I and II) it can be observed that the shapes of the curves at near growth boundary conditions are different. Where KCl shows tailing towards the growth boundary, NaCl shows an acute and rapid decrease towards the growth boundary, a so called cliff edge. A reason for this difference could not be found and is of interest for future studies.

Evaluation of the gamma hypothesis

Model 9 and the pH model of Equation 2 were combined into a gamma model which was used to asses the combined effect of a_w lowering solutes and pH on μ_{max} and the growth boundary of *B. cereus* F4810/72. This newly constructed gamma model was compared to the synergy models of Le Marc *et al*. (19) and Augustin and Carlier (4). The maximum specific growth rate was underestimated for the three solutes tested when predictions on the effect of combined low pH values (pH 5 and pH 5.5) and low concentrations of a_w lowering solute were made. The underlying cause for this low prediction as compared to the real data is as yet unknown. No systematic differences in pH of the broth were measured when re-measuring the pH with other pH meters, and before and after filter sterilizing. The same batch of BHI was used for all experiments, but the time frame between the first experiments of determining the μ_{max} for pH effects, and the last experiments determining the effect of different concentrations of a_w lowering solute on μ_{max}, was two years. Whether it is possible that the μ_{max} had changed over this period of time is speculative, but an option to consider. However, when plotting the μ_{max} data of the combination experiments, performed when the solute concentrations were 0 M, in the same graph as the original pH experiments (Figure 3), it can be seen that small deviations in pH at near growth boundary conditions can cause very significant changes in μ_{max}-values. For instance, a two fold increase in μ_{max}-value can be caused by a 0.14 pH-point increase. This pH increase is two times bigger than the measuring error of a pH meter and the measured differences between the pH meters in the laboratory. This observation of structural differences in μ_{max}-values also explains the differences between data points and the models in Figure 2 when no a_w lowering solute is present.

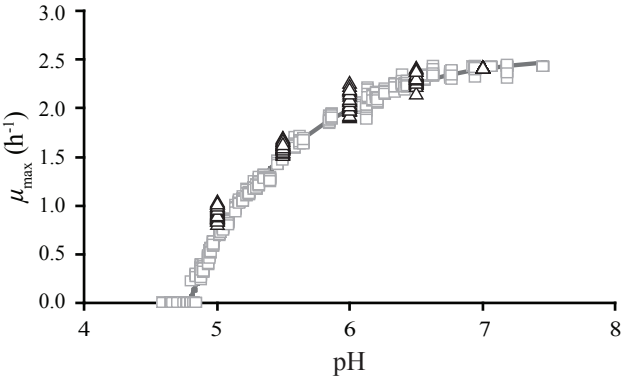

Figure 3. Maximum specific growth rate of emetic *B. cereus* as a function of pH, where the gray squares (□) represent the experimental data and the gray line depicts the fit of the most optimal pH model (Equation 2) to the original data sets; the black triangles (Δ) represent the data point of the experiments of group 3, where no a_w lowering solutes were added to the BHI broth.

Although not considered optimal data sets with respect to absolute μ_{max}-values, the data sets obtained in our study could still be used to draw conclusions about synergy, since the three models evaluated in this assessment differed in their growth boundary estimates and not in their μ_{max} when the a_w lowering solute was absent. For all models higher MSE-values were noted, but this was consistent for all three models tested and thus would not influence any further conclusions about the validity of the gamma hypothesis.

Different trends could be seen for the various predictions of the salts and the glucose curves combined with different pH values. The glucose curves clearly had a different shape compared to those of the salts. For the two salts evaluated, the gamma model extensively overestimated the growth boundary. For glucose, the growth boundary was underestimated by the gamma model. This could be explained by the fact that glucose may have a growth stimulating effect as well as a growth limiting effect and that the two opposing effects balanced each other's impact out. As a consequence, a shift of the growth boundary was not apparent, and the non-synergistic gamma model was able to predict the growth rate curve well. Since the curves of the salts and glucose were so different, drawing conclusions on the MSE_{sum}-values appeared not to be specific enough to judge the quality of predictions. However, the use of MSE-values seems unavoidable when an objective, quantitative judgment about the model performance is to be made.

When assessing MSE_{sum}, the sum of the MSE-values between data and prediction, for all three solutes used (NaCl, KCl and glucose), for all concentrations and for all 5 pH values tested (pH 5.0, 5.5, 6.0, 6.5, and 7.0), the newly composed gamma model had the lowest value and was judged to be performing the best. When focusing on specific, single MSE-values and visual analysing Figure 2, this conclusion was not unambiguously proven. As could be seen, the gamma model overestimated the boundary for NaCl and KCl, especially for low pH values, i.e. pH 5 and 5.5, and the introduction of a synergy factor as in the model of Le Marc *et al.* improved the estimate of the growth boundary. Assessing the MSE_{sum}-values for the two salts only and neglecting the glucose data ($MSE_{sum,NaCl+KCl}$), actually revealed that the synergy model performed better ($MSE_{sum,NaCl+KCl}$ = 0.5980 for the gamma model and $MSE_{sum,NaCl+KCl}$ = 0.5725 for the synergy model of Le Marc *et al.*). This would indicate that there was indeed a shift of the growth boundary which might have been caused by synergy. Notably, the synergy model of Augustin and Carlier underestimated the growth boundary by assuming synergy ($MSE_{sum,NaCl+KCl}$ = 1.371).

Since the growth boundary was estimated differently by all three methods, it was decided to re-test the growth boundaries. Re-testing has elsewhere been found to

Table 3. MSE-values between experiments and predictions obtained with various combinations of a_w lowering solute models and the pH model (Equation 2), combined into the non-synergistic gamma model, for NaCl, KCl and glucose[1]

model	NaCl					KCl				
	pH 5.0	pH 5.5	pH 6.0	pH 6.5	pH 7.0	pH 5.0	pH 5.5	pH 6.0	pH 6.5	pH 7.0
1	**0.0553**	0.0792	0.0970	0.1239	0.1203	**0.0431**	0.0575	**0.0294**	**0.0176**	0.0401
2	0.0621	**0.0634**	**0.0671**	**0.0930**	**0.0712**	**0.0464**	**0.0423**	**0.0300**	**0.0233**	**0.0318**
3	**0.0413**	**0.0549**	0.2566	0.3751	0.4427	**0.0354**	0.1230	0.3578	0.4615	0.5021
4	0.0640	0.1309	0.2386	0.3383	0.2766	0.0527	0.0875	0.1743	0.1939	0.1578
5	**0.0564**	**0.0632**	0.0937	0.1358	0.1019	**0.0464**	**0.0485**	0.0485	0.0412	0.0436
6	0.0618	**0.0715**	0.0852	0.1194	0.0814	**0.0468**	**0.0487**	0.0446	0.0389	0.0461
7	**0.0531**	**0.0541**	0.0897	0.1336	0.1021	0.0450	**0.0436**	0.0496	0.0490	0.0499
8	0.0660	0.0778	**0.0740**	**0.0989**	**0.0708**	**0.0471**	**0.0416**	**0.0300**	**0.0241**	**0.0318**
9	0.0625	0.0716	0.0797	0.1096	0.0760	0.0477	0.0496	0.0369	0.0294	0.0350
10	0.0540	0.0984	0.1909	0.2719	0.2255	0.0448	0.0711	0.1281	0.1306	0.1217
11	0.0637	0.1602	0.2880	0.4010	0.3331	0.0535	0.1101	0.1871	0.1935	0.1727
12	**0.0583**	0.0808	0.1260	0.1779	0.1398	**0.0468**	0.0507	0.0507	0.0407	0.0435

[1] in bold type face those MSE-values are highlighted that are smaller for the solute/pH indicated using the model indicated as compared to the combination with model 9 (highlighted with gray bar).

give useful insights. According to Vermeulen *et al*. (37) *Listeria monocytogenes* showed a significant increase in detection time (determined using optical density) of up to 30 days, when both pH and a_w were lowered simultaneously. This finding stresses the importance of re-testing of the boundary for the most stringent conditions, i.e. low pH and high concentrations of a_w lowering solute. The experiment validating the growth boundary for the strain of emetic *B. cereus* used in the current study, revealed that if cultures did not show growth within 3 days, growth was also not commencing in the 37 days following. So the experimental set-up used was sufficient to correctly determine the growth boundary.

All of the a_w lowering solute models were re-tested, since the incorrect prediction of the boundary might be caused by failure of the model selection criteria, and another combination of models possibly would improve the prediction of the combined pH and a_w lowering solute effect. The result of re-testing model combinations is displayed in Table 3, comparing MSE-values between experimental data and predictions. The initial combination of model 9 and the pH model is highlighted by a gray bar. For all combinations that perform better than the combination of model 9 and Equation 2, as indicated by a lower MSE-value, the MSE-value is marked in bold typeface.

Table 3 - *Continued*

model	glucose					# better than model 9	MSE_{sum}
	pH 5.0	pH 5.5	pH 6.0	pH 6.5	pH 7.0		
1	**0.0729**	0.2610	0.3660	0.7610	1.0773	5	3.2016
2	0.1939	0.1868	0.2541	0.2150	0.1493	9	1.5297
3	0.3040	0.4688	0.8689	0.7962	0.8439	3	5.9323
4	0.2791	0.3844	0.4866	0.6898	1.1474	0	4.7020
5	0.2166	0.2331	0.2884	0.2767	0.1886	4	1.8827
6	0.1962	0.2073	0.2639	0.2102	0.1057	3	1.6276
7	0.1894	0.1845	0.2264	0.1979	0.0935	3	1.5613
8	**0.1792**	**0.1615**	**0.2165**	**0.1707**	0.1016	12	1.3914
9	0.1874	0.1796	0.2230	0.1937	0.0920		1.4737
10	0.2520	0.3138	0.3914	0.4350	0.3470	0	3.0763
11	0.2658	0.3493	0.4127	0.5100	0.4009	0	3.9016
12	0.2149	0.2285	0.2787	0.2742	0.1808	2	1.9922

[1] in bold type face those MSE-values are highlighted that are smaller for the solute/pH indicated using the model indicated as compared to the combination with model 9 (highlighted with gray bar).

Evidently, no model was much better overall than model 9, although other models were better in some specific combinations and model 8 had a slightly lower MSE_{sum}. For example a combination with model 1 performed better in five out of 15 times. The improved performance of a combination was mostly observed at near growth boundary conditions. The improvement can be caused by a better estimation of the growth boundary by the gamma model. One model combination that was performing almost as well as model 9 combined, was model 8 of Lambert and Bidlas (15). This model gives better predictions in 12 out of 15 cases, though the improvements were relatively small. These improvements may have been due to a better shape of the curve, since the curve was first parabolic and showed tailing towards the growth boundary.

In previous work modeling combined effects of hurdles on the growth rate of microorganisms, good results often have been achieved using models without a synergy factor (15, 31, 38). In our study, predictions made using synergy models approached the growth boundary best for low pH conditions combined with different concentrations of a_w lowering solutes. For less stringent combinations of growth limiting factors, it was clearly found that the introduction of a synergy factor did not improve the predictions. A discussion is warranted whether non-optimal models predicting the effect of single hurdles should be incorporated in models predicting combined effects. Where the best performance in predictions of a combined effect is driving creation of synergy models, in effect poorer performance of the individual hurdles is generally accepted. This may result in a bias towards the synergy factor. Our study suggests that it may not be always possible to achieve the same level of good performance with the combined models and with the models of the single hurdles. However, as a best practice one should follow a systematic and quantitative approach to objectively identify the most optimal model for single effects that is to be used in assessing a combined effect. Such an approach was followed here and the fact that also one model was eliminated that had very good performance in a gamma model, proved that in order not to be biased for synergy, it is necessary to additionally use pre-set criteria for single factor effects first.

Acknowledgments

This work was financially supported by Nestlé Research Centre, Lausanne, Switzerland. Piet van der Zaal is acknowledged for experimental assistance in the a_w lowering solute experiments.

References

1. **Adams, M. R., and M. O. Moss.** 2000. Food Microbiology, 2 ed. The Royal Society of Chemistry.
2. **Aiba, S., M. Shoda, and M. Nagatani.** 1968. Kinetics of product inhibition in alcohol fermentation. Biotechnol. Bioeng. 10:845-864.
3. **Augustin, J.-C., and V. Carlier.** 2000. Mathematical modelling of the growth rate and lag time for *Listeria monocytogenes*. Int. J. Food Microbiol. 56:29-51.
4. **Augustin, J.-C., and V. Carlier.** 2000. Modelling the growth rate of *Listeria monocytogenes* with a multiplicative type model including interactions between environmental factors. Int. J. Food Microbiol. 56:53-70.
5. **Bidlas, E., and R. J. W. Lambert.** 2008. Comparing the antimicrobial effectiveness of NaCl and KCl with a view to salt/sodium replacement. Int. J. Food Microbiol. 124:98-102.
6. **Biesta-Peters, E. G., M. W. Reij, L. G. M. Gorris, and M. H. Zwietering.** 2010. Comparing nonsynergistic gamma models with interaction models to predict growth of emetic *Bacillus cereus* when using combinations of pH and individual undissociated acids as growth-limiting factors. Appl. Environ. Microbiol. 76:5791-5801.
7. **Biesta-Peters, E. G., M. W. Reij, H. Joosten, L. G. M. Gorris, and M. H. Zwietering.** 2010. Comparison of two optical density methods and a plate count method for estimation of growth parameters of *Bacillus cereus*. Appl. Environ. Microbiol. 76:1399-1405.
8. **Buchanan, R. L., and L. K. Bagi.** 1997. Effect of water activity and humectant identity on the growth kinetics of *Escherichia coli* O157:H7. Food Microbiol. 14:413-423.
9. **Choma, C., T. Clavel, H. Dominguez, N. Razafindramboa, H. Soumille, C. Nguyen-The, and P. Schmitt.** 2000. Effect of temperature on growth characteristics of *Bacillus cereus* TZ415. Int. J. Food Microbiol. 55:73-77.
10. **Cuppers, H. G., S. Oomes, and S. Brul.** 1997. A model for the combined effects of temperature and salt concentration on growth rate of food spoilage molds. Appl. Environ. Microbiol. 63:3764-3769.
11. **Den Besten, H. M. W., M. Mataragas, R. Moezelaar, T. Abee, and M. H. Zwietering.** 2006. Quantification of the effects of salt stress and physiological state on thermotolerance of *Bacillus cereus* ATCC 10987 and ATCC 14579. Appl. Environ. Microbiol. 72:5884-5894.
12. **Gould, G. W.** 1996. Methods for preservation and extension of shelf life. Int. J. Food Microbiol. 33:51-64.

13. **Houtsma, P. C., B. J. M. Kusters, J. C. de Wit, F. M. Rombouts, and M. H. Zwietering.** 1994. Modelling growth rates of *Listeria innocua* as a function of lactate concentration. Int. J. Food Microbiol. 24:113-123.

14. **Kotiranta, A., K. Lounatmaa, and M. Haapasalo.** 2000. Epidemiology and pathogenesis of *Bacillus cereus* infections. Microb. Infect. 2:189-198.

15. **Lambert, R. J. W., and E. Bidlas.** 2007. An investigation of the Gamma hypothesis: A predictive modelling study of the effect of combined inhibitors (salt, pH and weak acids) on the growth of *Aeromonas hydrophila*. Int. J. Food Microbiol. 115:12-28.

16. **Lambert, R. J. W., and E. Bidlas.** 2007. A study of the Gamma hypothesis: Predictive modelling of the growth and inhibition of *Enterobacter sakazakii*. Int. J. Food Microbiol. 115:204-213.

17. **Lanciotti, R., M. Sinigaglia, F. Gardini, L. Vannini, and M. E. Guerzoni.** 2001. Growth/no growth interfaces of *Bacillus cereus*, *Staphylococcus aureus* and *Salmonella enteritidis* in model systems based on water activity, pH, temperature and ethanol concentration. Food Microbiol. 18:659-668.

18. **Larsen, H. D., and K. Jørgensen.** 1999. Growth of *Bacillus cereus* in pasteurized milk products. Int. J. Food Microbiol. 46:173-176.

19. **Le Marc, Y., V. Huchet, C. M. Bourgeois, J. P. Guyonnet, P. Mafart, and D. Thuault.** 2002. Modelling the growth kinetics of *Listeria* as a function of temperature, pH and organic acid concentration. Int. J. Food Microbiol. 73:219-237.

20. **Leistner, L., and L. G. M. Gorris.** 1995. Food preservation by hurdle technology. Trends Food Sci. Technol. 6:41-46.

21. **Levenspiel, O.** 1980. The Monod equation: a revisit and a generalization to product inhibition situations. Biotechnol. Bioeng. 22:1671-1688.

22. **Luong, J. H. T.** 1985. Kinetics of ethanol inhibition in alcohol fermentation. Biotechnol. Bioeng. 27:280-285.

23. **McMeekin, T. A., R. E. Chandler, P. E. Doe, C. D. Garland, J. Olley, S. Putro, and D. A. Ratkowsky.** 1987. Model for combined effect of temperature and salt concentration/water activity on the growth rate of *Staphylococcus xylosus*. J. Appl. Microbiol. 62:543-550.

24. **McMeekin, T. A., K. Presser, D. A. Ratkowsky, T. Ross, M. Salter, and S. Tienungoon.** 2000. Quantifying the hurdle concept by modelling the bacterial growth/no growth interface. Int. J. Food Microbiol. 55:93-98.

25. **Mellefont, L. A., T. A. McMeekin, and T. Ross.** 2003. Performance evaluation of a model describing the effects of temperature, water activity, pH and lactic acid concentration on the growth of *Escherichia coli*. Int. J. Food Microbiol. 82:45-58.

26. **Neumeyer, K., T. Ross, and T. A. McMeekin.** 1997. Development of a predictive model to describe the effects of temperature and water activity on the growth of spoilage pseudomonads. Int. J. Food Microbiol. 38:45-54.

27. **Pasos, F. V., H. P. Fleming, D. F. Ollis, D. F. Hassan, and R. M. Felder.** 1993. Modeling the specific growth rate of *Lactobacillus plantarum* in cucumber extract. Appl. Microbiol. Biotechnol. 40:143-150.

28. **Presser, K. A., T. Ross, and D. A. Ratkowsky.** 1998. Modelling the growth limits (growth/no growth interface) of *Escherichia coli* as a function of temperature, pH, lactic acid concentration, and water activity. Appl. Environ. Microbiol. 64:1773-1779.

29. **Rödel, W., and R. Scheuer.** 2007. Recent results on the hurdle technology - measuring of combined hurdles. Mitteilungsblatt der Fleischforschung Kulmbach 46:3-10.

30. **Ross, T.** 1996. Indices for performance evaluation of predictive models in food microbiology. J. Appl. Bacteriol. 81:501-508.

31. **Ross, T., D. A. Ratkowsky, L. A. Mellefont, and T. A. McMeekin.** 2003. Modelling the effects of temperature, water activity, pH and lactic acid concentration on the growth rate of *Escherichia coli*. Int. J. Food Microbiol. 82:33-43.

32. **Rosso, L., and T. P. Robinson.** 2001. A cardinal model to describe the effect of water activity on the growth of moulds. Int. J. Food Microbiol. 63:265-273.

33. **Samapundo, S., T. Anthierens, R. Xhaferi, and F. Devlieghere.** Development of a validated model to describe the individual and combined water activity depressing effects of water soluble salt, sugar and fat replacers. J. Food Eng. 96:433-439.

34. **Stenfors Arnesen, L. P., A. Fagerlund, and P. E. Granum.** 2008. From soil to gut: *Bacillus cereus* and its food poisoning toxins. FEMS Microbiol. Rev. 32:579-606.

35. **Taylor, A. J., and R. J. Gilbert.** 1975. *Bacillus cereus* food poisoning: a provisional serotyping scheme. J. Med. Microbiol. 8:543-550.

36. **Te Giffel, M. C., and M. H. Zwietering.** 1999. Validation of predictive models describing the growth of *Listeria monocytogenes*. Int. J. Food Microbiol. 46:135-149.

37. **Vermeulen, A., K. P. M. Gysemans, K. Bernaerts, A. H. Geeraerd, J. F. Van Impe, J. Debevere, and F. Devlieghere.** 2007. Influence of pH, water activity and acetic acid concentration on *Listeria monocytogenes* at 7°C: Data collection for the development of a growth/no growth model. Int. J. Food Microbiol. 114:332-341.

38. **Wijtzes, T., F. M. Rombouts, M. L. T. Kant-Muermans, K. van 't Riet, and M. H. Zwietering.** 2001. Development and validation of a combined temperature,

water activity, pH model for bacterial growth rate of *Lactobacillus curvatus*. Int. J. Food Microbiol. 63:57-64.

39. **Zwietering, M. H., T. Wijtzes, J. C. de Wit, and K. van 't Riet.** 1992. A decision support system for prediction of the microbial spoilage in foods. J. Food Prot. 55:973-979.

Chapter 6

Quantification of the emetic toxin cereulide in food products by liquid chromatography-mass spectrometry using synthetic cereulide as a standard

Elisabeth G. Biesta-Peters, Martine W. Reij, Richard H. Blaauw, Paul H. in 't Veld, Andreja Rajkovic, Monika Ehling-Schulz, Tjakko Abee

Published in Applied and Environmental Microbiology (2010), Vol. 76, No. 22, p. 7466-7472

Abstract

Bacillus cereus *produces the emetic toxin cereulide, a cyclic dodecadepsipeptide that can act as a K^+ ionophore, dissipating the transmembrane potential in mitochondria of eukaryotic cells. Because pure cereulide has not been commercially available, cereulide content in food samples has been expressed in valinomycin equivalents, a highly similar cyclic potassium ionophore that is commercially available. This research tested the biological activity of synthetic cereulide and validated its use as a standard in the quantification of cereulide contents in food samples. The synthesis route consists of 10 steps that result in a high yield of synthetic cereulide that showed biological activity in the HEp-2 cell assay and the boar sperm motility assay. The activity is different in both methods, which may be attributed to differences in K^+ content of the test media used. Using cereulide or valinomycin as a standard to quantify cereulide based on liquid chromatography-mass spectrometry (LC-MS), the concentration determined with cereulide as a standard was on average 89.9 % of the concentration determined using valinomycin as a standard. The recovery experiments using cereulide-spiked food products and acetonitrile as extraction solute showed that the LC-MS method with cereulide as a standard is a reliable and accurate method to quantify cereulide in food, because the recovery rate was close to 100 % over a wide concentration range.*

Introduction

The emetic type toxin cereulide is produced in food products, such as rice, pasta, and noodles, by cells of *Bacillus cereus*. This happens during temperature abuse, and the cereulide causes vomiting upon ingestion (9, 16). Data on the frequency of outbreaks of emetic food poisoning are scarce, since the symptoms are often mild and therefore not reported. One fatal outbreak was reported in Belgium in 2003, where a child died due to the presence of emetic toxin in pasta salad eaten during a picnic (5). In the Netherlands an outbreak occurred in 2000, where 116 students got ill after consumption of a rice dish containing emetic toxin (7).

The emetic toxin, cereulide, is a cyclic dodecadepsipeptide (D-*O*-Leu-D-Ala-L-*O*-Val-L-Val)$_3$ (1). The toxic effects of cereulide are caused by the ionophoric uptake of K^+, resulting in dissipation of the transmembrane potential, stimulating swelling and respiration in mitochondria, and finally resulting in their inactivation (18). Cereulide structurally resembles valinomycin, another cyclic potassium ionophore (1). Both toxins form complexes with alkali metal ions but cereulide has been suggested to have a higher toxicity than valinomycin due to its higher affinity for potassium (23). The described effect of cereulide on mitochondria is used in several assays to detect the presence of cereulide in food products, like the sperm motility inhibition assay (2, 11, 19) and the HEp-2 (human carcinoma of the larynx) cell vacuolation assay (6, 8, 14).

Chemical assays for cereulide quantification using liquid chromatography-mass spectrometry (LC-MS) have been described in the literature by Häggblom *et al*., Bauer *et al*., and Hormazábal *et al*. (4, 10, 12). This quantitative method is based on high-performance LC (HPLC) connected to ion trap MS, which enables very accurate detection of low cereulide concentrations in food and with small between-experiment variations.

For all three methods, a solution with a known concentration of cereulide is needed as an external standard in order to quantify the cereulide level in a sample. To date, such an external standard of cereulide could not be prepared due to the lack of commercially available pure cereulide. As an alternative, the cereulide-like ionophore valinomycin has been used as a standard, since it is commercially available in known concentrations and purity. The use of valinomycin as a standard results in quantification of cereulide in terms of valinomycin equivalents, which is an elegant method but also scientifically debatable, since the compounds are different and might therefore show different behaviour in biological and chemical assays. In 1995 Isobe *et al*. (15) chemically

synthesized cereulide which was identical to cereulide produced by emetic *B. cereus* and also showed biological activity.

This study describes an improved synthesis route for cereulide, resulting in a higher yield and a more pure final product. Additionally, the cereulide MS pattern was compared to that of valinomycin by using an improved LC-MS analysis method. The synthetic cereulide was tested for its biological activity in both the HEp-2 cell culture assay and the boar sperm motility assay. Finally, cereulide recovery from three cereulide-spiked food products was evaluated using acetonitrile as the extraction medium and the LC-MS method for detection and quantification, with an external standard of cereulide prepared according to the improved protocol.

Materials and methods

Cereulide synthesis

The cyclic dodecadepsipeptide cereulide was synthesized from readily available Boc-D-Ala-OH, H-L-*O*-Val-OBn, Boc-L-Val-OH and H-L-*O*-Leu-OBn (Chiralix B.V., Nijmegen, Netherlands). First, Boc-D-Ala-OH and H-L-*O*-Val-OBn were coupled to give a depsipeptide building block, which was subjected to acidolysis of the Boc protecting group. Analogously, Boc-L-Val-OH and H-L-*O*-Leu-OBn were coupled, but with inversion of the configuration of L-*O*-Leu, affording the corresponding D-O-Leu-containing depsipeptide building block. This building block was then debenzylated by hydrogenolysis. Both building blocks were subjected to peptide coupling conditions to form a tetrapeptide having again *N*-Boc and *O*-benzyl protection. Selective deprotection of this tetrapeptide resulted in either the corresponding free amine or the free acid, followed by sequential coupling, resulting in a linear dodecapeptide which was finally cyclized to obtain cereulide. The complete synthesis route, including all intermediate steps, is described in the appendix.

LC-MS analysis of synthetic cereulide and valinomycin

Ten milligrams of the synthetic cereulide (Chiralix B.V., Nijmegen, Netherlands) was dissolved in 1 ml methanol (Merck KGaA, Darmstadt, Germany). Solution A was obtained by diluting this stock solution in methanol to a concentration of 50 µg/ml. Solution A was diluted in acetonitrile (Merck KGaA, Darmstadt, Germany) to a concentration of 1,000 ng/ml (solution B). The working stock solution C was obtained by diluting solution B in acetonitrile to a final concentration of 10 ng/ml. The same procedure as described for

dilution of synthetic cereulide was used for valinomycin (Sigma-Aldrich GmbH, Steinheim, Germany) to obtain a working stock solution of 10 ng/ml.

For both components, samples for LC-MS analysis were prepared by adding 200, 160, 120, 80, or 40 µl of solution C to an LC-MS vial. The vials were filled with additional acetonitrile to reach a total volume of 240 µl to obtain a concentration range of solution C. Subsequently, 30 Milli-Q water was added to the vials, resulting in final concentrations of cereulide or valinomycin of 1.5, 3, 4.5, 6, and 7.5 ng/ml. The samples were analysed using an LC-MS method derived from the method described by Häggblom *et al.* (10). The samples were analysed on an ion trap LC-MS apparatus by injecting 10-µl aliquots of the samples and subsequent elution and analysis using the positive electrospray ionization mode using either a Thermofinnigan LCQ Advantage setup (Thermo Fisher Scientific, Waltham, MA) with a C_{18} column (100 mm by 2.1 mm by 5 µm; Discovery, Supelco, Bellefonte, PA) or a Thermo Scientific LTQ XL setup (Thermo Fisher Scientific, Waltham, MA) with a C_{18} column (100 mm by 2.1 mm by 5 µm; Acquity UPLC, Waters Ltd., Hertfordshire, United Kingdom). The column was eluted at a flow rate of 0.2 ml/min with the following gradient: from 0 to 18 min, 13 % solution A and 87 % solution B; from 18 to 35 min, 100 % B; from 35 to 50 min, 13 % A and 87 % B, with phase A being 2 % (vol/vol) trifluoracetic acid anhydride (TFA; Merck KGaA, Darmstadt, Germany) in Milli-Q water with additional NH_4^+ (added as ammonium acetate [Merck, Darmstadt, Germany]) at a concentration of 10 mM and phase B being acetonitrile. The NH_4^+ adducts of both compounds were used for quantification (m/z for valinomycin, 1,128.5; m/z for cereulide, 1,170.7). The peak surface of every sample was plotted as a function of the concentration of the sample, resulting in two calibration curves for both synthetic cereulide and valinomycin.

Natural cereulide was produced by culturing *Bacillus cereus* (NCTC 11143) on tryptone soya agar (Oxoid CM 131) plates for 24 h at 28°C. After incubation the cells were harvested by using a 10 µl loop. The biomass was transferred to a screw-cap bottle and suspended in methanol (HPLC grade; Merck 1.06007) for extraction (10 ml methanol per g of biomass). The methanol extract was dried by evaporation over nitrogen, and the residue was suspended in 50 ml pentane (Merck 1.07177) and filtered over a paper filter (Schleicher & Schuell 589/3) to trap the undissolved particles. The pentane solution was subsequently dried by evaporation over nitrogen, and the residue was dissolved in 100 ml methanol. This solution was used to make a calibration curve consisting of various

dilutions of natural cereulide of unknown purity (containing 1.5, 3, 4.5, 6, and 7.5 ng/ml valinomycin equivalents). A sample of synthetic cereulide with a final concentration of 4.95 ng/ml was quantified using this natural cereulide calibration curve, with the cereulide content expressed in valinomycin equivalents.

Testing biological activity of synthetic cereulide in a HEp-2 cell assay

The biological activity of the synthetic cereulide was determined using the HEp-2 cell assay as described by Ehling-Schulz *et al*. (6). In short, Earle's minimal essential cell culture medium (MEM) with supplements was mixed with 2 % ethanol as a diluent, and 50 µl was added to every well of a 96-well plate. Valinomycin or cereulide was added to the first well of a row at an initial concentration of 500 ng/ml per well, and the content was serially diluted up to the 10th (valinomycin) or the 20th (cereulide) well, respectively. The HEp-2 cells were prepared and counted, and 150 µl of the HEp-2 cell suspension was added to all wells by using a multichannel pipette. The 96-well plates were incubated at 37°C for 48 h under a 5 % CO_2 atmosphere. The cells were investigated microscopically for toxicity, since intoxicated cells will show malformations. Subsequently, 100 µl of the liquid was removed from each well. Ten microliters of the cell proliferation reagent WST-1 was added to every well, and the plate was incubated for 20 min at 37°C. The absorption of every well was measured at 450/620 nm to determine the live/dead cell ratio.

Testing biological activity of synthetic cereulide in the boar sperm motility assay

The effect of the synthetic cereulide on boar sperm was compared to valinomycin of known concentrations according to the modified protocol of Rajkovic *et al*. (20, 21). The aliquot of the stock solution of 50 ng cereulide per ml of methanol was evaporated under N_2 and diluted in 2-fold serial dilutions to 0.78 ng/ml using dimethyl sulfoxide (DMSO; Sigma-Aldrich, Steinheim, Germany) as the diluent. Volumes of 5 µl of each dilution were mixed with 195 µl of sperm (from the Belgian Piétrain extramuscled boar breed; standardized to a concentration of approximately 30 million cells per milliliter) in wells of a microtiter plate. The mixture was immediately transferred into a 37°C prewarmed counting slide (standard count two-chamber 20-µm slide; Leja, Nieuw-Vennep, Netherlands). The motility behavior was observed for 10 min, and the time to complete cessation of motility was recorded. The lowest concentration at which motility ceased within 10 min was taken as the limit of detection. Exposure was limited to 10 min, as any

longer exposure of semen to DMSO had toxic effects that resulted in impaired motility. Semen alone and semen mixed with 5 µl of methanol served as a negative control and blank, respectively.

Extraction and detection of cereulide from food products spiked with cereulide

Cooked rice, a Chinese noodle dish, and french fries were used as model systems to test the extraction of cereulide from foods by using acetonitrile. The samples were spiked with natural cereulide of known purity. The chosen concentrations of the spiked cereulide in the food product were based on the estimated limits of quantification (1.5, 3, and 4.5 times the limit of quantification [LOQ] for the low concentration level and 7.5, 15, and 22.5 times the limit of quantification for the high concentration level). The low concentration level corresponded to 6.1, 12.3, and 18.4 µg cereulide/kg of sample, and the high concentration level corresponded to 30.7, 46.1, and 92.2 µg cereulide/kg sample. The precision of the method was determined as the standard deviation of replicate measurements of the same sample (SD_r) and standard deviation of the replicate experiment within the same laboratory (SD_{RL}). Five grams of every food sample was extracted with 50 ml acetonitrile (HPLC grade; Labscan C02C11X) by shaking it for 1 h at 100 rpm on an orbital shaker. The sample was left to settle after shaking, and 1,000 µl of the clear upper layer was transferred to a vial. To each vial 200 µl internal standard (valinomycin at a concentration of 25 ng/ml) and 150 Milli-Q water (HPLC grade) were added, mixed, and sealed. If the solution turned turbid, it was centrifuged for 10 min at ≥ 10,000 × *g*, and the clear supernatant was transferred to a new vial. The concentration of cereulide was determined by LC-MS with the settings described above.

Results

Cereulide synthesis and LC-MS analysis

The synthesis route as described in this study (see the appendix) consists of 10 steps, compared to 11 steps in the synthesis route reported by Isobe *et al*. (15). The overall yield of this synthesis was 28.5 %, a 3-fold improvement over the yield of the synthesis route proposed by Isobe *et al*. The purity of the solution was > 95 %. Figures 1A to D present the chromatogram and MS scans for, respectively, valinomycin and synthetic cereulide. Figure 1A represents the chromatogram (time versus relative abundance) of the valinomycin NH_4^+ adduct, and Figure 1C shows the cereulide NH_4^+ adducts. Figure 1B

shows the typical mass spectrum of the valinomycin NH_4^+ adduct, and Figure 1D shows that of the cereulide NH_4^+ adduct. The NH_4^+ adducts of valinomycin and cereulide had molecular weights of 1,128.6 and 1,170.6, respectively. The MS scans for synthetic and natural cereulide proved to be identical (results not shown).

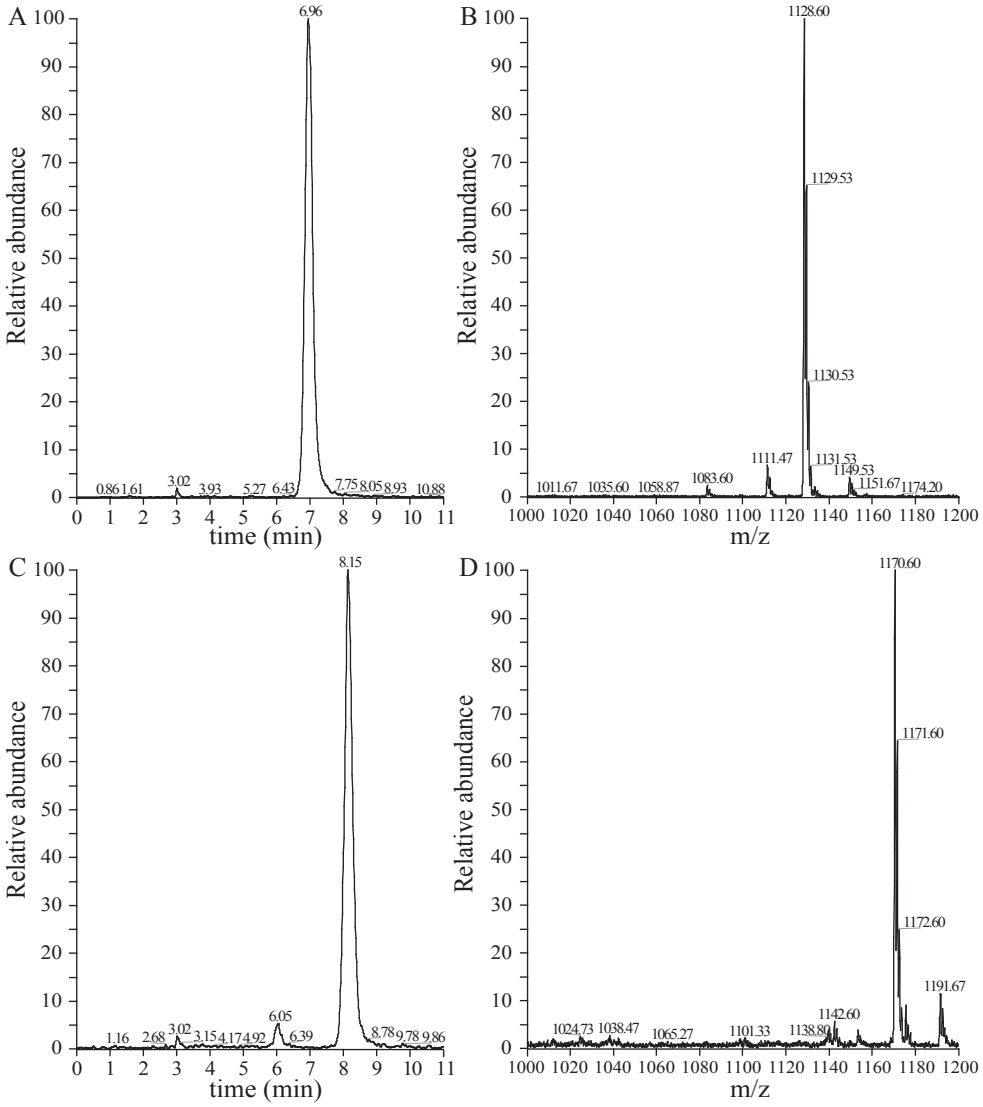

Figure 1. A: LC chromatogram of valinomycin with elution of the compound after 7 min. B: Full ion spectrum of valinomycin with m/z 1,128.6. C: LC chromatogram of cereulide with elution of the compound after 8 min. D: Full ion spectrum of cereulide with m/z 1,170.60.

Figure 2 presents the calibration curves for synthetic cereulide and valinomycin in the concentration range of 1.5 to 7.5 ng/ml. The results prove that the LC-MS response was linear over this range. The difference in peak areas for equal concentrations of the two components was 10.3 %, indicating that the cereulide content of a sample that was estimated by using valinomycin to establish the calibration curve resulted in an overestimation of the cereulide content by 10.3%.

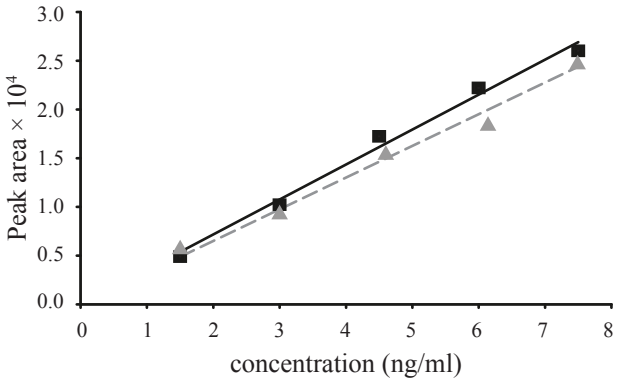

Figure 2. Calibration curve of synthetic cereulide (■) and valinomycin (▲), with the peak area of the compound measured based on LC-MS results as a function of known initial concentrations.

The reverse approach, in which natural cereulide of unknown purity was used to establish a calibration curve (cereulide concentration expressed as valinomycin equivalents) and the peak area of synthetic cereulide with a known concentration of 4.95 ng/ml was compared to the calibration curve, gave similar results. The synthetic cereulide concentration determined was on average 5.520 ng/ml with a standard deviation of 0.205 ng/ml (n = 11), 89.9 % of the valinomycin concentration.

Testing the biological activity of synthetic cereulide

The effects of various concentrations of valinomycin and cereulide on HEp-2 cells as a function of the toxin concentration are displayed in Figure 3A. When the toxin concentration was above 7.81 ng/ml (cereulide) or 62.5 ng/ml (valinomycin), less than 10 % of the HEp-2 cells survived the 48 h of incubation. An increase in surviving cells was observed with a serial decrease in toxin concentration. The toxic effect of valinomycin decreased faster along dilution series of equal initial concentrations compared to cereulide. The 50 %

effective concentrations for valinomycin and cereulide, the amounts of toxin required to inactivate half of the cells, showed a 15-fold difference, indicating that cereulide was 15 times more toxic to the cells than valinomycin at an equal incubation concentration. Concentrations of cereulide of 1 ng/ml did not result in a measurable toxic effect to the cells. The effects of equal concentrations of synthetic and natural cereulide on the HEp-2 cells were similar (data not shown).

The effects of various concentrations of valinomycin and cereulide on the motility of the boar sperm are represented as a function of the toxin concentration in Figure 3B.

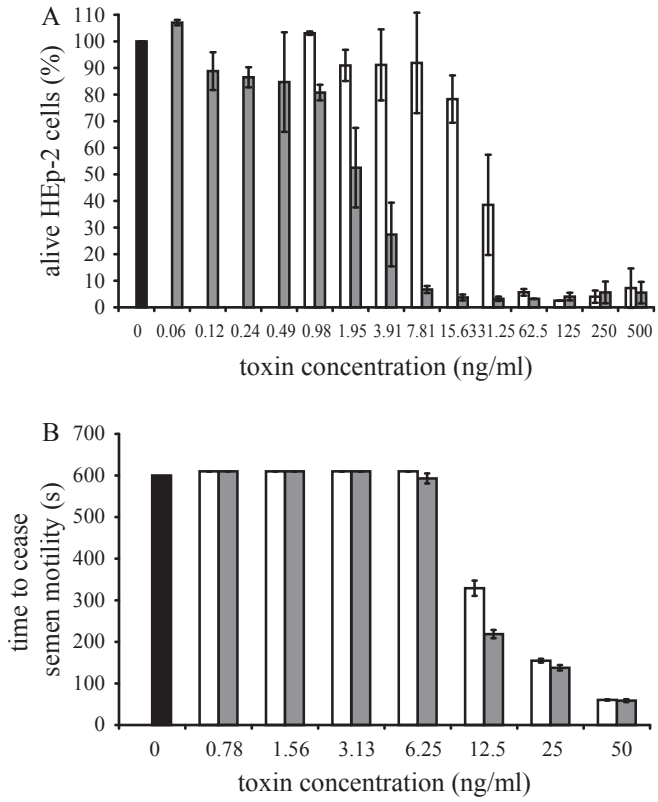

Figure 3. A: Live HEp-2 cells, incubated with 2-fold-diluted concentrations of cereulide and valinomycin, as a function of nonincubated HEp-2 cells. B: Time needed for boar semen to lose motility in the presence of 2-fold-diluted concentrations of cereulide and valinomycin. For both panels, white bars represent valinomycin, gray bars represent cereulide, and black bars represent nonincubated HEp-2 cells or semen.

When the toxin concentration was higher than 6.25 ng/ml, the boar semen lost their motility. A serial decrease in toxin concentration resulted in an increase in time required to reduce semen motility. The results indicated that synthetic cereulide in the range of 6.25 to 25 ng/ml resulted in a shorter time to complete cessation of semen motility than with equal concentrations of valinomycin. Although statistically significant (*t* test, $P < 0.05$), this difference was not as extensive as the difference observed with the HEp-2 cell assay. For both compounds, concentrations below 6.25 ng/ml did not result in complete cessation of motility within 10 min. At 50 ng/ml both synthetic cereulide and valinomycin were too toxic (complete cessation of semen motility within a minute of exposure).

Detection of cereulide from a food product spiked with cereulide

The results for recovery, expressed as the SD_r and the SD_{RL} for both high and low concentrations of cereulide as determined in the matrices cooked rice, a Chinese noodle dish, and french fries, are presented in Table 1. The concentrations used to determine the recovery were based on the LOQ. The LOQ (defined as six times the background noise) was determined to be 4.1 µg/kg of sample. The values for recovery ranged between 96.7 % and 107.6 %. The values for SD_r and SD_{RL} were the lowest in cooked rice and the highest in french fries, although the differences between the results were not significant.

Table 1: Recovery and precision data for the quantification of cereulide from cooked rice, a Chinese noodle dish, and french fries

Matrix	% Recovery		SD_r		SD_{RL}	
	Low level[a]	High level[b]	Low level	High level	Low level	High level
Cooked rice	96.7	98.2	1.93	3.09	2.85	4.56
Chinese noodle dish	98.0	102.5	2.74	4.38	2.88	4.60
French fries	101.1	106.7	2.47	3.96	3.42	5.47

[a] Low-level samples were spiked with 6.1 to 18.4 µg of cereulide/kg of sample.

[b] High-level samples were spiked with 30.7 to 92.2 µg of cereulide/kg of sample.

Discussion

The key differences of the new synthesis route, compared to the synthesis route described by Isobe *et al*., were that in the new strategy the dipeptide building blocks were constructed by ester bond formation and subsequent couplings of the building blocks and that the final cyclization was achieved by amide bond formation. In contrast, in the Isobe *et al*. synthesis method the dipeptides were prepared by amide bond formation,

and the subsequent couplings of the building blocks and the final cyclization were done by ester bond formation. Since amide bond formation is generally more facile than ester bond formation, the new strategy resulted in a more efficient synthesis, with significantly higher overall yield (10 steps with a 28.5 % overall yield, compared to 11 steps with a 9.3 % overall yield with the Isobe *et al*. synthesis method).

The mass spectra of natural and synthetic cereulide were identical (data not shown). Using synthesized cereulide allows the direct determination of the concentration of cereulide in (food) samples, instead of expressing the cereulide concentration in terms of valinomycin equivalents. Quantification of cereulide in samples by using valinomycin as the standard overestimated the concentration compared to that obtained using synthetic cereulide as the standard. Using valinomycin, the levels were approximately 10 % higher. This is in correspondence with observations of Häggblom *et al*. (10), who found that MS results for valinomycin and cereulide are within 10 %.

Both the HEp-2 cell assay and the boar sperm motility assay proved that the synthetic cereulide is biologically active. In the HEp-2 cell assay synthetic cereulide had a 15-fold-higher toxic effect than valinomycin at the same concentration (Figure 3A). In the boar sperm motility assay this difference was of a lesser extent (Figure 3B). These results are in agreement with the findings of Teplova *et al*. and Makarasen *et al*. (17, 23), who suggested that the differences are caused by the different potassium levels in the two assay mixtures, i.e., the boar semen assay mixture contains 10 to 19 mM and the HEp-2 cell assay mixture contains around 1 mM. The lower concentration of potassium in the HEp-2 cell proliferation assay favors the activity of cereulide, based on its higher affinity for potassium.

The current study also demonstrates that it is possible to quantify cereulide in a variety of starch-rich food products at low concentration levels (5 µg cereulide/kg of sample) with good reproducibility. The low concentration could be detected by increasing the volume injected in the LC-MS apparatus to 20 µl instead of the 1 µl used by Häggblom *et al*. (10). In addition, methanol was replaced by acetonitrile for extraction in order to optimize peak shape in the LC chromatogram (data not shown). The acetonitrile itself might also enhance the extraction of cereulide from the food, since the solvent is more apolar than methanol (polarity indices, 5.8 versus 5.1). An alternative approach to increase the accuracy of cereulide quantification was recently published and is based on the addition of a $^{13}C_6$ cereulide isotopologue to each sample during extraction,

dilution with water, and quantification by liquid chromatography (4). The $^{13}C_6$ cereulide isotopologue can be considered the perfect internal standard for cereulide extraction and therefore has promising implications for further research concerning cereulide extraction. On the other hand, our study proposes extraction of cereulide with acetonitrile, without dilution in water, and to increase the injection volume into the LC-MS apparatus. This relatively simple protocol can be applied both for research purposes and during routine analysis of (food) samples. Commercially available cereulide may be used as a standard of known concentration, and it can also be considered the perfect standard for recovery and detection experiments.

The values for recovery with the method used were good (ranging between 96.7 % and 107.6 %) and were well within the laboratory's internal limits (acceptability range, 60 to 115 % at a level of 10 µg/kg), which are based upon the AOAC peerverified methods program (3). The values found for SD_r and SD_{RL} were compared to the Horwitz ratio, the index of method performance with respect to precision, or HorRat values (13), and all values were at least three times lower than the Horwitz values, indicating the good precision of the method.

In conclusion, this research provides a novel route for the synthesis of biologically active cereulide, with a high yield and purity. Recovery rates of cereulide from three tested food matrices, using acetonitrile as extraction solvent, were close to 100 %, with low SD values by LC-MS analysis. The commercial availability of cereulide should encourage method development for cereulide detection and quantification, since results no longer need to be extrapolated due to the use of nonidentical standards.

Acknowledgments

This work was financially supported by Nestlé Research Centre, Lausanne, Switzerland.
We acknowledge Bas Gruijters and Roel Wijtmans from Chiralix B.V. for their contribution to the synthesis of the cereulide. We acknowledge Romy Renner and Genia Lücking from the Technical University of Munich for skillful technical assistance with the Hep-2 cell assay. We acknowledge Leo van der Laak and Serge Dissel from the Food and Consumer Product Safety Authority, Region South, for their work on the development and validation of the LC-MS method for the quantification of cereulide in food samples.

References

1. **Agata, N., M. Mori, M. Ohta, S. Suwan, I. Ohtani, and M. Isobe.** 1994. A novel dodecadepsipeptide, cereulide, isolated from *Bacillus cereus* causes vacuole formation in HEp-2 cells. FEMS Microbiol. Lett. 121:31-34.

2. **Andersson, M. A., E. L. Jaaskelainen, R. Shaheen, T. Pirhonen, L. M. Wijnands, and S. Salkinoja-Salonen.** 2004. Sperm bioassay for rapid detection of cereulide-producing *Bacillus cereus* in food and related articles. Int. J. Food Microbiol. 94:175-183.

3. **AOAC.** 1995. Verified methods program, manual on policies and procedures.

4. **Bauer, T., T. Stark, T. Hofmann, and M. Ehling-Schulz.** 2010. Development of a stable isotope dilution analysis for the quantification of the *Bacillus cereus* toxin cereulide in foods. J. Agricult. Food Chem. 58:1420-1428.

5. **Dierick, K., E. Van Coillie, I. Swiecicka, G. Meyfroidt, H. Devlieger, A. Meulemans, G. Hoedemaekers, L. Fourie, M. Heyndrickx, and J. Mahillon.** 2005. Fatal family outbreak of *Bacillus cereus*-associated food poisoning. J. Clin. Microbiol. 43:4277-4279.

6. **Ehling-Schulz, M., N. Vukov, A. Schulz, R. Shaheen, M. Andersson, E. Martbauer, and S. Scherer.** 2005. Identification and partial characterization of the Nonribosomal peptide synthetase gene responsible for cereulide production in emetic *Bacillus cereus*. Appl. Environ. Microbiol. 71:105-113.

7. **Essen, R., C. de Ruiter, and M. de Wit.** 2000. Massale voedselvergiftiging in het Kotterbos te Almere. Infectieziekten bulletin 11:205-207 (in Dutch).

8. **Finlay, W. J. J., N. A. Logan, and A. D. Sutherland.** 1999. Semiautomated metabolic staining assay for *Bacillus cereus* emetic toxin. Appl. Environ. Microbiol. 65:1811-1812.

9. **Granum, P. E., and T. Lund.** 1997. *Bacillus cereus* and its food poisoning toxins. FEMS Microbiol. Lett. 157:223-228.

10. **Häggblom, M. M., C. Apetroaie, M. A. Andersson, and M. S. Salkinoja-Salonen.** 2002. Quantitative analysis of cereulide, the emetic toxin of *Bacillus cereus* produced under various conditions. Appl. Environ. Microbiol. 68:2479-2483.

11. **Hoornstra, D., M. A. Andersson, R. Mikkola, and M. S. Salkinoja-Salonen.** 2003. A new method for in vitro detection of microbially produced mitochondrial toxins. Toxicol. in Vitro 17:745-751.

12. **Hormazábal, V., Ø. Østensvik, K. O' Sullivan, and P. E. Granum.** 2004. Quantification of *Bacillus cereus* emetic toxin (cereulide) in figs using LC.MS. J. Liq. Chromatogr. Related Technol. 27:2531-2538.

13. **Horwitz, W., and R. Albert.** 2006. The Horwitz ratio (HorRat): a useful index of

method performance with respect to precision. J. AOAC. Int. 89:1095-1109.

14. **Hughes, S., B. Bartholomew, J. C. Hardy, and J. M. Kramer.** 1988. Potential application of a HEp-2 cell assay in the investigation of *Bacillus cereus* emetic-syndrome food poisoning. FEMS Microbiol. Lett. 52:7-11.

15. **Isobe, M., T. Ishikawa, S. Suwan, N. Agata, and M. Ohta.** 1995. Synthesis and activity of cereulide, a cyclic dodecadepsipeptide ionophore as emetic toxin from *Bacillus cereus*. Bioorg. Med. Chem. Lett. 5:2855-2858.

16. **Kramer, J. M., and R. J. Gilbert.** 1989. *Bacillus cereus* and other *Bacillus* species. M. Dekker, New York (USA).

17. **Makarasen, A., K. Yoza, and M. Isobe.** 2009. Higher structure of cereulide, an emetic toxin from *Bacillus cereus*, and special comparison with valinomycin, an antibiotic from Streptomyces *fulvissimus*. Chem. Asian J. 4:688-698.

18. **Mikkola, R., N. E. L. Saris, P. A. Grigoriev, M. A. Andersson, and M. S. Salkinoja-Salonen.** 1999. Ionophoretic properties and mitochondrial effects of cereulide. Eur. J. Biochem. 263:112-117.

19. **Rajkovic, A., M. Uyttendaele, and J. Debevere.** 2007. Computer aided boar semen motility analysis for cereulide detection in different food matrices. Int. J. Food Microbiol. 114:92-99.

20. **Rajkovic, A., M. Uyttendaele, W. Deley, A. Van Soom, T. Rijsselaere, and J. Debevere.** 2006. Dynamics of boar semen motility inhibition as a semi-quantitative measurement of *Bacillus cereus* emetic toxin (cereulide). J. Microbiol. Meth. 65:525-534.

21. **Rajkovic, A., M. Uyttendaele, S.-A. Ombregt, E. Jaaskelainen, M. Salkinoja-Salonen, and J. Debevere.** 2006. Influence of type of food on the kinetics and overall production of *Bacillus cereus* emetic toxin. J. Food Prot. 69:847-852.

22. **Suwan, S., M. Isobe, I. Ohtani, N. Agata, M. Mori, and M. Ohta.** 1995. Structure of cereulide, a cyclic dodecadepsipeptide toxin from *Bacillus cereus* and studies on NMR characteristics of its alkali metal complexes including a conformational structure of the K^+ complex. J. Chem. Soc., Perkin Trans. 17:765-775.

23. **Teplova, V., R. Mikkola, A. Tonshin, N. Saris, and M. Salkinoja-Salonen.** 2006. The higher toxicity of cereulide relative to valinomycin is due to its higher affinity for potassium at physiological plasma concentration. Toxicol. Appl. Pharmacol. 210:39-46.

Appendix

Unless noted otherwise, materials were purchased from commercial suppliers (Sigma-Aldrich GmbH, Steinheim, Germany, or Acros, Thermo Fisher Scientific, Geel, Belgium) and used without purification. CH_2Cl_2 was freshly distilled from calcium hydride. Celite was obtained from Sigma-Aldrich. All air- and moisture-sensitive reactions were carried out under an inert atmosphere of dry argon. Column chromatography was performed using Acros silica gel (0.035 to 0.070 mm, 6 nm). Thin-layer chromatography was performed using silica gelcoated glass plates (Merck 60 F254), and compounds were detected with UV light (254 nm) and/or with potassium permanganate.

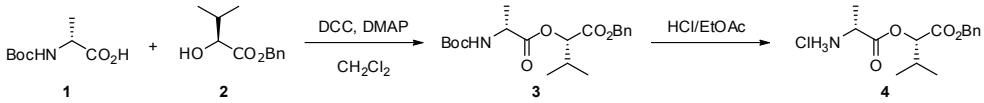

Boc-(D-Ala-L-*O*-Val)-OBn (compound 3). DCC (*N*,*N*'-dicyclohexylcarbodiimide) (219 mg, 1.06 mmol) was added to a stirred solution of compound 1 (200 mg, 1.06 mmol), compound 2[i] (208 mg, 1.00 mmol) (6), and DMAP [4-(dimethylamino)pyridine] (24 mg, 0.20 mmol) in CH_2Cl_2 (5 ml) at 0°C. The resulting suspension was allowed to warm to room temperature and stirred for 2 h. The suspension was filtered, and the residue was washed with CH_2Cl_2 (5 ml). The combined filtrates were concentrated *in vacuo*. Purification by flash column chromatography (ethyl acetate [EtOAc]/heptane, 1:4; R_f, 0.28) afforded compound 3 (330 mg, 87 %) as a colorless oil.

H-(D-Ala-L-*O*-Val)-OBn · HCl (compound 4). A freshly prepared solution of $HCl_{(g)}$ (i.e., added as a gas by continuous injection in the solution) in EtOAc (2.6 M, 10 ml) was added to a stirred solution of compound 3 (317 mg, 0.83 mmol) in EtOAc (3 ml) at room temperature. The resulting mixture was stirred for 45 min and then concentrated *in vacuo*, to afford compound 4 (261 mg, 99 %) as a colorless viscous oil, which was used without further purification.

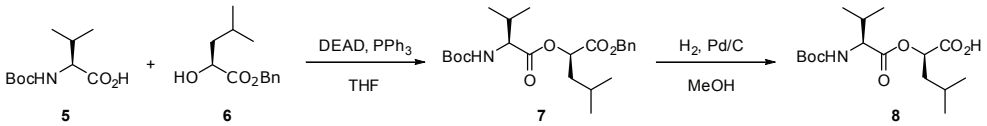

Boc-(L-Val-D-*O*-Leu)-OBn (compound 7). At 0°C, triphenylphosphine (976 mg, 3.72 mmol) was added to a stirred solution of compound 5 (270 mg, 1.24 mmol) and compound 6[ii] (276 mg, 1.24 mmol) in dry tetrahydrofuran (THF) (10 ml). Next, DEAD (diethyl azodicarboxylate) (40 wt % in toluene, 1.70 ml, 3.72 mmol) was added dropwise. The resulting yellow solution was allowed to warm to room temperature and stirred for 1 h. Subsequently, the mixture was concentrated *in vacuo*, redissolved in EtOAc (25 ml), and washed with saturated aqueous $NaHSO_4$ (three 10-ml volumes). The organic phase was dried over Na_2SO_4, filtered, and concentrated *in vacuo*. Purification by flash column chromatography (EtOAc/heptane, 1:9; R_f, 0.25) afforded compound 7 (398 mg, 76 %) as a colorless oil.

Boc-(L-Val-D-*O*-Leu)-OH (compound 8). Palladium on carbon (10 % [wt/wt] Pd, 94 mg, 0.088 mmol) was added to a stirred solution of compound 7 (371 mg, 0.88 mmol) in methanol (MeOH; 10 ml) at room temperature. The resulting mixture was placed under a hydrogen atmosphere and stirred vigorously for 1 h. Next, the mixture was filtered over Celite and concentrated *in vacuo* to afford compound 8 (288 mg, 99 %) as a colorless oil, which was used without further purification.

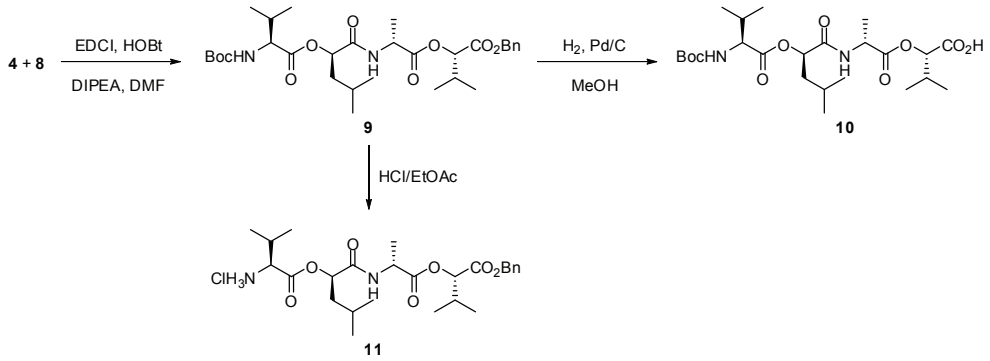

Boc-(L-Val-D-*O*-Leu-D-Ala-L-*O*-Val)-OBn (compound 9). DIPEA (diisopropylethylamine) (0.30 ml, 1.7 mmol) was added dropwise to a stirred solution of compound 8 (225 mg, 0.68 mmol) in DMF (dimethylformamide) (4 ml) at 0°C. Next, HOBt (1-hydroxybenzotriazole) (101 mg, 0.75 mmol) and EDCI [*N*-(3-dimethylaminopropyl)-*N*'-ethylcarbodiimide] (144 mg, 0.75 mmol) were added successively. Finally, a solution of compound 4 (225 mg, 0.71 mmol) in DMF (2 ml) was added dropwise. The resulting mixture was allowed to

warm to room temperature and stirred for 16 h. Next, the mixture was diluted with EtOAc (30 ml). The organic phase was washed with aqueous citric acid (10 % [wt/wt], two times with 5 ml), water (once with 5 ml), saturated aqueous $NaHCO_3$ (two times with 5 ml), water (once with 5 ml), and brine (once with 5 ml), dried over Na_2SO_4, filtered, and concentrated *in vacuo*. Purification by flash column chromatography (EtOAc/heptane, 1:3; R_f, 0.23) afforded compound 9 (250 mg, 62 %) as a colorless oil.

Boc-(L-Val-D-*O*-Leu-D-Ala-L-*O*-Val)-OH (compound 10). Palladium on carbon (10 % [wt/wt] Pd, 13 mg, 0.01 mmol) was added to a stirred solution of compound 9 (72 mg, 0.12 mmol) in MeOH (3 ml) at room temperature. The resulting mixture was placed under a hydrogen atmosphere and stirred vigorously for 1 h. Next, the mixture was filtered over Celite and concentrated *in vacuo* to afford compound 10 (61 mg, 99 %) as a white solid, which was used without further purification.

H-(L-Val-D-*O*-Leu-D-Ala-L-*O*-Val)-OBn · HCl (compound 11). A freshly prepared solution of $HCl_{(g)}$ in EtOAc (2.6 M, 4 ml) was added to a stirred solution of compound 9 (125 mg, 0.21 mmol) in EtOAc (1 ml) at room temperature. The resulting mixture was stirred for 45 min and then concentrated *in vacuo* to obtain compound 11 (106 mg, 95 %) as a colorless viscous oil, which was used without further purification.

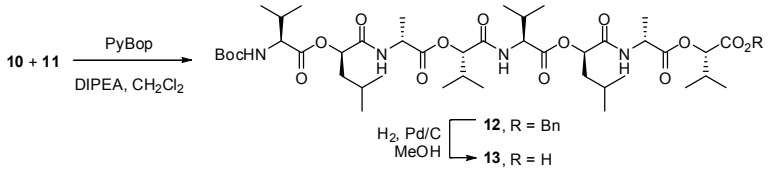

Boc-(L-Val-D-*O*-Leu-D-Ala-L-*O*-Val-L-Val-D-*O*-Leu-D-Ala-L-*O*-Val)-OBn (compound 12). DIPEA (34 µl, 0.19 mmol) was added to a stirred solution of compound 10 (44 mg, 0.088 mmol) in CH_2Cl_2 (2 ml) at room temperature, followed by addition to a solution of compound 11 (48 mg, 0.091 mmol) in CH_2Cl_2 (1 ml). Finally, PyBop [(benzotriazol-1-yloxy)tripyrrolidinophosphonium] (48 mg, 0.092 mmol) was added, and the mixture was stirred for 40 min. Next, the mixture was diluted with EtOAc (15 ml). The organic phase was washed with aqueous citric acid (10% [wt/wt], twice with 5 ml), water (once with 5 ml), saturated aqueous $NaHCO_3$ (twice with 5 ml), water (once with 5 ml), and brine (once with 5 ml), dried over Na_2SO_4, filtered, and concentrated *in vacuo*. Purification by flash

column chromatography (EtOAc/heptane, 1:2; R_f, 0.23) afforded compound 12 (79 mg, 92 %) as a white solid.

Boc-(L-Val-D-*O*-Leu-D-Ala-L-*O*-Val-L-Val-D-*O*-Leu-D-Ala-L-*O*-Val)-OH (compound 13). Palladium on carbon (10 % [wt/wt] Pd, 8 mg, 0.007 mmol) was added to a stirred solution of 12 (72 mg, 0.074 mmol) in MeOH (2 ml) at room temperature. The resulting mixture was placed under a hydrogen atmosphere and stirred vigorously for 1 h. Next, the mixture was filtered over Celite and concentrated *in vacuo* to obtain compound 13 (65 mg, 99 %) as a white solid, which was used without further purification.

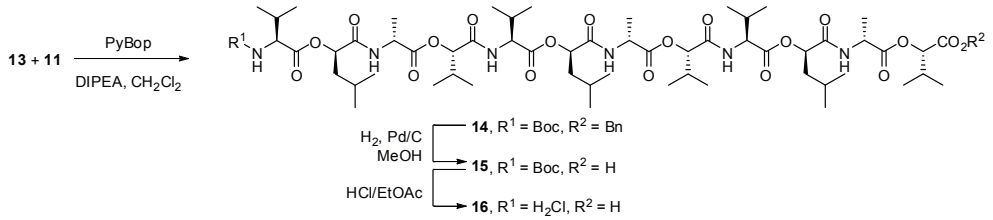

Boc-(L-Val-D-*O*-Leu-D-Ala-L-*O*-Val-L-Val-D-*O*-Leu-D-Ala-L-*O*-Val-L-Val-D-*O*-Leu-D-Ala-L-*O*-Val)-OBn (compound 14). DIPEA (26 µl, 0.15 mmol) was added to a stirred solution of compound 13 (59 mg, 0.067 mmol) in CH_2Cl_2 (1.5 ml) at room temperature, followed by a solution of compound 11 (36 mg, 0.068 mmol) in CH_2Cl_2 (0.75 ml). Finally, PyBop (37 mg, 0.70 mmol) was added, and the mixture was stirred for 1 h. Next, the mixture was diluted with EtOAc (15 ml). The organic phase was washed with aqueous citric acid (10 % [wt/wt], twice with 5 ml), water (once with 5 ml), saturated aqueous $NaHCO_3$ (twice with 5 ml), water (once with 5 ml), and brine (once with 5 ml), dried over Na_2SO_4, filtered, and concentrated *in vacuo*. Purification by flash column chromatography (EtOAc/heptane, 2:3; R_f, 0.26) afforded compound 14 (87 mg, 96 %) as a white solid.

Boc-(L-Val-D-*O*-Leu-D-Ala-L-*O*-Val-L-Val-D-*O*-Leu-D-Ala-L-*O*-Val-L-Val-D-*O*-Leu-D-Ala-L-*O*-Val)-OH (compound 15). Palladium on carbon (10 % [wt/wt] Pd, 6 mg, 0.005 mmol) was added to a stirred solution of compound 14 (78 mg, 0.057 mmol) in MeOH (2.5 ml) at room temperature. The resulting mixture was placed under a hydrogen atmosphere and stirred vigorously for 1 h. Next, the mixture was filtered over Celite and concentrated *in vacuo* to afford compound 15 (72 mg, 100 %) as a white solid, which was used without further purification.

H-(L-Val-D-*O*-Leu-D-Ala-L-*O*-Val-L-Val-D-*O*-Leu-D-Ala-L-*O*-Val-L-Val-D-*O*-Leu-D-Ala-L-*O*-Val)-OH · HCl (compound 16). A freshly prepared solution of $HCl_{(g)}$ in EtOAc (2.6 M, 4 ml) was added to a stirred solution of compound 15 (66 mg, 0.052 mmol) in EtOAc (1 ml) at room temperature. The resulting mixture was stirred for 45 min and then concentrated *in vacuo*, to obtain compound 16 (61 mg, 98 %) as a white solid, which was used without further purification.

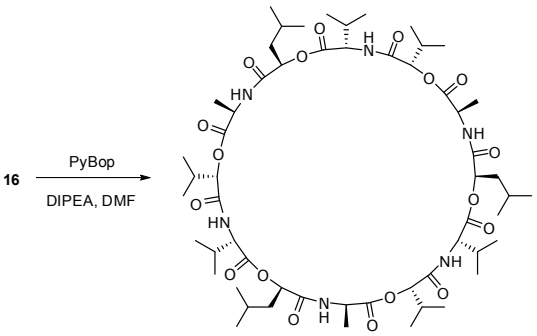

cereulide

Cereulide. DIPEA (22 µl, 0.12 mmol) was added to a stirred solution of compound 16 (50 mg, 0.041 mmol) in DMF (40 ml) at room temperature, followed by PyBop (23 mg, 0.043 mmol), and the mixture was stirred for 16 h. Next, the mixture was diluted with EtOAc (200 ml). The organic phase was washed with aqueous citric acid (10 % [wt/wt]; twice with 50 ml), water (once with 50 ml), saturated aqueous $NaHCO_3$ (twice with 50 ml), water (once with 50 ml), and brine (once with 50 ml), dried over Na_2SO_4, filtered, and concentrated *in vacuo*. Purification by flash column chromatography (EtOAc/heptane, 1:3; R_f, 0.28) afforded cereulide (34 mg, 72 %) as a white solid.

[i] Dinh, T.Q., Du, X., Armstrong, R.W. (1996). J. Org. Chem. 61: 6606–6616.
[ii] Ghosh, A.K., Bischoff, A. (2000). Org. Lett. 2: 1573–1576.

Chapter 7

Kinetics of cereulide production by *Bacillus cereus* F4810/72 as influenced by water activity

Elisabeth G. Biesta-Peters, Martine W. Reij, Han Joosten, Leon G.M. Gorris, Marcel H. Zwietering

Submitted for publication

7

Abstract

Culturing emetic Bacillus cereus *F4810/72 in water activity modified broth caused a delay in onset of cereulide production compared to standard broth. There was a large difference in onset of cereulide production between experiments conducted under identical conditions, which may be explained by variation in growth rate and/or lag phase.*

Some strains of *Bacillus cereus* produce the emetic toxin cereulide, which may cause vomiting upon ingestion (3). Cereulide is a cyclic dodecadepsipeptide and is mainly produced in farinaceous foods such as pastas, noodles and rice dishes (3). Cereulide production is generally considered to commence at the end of the exponential phase, but to be independent of sporulation (2, 4). This research was undertaken to study the kinetics of cereulide production in more detail in relation to cell numbers and/or sporulation under specific culture conditions. The culture conditions studied were Brain Heart Infusion (BHI) broth as control medium and water activity (a_w) modified BHI broth amended by two aw lowering solutes, i.e. sodium chloride (NaCl) and potassium chloride (KCl).

B. cereus F4810/72 was cultured in triplicate in BHI broth (Becton Dickinson and Company; Le Pont de Claix, France) not supplemented with salts, and in BHI broth supplemented with 0.3 M NaCl, 0.7 M NaCl and 0.7 M KCl. A pre-culture of *B. cereus* F4810/72, incubated overnight in BHI broth at 30°C while shaking was added to the broth, to obtain approximately 10^4 cells/ml. The cultures were then incubated at 30°C while shaking and samples of the time points 0 h to 32 h were taken. *B. cereus* was enumerated by plating on BHI agar plates (BHI broth supplemented with 1.5 % bacteriological agar, Oxoid, Basingstoke, Hampshire, England). Samples were enumerated in duplicate. The growth curves obtained with non-supplemented BHI and BHI with 0.3 M NaCl are displayed in Figure 1A. Part of each sample taken was heated at 70°C for 15 minutes before plating, to determine the number of spores. On the basis of the cell counts the maximum specific growth rate (μ_{max}) and the lag phase (λ) were determined using the modified Gompertz equation (Equation 1) (7).

$$\ln\left(\frac{N_t}{N_0}\right) = A\,\exp\left\{-\exp\left[\frac{\mu_{max}\mathrm{e}}{A}\left(\lambda - t\right)+1\right]\right\} \qquad (1)$$

The μ_{max}-values and λ-values derived for the four conditions tested and their standard deviations are provided in Table 1 and incorporated in Figure 2 A. The standard deviations observed are comparable to the within-strain-variability as observed in literature (6). Addition of 0.3 M NaCl to the BHI led to a reduction of μ_{max} but had no influence on the length of the lag phase. At 0.7 M NaCl μ_{max} was further reduced and a longer lag phase was observed. The results of equal concentrations of NaCl and KCl were comparable. Less

than 1 % of the total population was present as spores for all conditions tested, once the cells had entered the stationary phase (data not shown). The average, minimum and maximum time for the bacteria to multiply from the initial level of approximately 10^4 cells/ml to a level of 10^9 cells/ml was calculated for every condition using the modified Gompertz equation (Equation 1) and the average parameter or the average parameter plus or minus their standard deviation. These results are also given in Table 1. For BHI the time difference due to variations in parameters of a culture to reach 10^9 cells/ml can be up to 2 h. For BHI supplemented with 0.3 M NaCl, 0.7 M NaCl or 0.7 M KCl this was calculated to be around 1.5 h, 6 h and 12 h, respectively.

Table 1. Maximum specific growth rates and lag phase durations, with standard deviations, for *B. cereus* F4810/72 cultured at 30°C in BHI and in BHI supplemented with either 0.3 M NaCl, 0.7 M NaCl or 0.7 M KCl; minimal and maximal time to reach stationary phase (10^9 cells/ml), and average time to onset of cereulide production

Condition	μ_{max} (h^{-1}) (SE)[a]	λ (h) (SE)[b]	time (h) to 10^9 cells/ml using average parameter estimates	Minimal time (h) to 10^9 cells/ml	Maximal time (h) to 10^9 cells/ml	Onset of cereulide production (h) (SE)[c]
0 M salt	3.22 (0.54)	2.78 (0.50)	6.36	5.35	7.58	20.2 (4.0)
0.3 M NaCl	2.47 (0.26)	2.61 (0.23)	7.27	6.59	8.05	21.7 (4.2)
0.7 M NaCl	1.27 (0.28)	5.72 (0.67)	14.79	12.48	18.03	25.3 (2.3)
0.7 M KCl	1.08 (0.20)	4.02 (4.26)	16.43	10.49	23.13	25.3 (2.3)

[a] Maximum specific growth rate with standard deviation in parentheses

[b] Lag phase with standard deviation in parentheses

[c] Average time of onset of cereulide production with standard deviation in parentheses

Samples for cereulide quantification were collected in triplicate from the cultures every hour from 13 h up to 26 h for 0 M salt and 0.3 M NaCl, and up to 28 h for 0.7 M NaCl and 0.7 M KCl. Three sets of additional experiments were performed focusing on the detection of the onset of cereulide production, but not following cereulide production further in time. Cereulide was extracted from the samples, and the sample vials and standards were prepared as previously described (1). The extracts were analyzed on an ion trap LC-MS (liquid chromatography-mass spectrometry, Thermo Scientific LTQ XL setup, Waltham, MA) using a method based on the methods described by Häggblom *et al*. (4) and by Thorsen *et al*. (5). Ten µl extract was injected onto the column (Aquity UPLC BEH 300, C4 1.7 µm 2.1×100 mm, Waters, Dublin, Ireland), and eluted at a flow rate of 0.3 ml/min using the positive electrospray ionization mode. Milli-Q water (Biosolve ULC/MS grade, Valkenswaard, The Netherlands) with 10 mM additional NH_4^+ (added as ammonium formate, Fluka Chemie GmbH, Buchs, Switzerland) and 20 mM additional formic acid

(VWR international, Fontenay-sous-Bois, France), and acetonitrile with 20 mM additional formic acid were used as eluents. The peak surface of the cereulide adduct (m/z 1,170.7) was determined on the basis of the LC-MS output registration and related to the peak surfaces of the calibration curves of the standards with known concentrations.

Figure 1B shows the effect of the addition of 0.3 M NaCl to the BHI broth on the time to onset of cereulide production, as compared to non-supplemented BHI broth. It was observed that the cereulide production was delayed by the addition of NaCl and that the increase of the cereulide level was slowed down. Figure 1C displays the cereulide production on a log scale, including the detection limit of the LC-MS of 0.3 ng /ml. For non-supplemented BHI it can be observed that the first time point above the detection limit is to be expected after 14 h, considering the trend of cereulide production. The production of cereulide for *B. cereus* F4810/72 therefore seems to commence in the stationary phase of the culture, which can be derived from Figure 1A. The average cereulide level at the average first time point showing production was 1.9 ng/ml at t = 18 h for non-supplemented BHI and 1.8 ng/ml at t = 20 h for BHI supplemented with 0.3 M NaCl. The level of cereulide reached after 24 h in non-supplemented BHI was around 50 ng ml^{-1}. The variability in cereulide levels observed are comparable to the variability in cereulide levels as observed by Dommel *et al*. (2), who also reported a reduction in cereulide levels due to the addition of salt.

The times to onset of cereulide production are depicted in Figure 2 A, which shows that the times to onset were variable, even for identical, standardized, culture conditions. Out of six experiments for BHI supplemented with 0.7 M NaCl or 0.7 M KCl cereulide was detected twice during the course of the experiment. There was no measureable effect on the time to onset of cereulide production for the use of either NaCl or KCl at equal concentrations. For BHI without supplements, the earliest time point at which cereulide production was observed was 13 h whereas the latest time point was 23 h. Such a variety was also observed for the other conditions, i.e. 0.3 M NaCl, 0.7 M NaCl and 0.7 M KCl, for which the variety was about 12 h, 5 h and 5 h, respectively. The variability in the time to onset of cereulide production and in the levels measured may be caused by the variability of the parameters for growth between various experiments. In our experiments there was a time difference of 13.8, 14.4, 10.5, and 10.6 h between reaching stationary phase and cereulide production in BHI supplemented with 0 M salt, 0.3 M NaCl, 0.7 M NaCl and 0.7 M KCl, respectively.

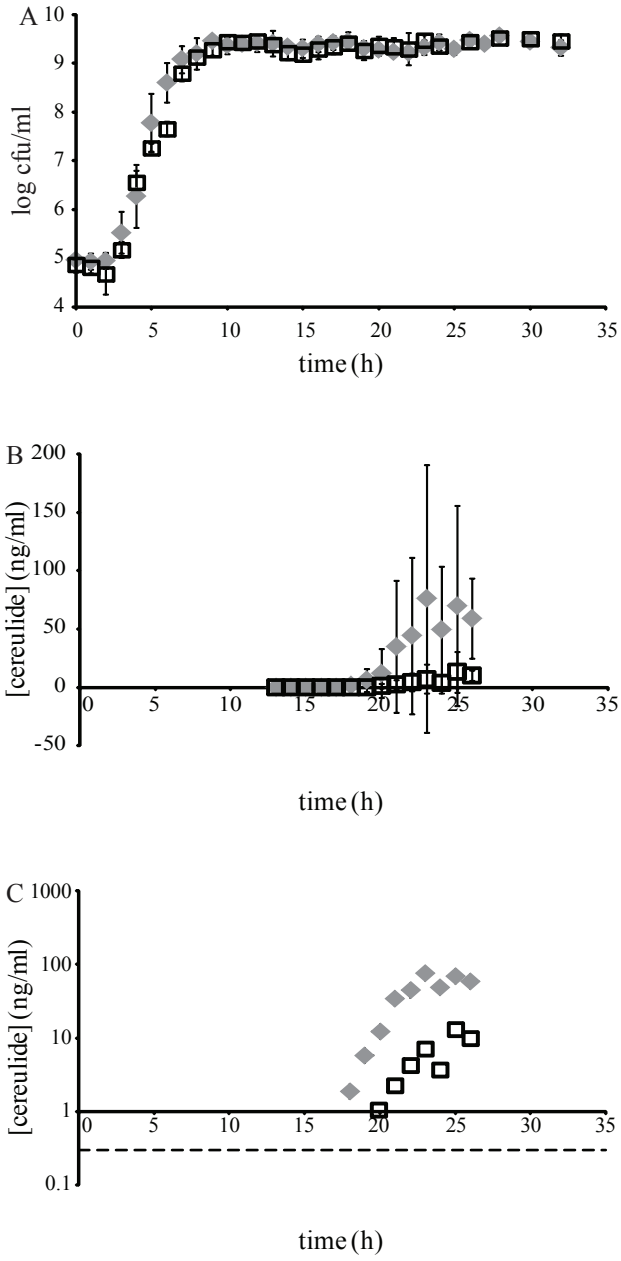

Figure 1. Cell levels (A), cereulide production (B) and cereulide production on log scale with detection limit of the LC-MS (dashed line) (C) over the course of incubation time for *B. cereus* F4810/72 cultured at 30°C in BHI broth (◆) and BHI broth supplemented with 0.3 M NaCl (□).

Comparing the average time to reach stationary phase to the average time to cereulide production it can be concluded that there is at least a 10 h time difference between these two stages. Figure 2B shows that for the tested conditions there is a linear correlation between the decrease in average μ_{max} values and the increase in average time to cereulide production for increasing salt concentrations.

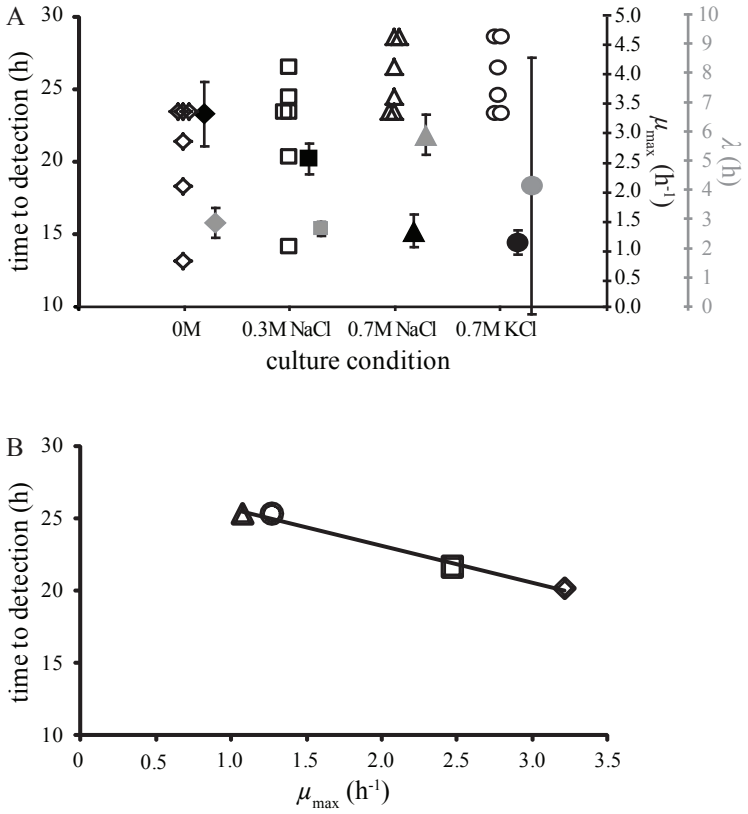

Figure 2. First onset of cereulide production (open symbols), maximum specific growth rate (black closed symbols) and lag time (gray closed symbols) (A) and average time to cereulide detection as a function of the average maximum specific growth rate (B) for *B. cereus* F4810/72 cultures cultured in BHI broth without supplements (◇), and BHI broth supplemented with 0.3 M NaCl (□), 0.7 M NaCl (Δ) or 0.7 M KCl (○).

It can be concluded that an increase in salt concentration causes a decrease in maximum specific growth rate, which is linearly correlated to the increase in onset of cereulide production for our tested strain. Once cereulide production commences for *B. cereus* F4810/72, the cells are in their stationary phase. Variations in growth parameters, as observed, can cause variations in onset of cereulide production and measured levels. A link to the level of sporulation could not be made. Therefore it can be concluded that the presence of *B. cereus* F4810/72 poses a realistic risk only when the cells are in their stationary phase and cereulide is starting to be formed, which depends again on the prevailing μ_{max} and λ of the population concerned. This observation should however not be generalized, Firstly, this assumption might not be valid for all toxigenic strains of *B. cereus*. Secondly, because the presence of other micro-organisms in food products will limit the level of *B. cereus* cells reached in the stationary phase this might have consequences for the cereulide production. Thirdly there will be medium/food commodity effects. The main target for food safety should therefore be to avoid the presence and growth of *B. cereus* in food products. If cells are nevertheless present, cereulide production can be prevented by delaying the onset of growth and/or by reducing the rate of proliferation, in order to delay the time of the culture to reach stationary phase and to start subsequent cereulide production.

Acknowledgments

This work was financially supported by Nestlé Research Centre, Lausanne, Switzerland. Mark Sanders is acknowledged for technical assistance with the LC-MS experiments.

References

1. **Biesta-Peters, E. G., M. W. Reij, R. H. Blaauw, P. H. in 't Veld, A. Rajkovic, M. Ehling-Schulz, and T. Abee.** 2010. Quantification of the emetic toxin cereulide in food products by liquid chromatography-mass spectrometry using synthetic cereulide as a standard. Appl. Environ. Microbiol. 76:7466-7472.

2. **Dommel, M. K., G. Lücking, S. Scherer, and M. Ehling-Schulz.** 2011. Transcriptional kinetic analyses of cereulide synthetase genes with respect to growth, sporulation and emetic toxin production in *Bacillus cereus*. Food Microbiol. 28:284-290.

3. **Granum, P. E., and T. Lund.** 1997. *Bacillus cereus* and its food poisoning toxins. FEMS Microbiol. Lett. 157:223-228.

4. **Häggblom, M. M., C. Apetroaie, M. A. Andersson, and M. S. Salkinoja-Salonen.** 2002. Quantitative analysis of cereulide, the emetic toxin of *Bacillus cereus* produced under various conditions. Appl. Environ. Microbiol. 68:2479-2483.

5. **Thorsen, L., B. B. Budde, L. Henrichsen, T. Martinussen, and M. Jakobsen.** 2009. Cereulide formation by *Bacillus weihenstephanensis* and mesophilic emetic *Bacillus cereus* at temperature abuse depends on pre-incubation conditions. Int. J. Food Microbiol. 134:133-139.

6. **Zwietering, M. H., J. T. de Koos, B. E. Hasenack, J. C. de Wit, and K. van 't Riet.** 1991. Modeling of bacterial growth as a function of temperature. Appl. Environ. Microbiol. 57:1094-1101.

7. **Zwietering, M. H., I. Jongenburger, F. M. Rombouts, and K. van 't Riet.** 1990. Modeling the bacterial growth curve. Appl. Environ. Microbiol. 56:1875-1881.

Chapter 8

Summarising discussion

8

Introduction

Consumers expect to buy food that is safe and tasty within its given shelf life. In order to prevent or limit microbial growth resulting in spoilage or unsafe conditions, different preservatives can be added to the product or growth inhibiting conditions can be ensured in (e.g. low a_w, low pH) and around (e.g. low temperature, modified atmosphere) the food. Also combinations of such growth inhibiting factors (hurdles) can be used to achieve this, allowing the intensity of every single hurdle to be lower than when used individually, whilst still achieving the same overall effect (23). The quantification of the impact of the combined hurdles is still under discussion, since there are two different views on how the factors combine. One view considers that there is no synergy between the hurdles, the so called gamma hypothesis (37), while the other view states that there is synergy occurring between the hurdles. The occurrence of synergy might not be consistent, but might be dependent on the type of microorganism targeted or the specific combination of hurdles used. Table 1 gives an overview of literature reporting on the effect of combined hurdles on microbial growth.

Table 1. Literature overview of combinations of hurdles and their effect on microbial growth

Hurdles	Microorganism	Synergy?	Reference
pH, a_w, temperature	*Listeria monocytogenes*	Yes	(4)
Heating & low pH, HHP & mild heating	*Clostridium botulinum*	Yes	(13)
Salt, pH, weak acid	*Aeromonas hydrophila*	No	(18)
Weak acids, pH, salt, temperature	*Cronobacter* spp.	No	(19)
Temperature, pH, organic acids	*Listeria innocua*	Yes	(22)
Temperature & pH, Temperature & a_w	Not specified	Yes (at boundary)	(27)
Heat, nisin	*Listeria monocytogenes*	Yes	(28)
Temperature, a_w, sodium nitrite	*Escherichia coli*	Yes	(30)
Temperature, pH, a_w	*Listeria monocytogenes*	No	(33)
Nisin, ultrahigh-pressure treatment	*Lactobacillus plantarum* *Escherichia coli* *Saccharomyces cerevisiae*	Yes	(34)
Lactic acid, monolaurin, nisin	*Listeria monocytogenes*	Yes	(35)
Temperature, a_w, pH	*Lactobacillus curvatus*	No	(36)
pH, a_w, temperature, oxygen availability	Several	No	(37)

The overall aim of the project was to examine the gamma hypothesis for microbial growth for the microorganism *Bacillus cereus*. Additionally, the effect of the hurdle water activity (a_w) on the production of the emetic toxin cereulide produced by *B. cereus* F4810/72

was investigated. Several new lines of research were set-up to achieve these aims. This chapter provides an integrated discussion of all research topics addressed and focuses on the implication of the results for future research and for application in food safety management by government and food industry.

Gamma hypothesis for growth

The definition of synergy

The definition of synergy is of key importance when discussing its occurrence. When reducing microbial growth by two hurdles such as pH and a_w, the growth rate will be logically lower when both hurdles are present simultaneously, as compared to one of the hurdles, such as only pH, being present as a single hurdle at the same intensity as in the combined situation. Often this reduction in growth rate is defined as synergy, while the effect could be simply multiplicative. This might be better visualized when picturing an athlete with glue to his/her shoes while running, and running with the wind blowing in his/her face. Clearly the athlete will run much faster when it is a nice windless summer day, but the reduction in running speed is not caused by synergy when both the glue and the wind are present, but simply by a multiplication of factors. When the air temperature would however cause the glue to become stickier, and this was not included as a parameter when predicting the speed of the athlete, the speed of the athlete is even further reduced, which can be considered synergy. The definition of synergy is amongst others discussed by Lambert *et al*. (20) and Berenbaum (5, 6). Lambert *et al*. (21) suggests that no synergy occurs as long as the dose-responses of the used hurdles (in this case antimicrobials) are equal. The authors in fact advocate that the emphasis within the literature of seeking interactions or synergies between environmental factors should be replaced with emphasizing the falsification of the gamma hypothesis. They suggest doing this by examining the relative ratios of the gamma factors for hurdles applied in combination as compared to their single use (7), as was done in this thesis. Although the results obtained in this thesis confirm that conclusions on synergy cannot always be made consistently and unequivocally, the best way forward is believed to be the combination of systematic selection of single hurdle models based on pre-set criteria and adherence to a science-based definition of synergy. An open discussion about the definition of synergy is therefore of utmost importance, next to testing of the hypothesis.

Model selection for gamma hypothesis validation

Information about the existence of synergy will limit the need for extensive challenge testing of different combinations of hurdles in different amounts for application in food industry, in order to reveal possible interactive effects. Therefore, throughout literature gamma hypothesis validation is a recurrent topic. So far no conclusive results are presented about the validity, which might be caused by the different models used to describe the growth data and to validate the hypothesis for combined effects of hurdles. For example, the best model to describe the effect of undissociated acid on μ_{max} of *B. cereus* is the model of Luong (24) (Equation 1) according to our study in Chapter 4.

$$\mu_{max} = \mu_{opt}\left[1 - \left(\frac{[HA]}{[HA]_{max}}\right)^{a}\right] \quad (1)$$

This model was selected as the best model based on two criteria: it showed the lowest MSE of all models tested and the standard deviations of the parameter estimates were lower than the estimate itself. Le Marc *et al*. (22) uses another model to describe the undissociated acid effect for *Listeria innocua* (Equation 2).

$$\mu_{max} = \mu_{opt}\left(1 - \sqrt{\frac{[HA]}{[HA]_{max}}}\right) \quad (2)$$

When fitting both of these models to the same data set of *B. cereus* testing the effect of undissociated acetic acid (HAc) on μ_{max}, the MSE between data and fit is 0.0014 for Equation 1 and 0.0028 for Equation 2. As shown in Chapter 5 (Table 3) of this thesis, the choice for non-optimal models for single hurdles does usually not result in a better description of the combined effect compared to the use of optimal single hurdle models. This might be the reason why a synergy factor improves the prediction in the case of Le Marc *et al.*, while an equally good result could possibly have been obtained using another model, e.g. Equation 1, for the hurdle undissociated acid concentration.

In general, single hurdle models are not systematically selected from a list of available models, as was done in this thesis. They are chosen because they have a (reasonably) good fit, and no selection is made based on pre-set criteria such as the lowest MSE-value for the fit to the data across available models. It is recommended that

for future studies, a systematic approach is indeed used for model selection, which may allow for more conclusive results about the occurrence of synergy.

This study did not investigate the possibility of designing new single hurdle models. This might be necessary as well for gamma hypothesis validation. In the case of Figure 1A, for instance, it is clear that the effect of NaCl, in BHI medium of pH 6 causes a cliff edge effect at near growth boundary conditions. Figure 1B shows the effect of NaCl of pH 7 where no such a cliff edge is visible, but a smooth and gradual transition to no growth.

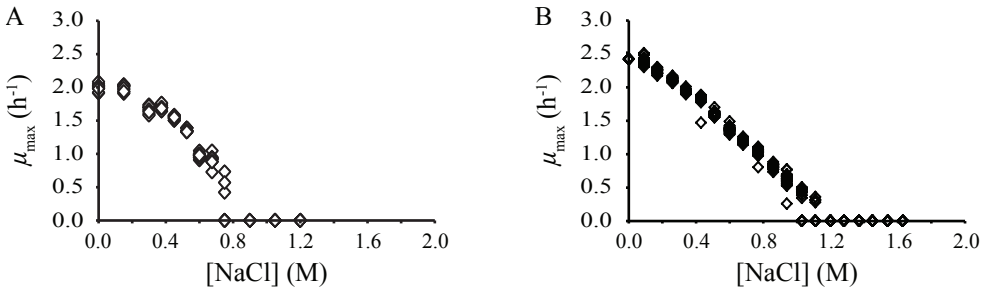

Figure 1. Specific growth rate data for the effect of concentrations of NaCl when cells are cultured in BHI medium at pH 6 (A) and pH 7 (B).

A 'cliff edge' is defined as the abrupt transition from growth to no growth caused by slight changes of growth influencing compounds and/or conditions (26). Cliff edges were also detected for the combined effects of NaCl or KCl with nisin when culturing *Listeria monocytogenes* Scott A (8). The prediction of the pH model of Luong is for Figure 1A not complying with the set criteria of an MSE-value below 0.01, since the MSE value is 0.08. The MSE value of Figure 1B using the same model of Luong is 0.006. This non-compliance in the first case is due to the fact that the model is not able to predict this cliff edge. For the future it would therefore be advisable to develop suitable new models that are able to describe microbial phenomena such as cliff edges. The current models seem to work satisfactorily for common and expected shapes of growth rate curves, but are not able to describe deviations from these, thereby introducing locally large errors when predicting microbial behavior. Since microorganisms may react differently in response to different stresses and to different food conditions as compared to standardized laboratory experiments, it is of key importance that such atypical behavior can be described by predictive models.

Hurdles and parameters for growth

Mode of action of hurdles and possible synergy

Some combinations of preservatives and other hurdles have been shown to have synergistic effects. The combination of high pressure and heat is such a combination, where the synergy is caused by the fact that pressure causes spores to germinate and the heat subsequently kills the germinated spores (13). Just application of heat or heat combined with another preservative would not have had the same effect. Also the combination of nisin with ultrahigh-pressure (UHP) treatment showed strong synergistic effects against *Lactobacillus plantarum* and *Escherichia coli* at reduced temperatures (<15°C). The assumed mode of action was that the reduced temperature or the addition of nisin affected the membrane fluidity and permeability, respectively, and therefore increased the efficacy of UHP treatment (34). A combination of nisin and heat was also reported to show synergistic effects on *Listeria monocytogenes* (28). Nisin makes pores (protein channels/holes) in the membrane causing leakage/permeability of the membrane. Heat and cold affect lipid composition and subsequent membrane characteristics including fluidity. The use of (weak-organic) acids induces other effects. Undissociated acids entering the cell will dissociate once inside and will cause the pH homeostasis systems to fail, which causes the internal H^+ concentration to rise to lethal levels (12). The accumulation of anions and protons inside the cell have been described to cause membrane disruption, inhibition of essential metabolic reactions, and stress on intracellular pH homeostasis (9). The addition of salt to growth medium results in a higher osmotic pressure outside the cell compared to the internal osmotic pressure in bacterial cells. Usually the internal pressure is higher (turgor pressure), exerting mechanical force for cell shape and elongation. A higher osmotic pressure outside the cell causes loss of cytoplasmic water, which requires accumulation of (preferably compatible) solutes, allowing uptake of water and restoration of turgor (2).

When assessing synergy, it is important to understand the mechanism(s) of action of the individual factors (6) and to understand whether or not these individual factors exert the same inhibitory impact at the same concentration, i.e. whether the factors have an identical response (21). The differences in modes of action might be an explanation for the occurrence of synergy. In case two different combined hurdles affect the same processes in the cell, they may be counteracted by the same homeostasis mechanism of the cell and then the effect can be multiplicative and they are not enforcing each other.

The cell does not have to divide the energy over different processes, but can spend the energy very efficiently on one process. When combinations affect different sites in the cell, for example nisin which influences membrane fluidity and pH which affects the pH homeostasis, it is can be more likely that synergistic effects occur. A bacterial cell trying to maintain membrane fluidity can spend less energy on maintaining osmotic pressure, considering there is limited availability of energy, and therefore it is likely that less high concentrations of compounds are needed to cause a lethal effect. The identical modes of action of pH and undissociated organic acids are therefore not expected to result in a synergistic effect, which is confirmed in Chapter 4, where no synergistic effects were apparent for combinations of these two hurdles.

Use of H_2SO_4 or HCl when investigating pH effects on growth

To investigate the effect of pH on μ_{max}, sulfuric acid (H_2SO_4) was chosen throughout this thesis to set the pH. Other strong acids could possibly also have been used to set the pH. It was tested if another acid, hydrochloric acid (HCl), initiated the same effects on μ_{max}, or if the sulfate or chloride ion initiated different effects on the growth of the culture. For example the chloride anion can bind to metallic elements in the medium which are required for growth, causing precipitation, or limit the bioavailability (15). Chloride ions are also known to inhibit phospholipid hydrolysis in *B. cereus* at concentrations of 25-200 mM, while the bivalent anion SO_4^{2-} was relatively ineffective at 100 mM (1). The effect of both H_2SO_4 and HCl on μ_{max} is presented in Figure 2A. As can be observed, the effects of both acids are in the same range and no effect of the chloride ion is observed. In order to avoid an effect on phospholipid hydrolysis and therefore on metabolic processes and growth, H_2SO_4 was used for further investigations in this thesis.

Use of strong and weak organic acids on growth parameters

Although the difference between the use of H_2SO_4 or HCl, both strong acids, on the growth rate is not apparent, the difference between strong acids and weak organic acids is much more pronounced. Whereas a boundary pH of 4.8 is defined for the use of H_2SO_4, the boundary pH for the use of lactic acid is 5.3, as shown in Figure 2B. Apart from the difference in growth boundary a cliff edge can be observed for the use of lactic acid, whereas this is absent for the use of sulfuric acid. This difference in growth boundary is caused by the only partial dissociation of the lactic acid when added to a liquid culture in

growth medium. The existing undissociated part is also toxic to the cells and this causes an increase of the boundary to a higher pH value.

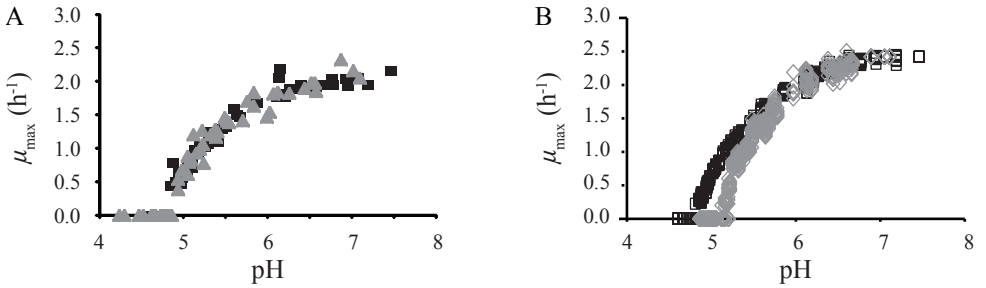

Figure 2. A: Effect of pH set with H_2SO_4 (■) and HCl (▲) on the maximum specific growth rate of *B. cereus* F4810/72, and B: Boundary pH and maximum specific growth rate of *B. cereus* F4810/72 affected by H_2SO_4 (□) and HLa (◇).

Interestingly, the use of strong or weak organic acids have identical effects on the processes in the cells in the lag phase and during onset to growth at their near growth boundary conditions, as shown in Chapter 3 of this thesis. The only difference is observed in the length of the lag phase at near growth boundary conditions, which is around 2 h for the use of H_2SO_4 and around 5h for the use of HLa. Identification of the processes during lag phase and onset to growth can be used to prevent microorganisms coming out of the lag phase. For example, it is shown that esterase activity, by means of low internal pH, and electron transport chain activity are increasing when the cells are entering the growth phase. Blocking these two mechanisms might prevent that microorganisms successfully enter the growth phase.

Effect of increased lag times on the use of the optical density methods

The observation that lag times increase at near growth boundary conditions is of importance for the method used to determine values for μ_{max}. In our study, the relative rate to detection (RRD) method was chosen because it allowed for the collection of larger datasets, as compared to the 2-fold dilution (2FD) method for which serial dilutions had to be made, needing more wells per test conditions. The latter method was able to distinguish between the parameters μ_{max} and λ, whereas the RRD method only determines μ_{max}. The effect of increasing lag phases at near growth boundary conditions using the RRD method is however not quantified. It was assumed that the increase in λ was proportional

to the decrease in μ_{max}, which made it not necessary to distinguish between these two parameters. A plot of the effect of H_2SO_4 on μ_{max} and λ (Figure 3A) however shows that λ increases to high levels at near growth boundary conditions. Although a plot of μ_{max} versus $\mu_{max} \times \lambda$ (Figure 3B) does give a scattered view of the dat apoints, it looks like there is a linear relationship, except for values approaching the growth boundary.

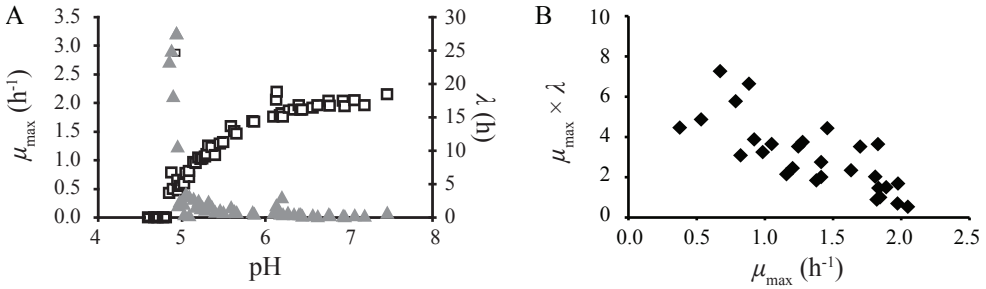

Figure 3. A: Values for μ_{max} (□)and λ *(▲)* for *B. cereus* F4810/72 when cultured in BHI at various pH values (set using H_2SO_4) and B: relation between μ_{max} and $\mu_{max} \times \lambda$ for the same culture conditions (◆).

The use of the two-fold dilution method at near growth boundary values at the other hand is no option, since due to the low numbers at the lowest dilution, the standard error for the estimate of λ and μ_{max} is very high, and the reliability of the estimates are therefore comparable to the use of the RRD method. The RRD method is therefore the method preferred to use, since λ and μ_{max} are mostly linearly correlated. However, most food products contain hurdles in the smallest levels possible but still disabling microbial growth. When creating near growth boundary conditions, the risk of fail dangerous predictions by underestimating the growth rates should be avoided, and this might occur when not taking into account the effect of increased lag phases. Therefore the plate count method will remain necessary to investigate the growth rate at the growth boundary, to avoid fail dangerous predictions by OD methods at the growth boundary.

Toxin formation

Use of a cereulide standard for quantification

It is of importance to have a good cereulide standard for accurate quantification. When medium and growth variability introduce uncertainty about the amount of cereulide produced, the uncertainty about the actual level and the estimated toxic dose should be as low as possible. Although valinomycin, used as a standard for cereulide quantification, structurally resembles cereulide, this study, as well as Häggblom *et al*. (14), proved that there is indeed a 10 % under-estimation in cereulide levels when using a valinomycin standard instead of a cereulide standard. Cereulide standards were not commercially available at the onset of this thesis, but synthesis routes had been described in literature. Isobe *et al*. (16) reported a synthesis route of 14 steps (16), and the synthesis route by Makarasen *et al*. (25) consisted of 14 steps with an overall yield of 23 %. The proposed synthesis route in this thesis for synthetic cereulide consisted of 10 steps and had an overall yield of 28.5 %, representing a significant improvement of the yield within fewer steps. This synthetic cereulide can now be obtained commercially. The standard can be used to quantify cereulide levels as real values, instead of expressing the level as valinomycin equivalents. Due to the commercial availability, it is recommended that this standard is used in all future cereulide research.

Effect of medium on cereulide production

Production of cereulide by emetic *B. cereus* has been studied previously (3, 14, 17, 31), and Figure 4 represents the effect of the type of liquid medium and growth conditions on cereulide production for two different strains of *B. cereus*. The toxin production is depending on static or shaken incubation, but it is also strain dependent. Often TSB is used for cereulide quantification because of the height of the obtained toxicity titers, but also other media such as skimmed milk media or complete amino acid defined medium (CADM) allow for the production of cereulide. Comparing the effect of BHI and TSB for equal culturing conditions and incubation time shows that the obtained level of cereulide is equal. In order to compare and relate the results of our cereulide research to the microbial growth data in this thesis, it was therefore decided to use BHI broth to investigate the effect of a_w lowering solutes on cereulide production. Figure 4 illustrates that the medium source and the incubation conditions all have an impact on cereulide production. When evaluating the results of our study and regarding real life cases and

outbreaks, it thus has to be taken into account that the type of broth or food product may have a considerable impact on the cereulide production and therefore on the validity of conclusions about risks associated with contaminated food products.

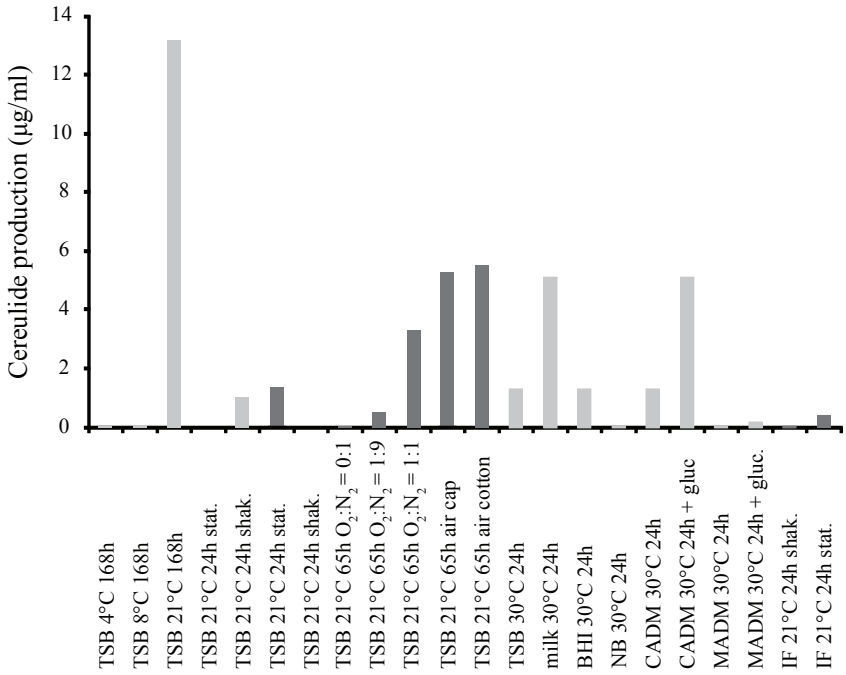

Figure 4: Effect of culture conditions on cereulide production of *B. cereus* NC7401 (light gray bars) and *B. cereus* F4810/72 (dark gray bars), selection of data from Agata *et al*., Häggblom *et al*., Jääskeläinen *et al*., and Shaheen *et al*. (3, 14, 17, 31).

Onset of cereulide production

Chapter 7 of this thesis concludes that the time to onset of cereulide production is dependent on the growth parameters of the culture. Even under optimally standardized conditions in a laboratory environment, the parameters μ_{max} and λ are variable, influencing the time to reach stationary phase. Since toxin production is thought to commence in cells that are at least 10 h in stationary phase, these growth parameters therefore also impact on the time point where cereulide production starts. The start of cereulide production in the stationary phase was also reported by Dommel *et al*. and Häggblom *et al*. (10, 14). It was also reported that cereulide production is independent of sporulation, although cereulide synthesis is part of the Spo0A regulon (10). In our study low levels of spores

(< 1 % of the total level of cells) were observed, but the onset of production of spores was not found to be related to the onset of cereulide production. The difference in time to onset of sporulation and cereulide production is not the proof that both processes are not related. Rather, the set-up of the research in this thesis does not allow for conclusions on this topic, but future studies might focus on this relationship. Both sporulation and cereulide production are unwanted processes in food products. A relation between both processes might make it easier to stop both unwanted phenomena, since interference with one will also affect the other.

It can be discussed if cereulide production starts already before the stationary phase but is still below the detection limit at earlier time-points. In the latter case cereulide production would be related to cell numbers and would not be growth phase dependent. In order to study this hypothesis Figure 5 was constructed.

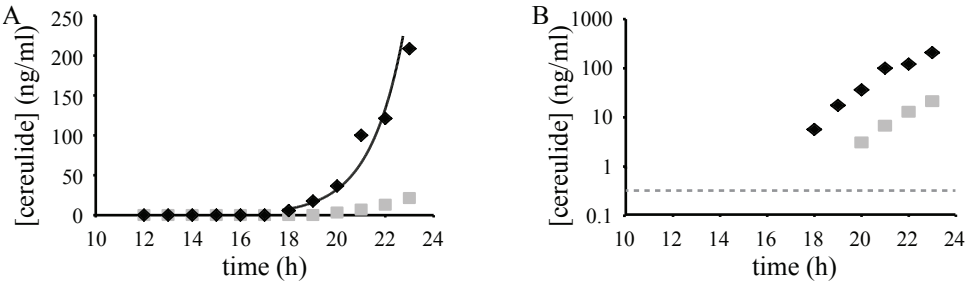

Figure 5. A: Cereulide production in time in *B. cereus* cultures in non-supplemented BHI broth (◆) and BHI broth supplemented with 0.3 M NaCl (■). The black line represents the trendline through the datapoints for non-supplemented BHI broth. B: Cereulide production as in Figure 5A, but plotted on a logarithmic scale, including cereulide detection limit (gray dashed line).

Figure 5 shows that once cereulide production commences for non-supplemented BHI, the production occurs exponentially. The addition of 0.3 M NaCl to the medium delays the time of onset of production and reduces the speed of production. Considering the first condition, standardised medium without supplements, the cells have reached stationary phase, defined as a level of 10^9 cells, after approximately 6.5 h, as calculated in Chapter 7 of this thesis. Since cereulide production shows exponential increase once commencing, an exponential trendline (Equation 3) can be drawn through the datapoints indicating cereulide production.

$$[\text{cereulide}] = 2 \times 10^{-5} e^{0.7092\,t} \quad (3)$$

Where *t* is the incubation time of the culture. Extrapolation of the line to the starting point of the stationary phase (t = 6.5 h) indicates that 0.002 ng/ml might be present at this time point. This level is too low to be measured, since the calibration curve covers the range of 0.3-7.5 ng/ml. The lowest quantifiable level of 0.3 ng/ml should be reached after 13 hours, as calculated per Equation 3. From Figure 5B, with the production of cereulide plotted on a logarithmic scale, it can be observed by extrapolation of the line to the detection limit that the first cereulide will be detected around 13 to 14h after inoculation of the culture. The fact that cereulide production occurs exponentially at equal cell concentrations can indicate that once cereulide production starts the cereulide itself triggers the speed of production. On average, the first cereulide production is measured after 20 hours of incubation. It can therefore be derived from our research that cereulide production occurs in mid- to end-stationary phase and is growth stage dependent for the strain tested.

The reason that some studies conclude that cereulide production occurs at the end of the exponential phase may be due to differences in measurement of the growth curve. When basing the conclusions on OD measurements, for instance, this will give a different conclusion as compared to using plate counts. Due to elongation/stretching of cells when they are no longer multiplying, the OD still rises while counts have already become stable. Before concluding about the growth stage supporting cereulide production, evidently, the experimental set-up and methodologies used should be better standardized.

Cereulide production in food

The results in this study are based on one strain (*B. cereus* F4810/72), and might not be representative for all emetic *B. cereus* strains. Moreover, these experiments were conducted in a laboratory environment in BHI broth, and even the same microorganism might act differently in a specific food environment. It was for example shown that *B. cereus* F4810/72 was able to produce cereulide in rice supplemented with salt in concentrations normally eliminating growth completely (data not shown). Due to uneven distribution of

salt in the rice, growth and cereulide production might still occur locally, while according to calculations it should not be possible. There are also differences observed between cereulide production in liquid media or on solid medium (32). As well, the cultures do not necessarily have to reach 10^9 cells before reaching stationary phase, since this level in the stationary phase might be lower due to nutrient limitations in the food product. Many factors affect the final level of microorganisms able to produce cereulide, and the growth phase allowing cereulide production might be different for different species. Our results do however show that for the investigated strain cereulide is produced in the stationary phase. If this holds for the other strains as well, it may be assumed that it is very unlikely that actively growing cultures are able to produce cereulide in a food product, and that foods will be showing signs of spoilage before *B. cereus* cultures have reached stationary phase. This in turn would mean that the presence of cereulide in foods does indicate serious abuse of the food product, since bacterial cells need temperatures higher than refrigerator temperatures to multiply, and they need considerable time to reach stationary phase and at least 10 hours should have passed once reaching stationary phase before cereulide production starts. These conditions do usually not occur in foods produced using good hygienic practices and with HACCP in place. The reported cases are indeed often related to catering events for large groups (11, 29), where food is prepared at least one day before consumption, warmed and presented au-bain-marie for prolonged times. Prevention of emetic toxin food poisoning outbreaks should therefore focus on good hygienic practices for food caterers, and the current maximum level of 10^5 cells of *B. cereus* per gram food product could still be adhered to in order to consider a product to be safe, especially since many strains of *B. cereus* can also cause toxico-infections.

Conclusions and future perspectives

The results described in this thesis provide insight into the ability of gamma models to describe microbial behaviour in food products, and into the possibility of *B. cereus* F4810/72 to produce cereulide in a_w altered broth. The selection criteria for single hurdle models proposed in this thesis can be used for future validation of the gamma hypothesis. The use of criteria is considered the best way forward for objective testing of the hypothesis without driving model creation due to the use of non-optimal models. Consequently, literature data used for validation of the gamma hypothesis can be retested using the criteria for model selection and if necessary other model combinations. This

might be useful for food industries and food safety professionals in government and academia, since knowledge of occurrence of synergy can contribute to the management of food safety. It would also be interesting to repeat the gamma hypothesis validation study with equal test conditions but another microorganism, to test if the set criteria for model selection do also apply for those cases. Additionally, the effect of inoculation levels on the gamma hypothesis can be investigated, since low inoculation levels, as occuring in foods, might show different behaviour towards applied hurdles, which might in turn affect the conclusion about the validity of the hypothesis. Also the development of new models which are better able to describe for example the phenomenon of cliff edges should be considered. The selection or development of models describing real life situations will prevent that fail-dangerous predictions about microbial growth and resulting product safety are made. The use of a cereulide standard for quantification puproses will allow making risk assessments with less uncertainty on the presence of cereulide in a food product and about the toxic dose. Together with the knowledge about the time to onset of cereulide production this can be used to more specifically target measures to prevent cereulide production in food and to evaluate the current criteria for presence of *B. cereus* in food products.

References

1. **Aakre, S. E., and C. L. Little.** 1982. Inhibition of *Bacillus cereus* phospholipase C by univalent anions. Biochem. J. 203:799-801.
2. **Abee, T., and J. A. Wouters.** 1999. Microbial stress response in minimal processing. Int. J. Food Microbiol. 50:65-91.
3. **Agata, N., M. Ohta, M. Mori, and K. Shibayama.** 1999. Growth conditions of and emetic toxin production by *Bacillus cereus* in a defined medium with amino acids. Microbiol. Immunol. 43:15-18.
4. **Augustin, J.-C., and V. Carlier.** 2000. Modelling the growth rate of *Listeria monocytogenes* with a multiplicative type model including interactions between environmental factors. Int. J. Food Microbiol. 56:53-70.
5. **Berenbaum, M. C.** 1977. Synergy, additivism and antagonism in immunosuppression. A critical review. Clin. Exp. Immunol. 28:1-18.
6. **Berenbaum, M. C.** 1989. What is synergy? Pharmacol. Rev. 41:93-141.
7. **Bidlas, E., and R. J. W. Lambert.** 2008. Quantification of hurdles: Predicting the combination of effects - Interaction vs. non-interaction. Int. J. Food Microbiol.

128:78-88.

8. **Boziaris, I. S., P. N. Skandamis, M. Anastasiadi, and G. J. E. Nychas.** 2007. Effect of NaCl and KCl on fate and growth/no growth interfaces of *Listeria monocytogenes* Scott A at different pH and nisin concentrations. J. Appl. Microbiol. 102:796-805.

9. **Brul, S., and P. Coote.** 1999. Preservative agents in foods: mode of action and microbial resistance mechanisms. Int. J. Food Microbiol. 50:1-17.

10. **Dommel, M. K., G. Lücking, S. Scherer, and M. Ehling-Schulz.** 2011. Transcriptional kinetic analyses of cereulide synthetase genes with respect to growth, sporulation and emetic toxin production in *Bacillus cereus*. Food Microbiol. 28:284-290.

11. **Essen, R., C. de Ruiter, and M de Wit.** 2000. Massale voedselvergiftiging in het Kotterbos te Almere. Infectieziekten bulletin 11:205-207.

12. **Foster, J. W.** 1995. Low pH adaptation and the acid tolerance response of *Salmonella typhimurium*. Crit. Rev. Microbiol. 21:215-237.

13. **Gould, G. W.** 1996. Methods for preservation and extension of shelf life. Int. J. Food Microbiol. 33:51-64.

14. **Häggblom, M. M., C. Apetroaie, M. A. Andersson, and M. S. Salkinoja-Salonen.** 2002. Quantitative analysis of cereulide, the emetic toxin of *Bacillus cereus* produced under various conditions. Appl. Environ. Microbiol. 68:2479-2483.

15. **Hughes, M. N., and R. K. Poole.** 1991. Metal speciation and microbial growth - the hard (and soft) facts J. Gen. Microbiol. 137:725-734.

16. **Isobe, M., T. Ishikawa, S. Suwan, N. Agata, and M. Ohta.** 1995. Synthesis and activity of cereulide, a cyclic dodecadepsipeptide ionophore as emetic toxin from *Bacillus cereus*. Bioorg. Med. Chem. Lett. 5:2855-2858.

17. **Jääskeläinen, E. L., M. M. Häggblom, M. A. Andersson, and M. S. Salkinoja-Salonen.** 2004. Atmospheric oxygen and other conditions affecting the production of cereulide by *Bacillus cereus* in food. Int. J. Food Microbiol. 96:75-83.

18. **Lambert, R. J. W., and E. Bidlas.** 2007. An investigation of the gamma hypothesis: A predictive modelling study of the effect of combined inhibitors (salt, pH and weak acids) on the growth of *Aeromonas hydrophila*. Int. J. Food Microbiol. 115:12-28.

19. **Lambert, R. J. W., and E. Bidlas.** 2007. A study of the gamma hypothesis: Predictive modelling of the growth and inhibition of *Enterobacter sakazakii*. Int. J. Food Microbiol. 115:204-213.

20. **Lambert, R. J. W., M. D. Johnston, G. W. Hanlon, and S. P. Denyer.** 2003. Theory of antimicrobial combinations: biocide mixtures - synergy or addition. J. Appl.

Microbiol. 94:747-759.

21. **Lambert, R. J. W., and R. Lambert.** 2003. A model for the efficacy of combined inhibitors. J. Appl. Microbiol. 95:734-743.

22. **Le Marc, Y., V. Huchet, C. M. Bourgeois, J. P. Guyonnet, P. Mafart, and D. Thuault.** 2002. Modelling the growth kinetics of *Listeria* as a function of temperature, pH and organic acid concentration. Int. J. Food Microbiol. 73:219-237.

23. **Leistner, L., and L. G. M. Gorris.** 1995. Food preservation by hurdle technology. Trends Food Sci. Technol. 6:41-46.

24. **Luong, J. H. T.** 1985. Kinetics of ethanol inhibition in alcohol fermentation. Biotechnol. Bioeng. 27:280-285.

25. **Makarasen, A., T. Nishikawa, and M. Isobe.** 2009. Synthesis of four lysine-linked cereulide analogues showing ionophoric activity towards potassium cations as lead compounds for emetic toxin-detection by immunoassays. Synth. 2009:2184-2204.

26. **McMeekin, T. A., J. Olley, D. A. Ratkowsky, and T. Ross.** 2002. Predictive microbiology: towards the interface and beyond. International Journal of Food Microbiology 73:395-407.

27. **McMeekin, T. A., K. Presser, D. A. Ratkowsky, T. Ross, M. Salter, and S. Tienungoon.** 2000. Quantifying the hurdle concept by modelling the bacterial growth/no growth interface. Int. J. Food Microbiol. 55:93-98.

28. **Modi, K. D., M. L. Chikindas, and T. J. Montville.** 2000. Sensitivity of nisin-resistant *Listeria monocytogenes* to heat and the synergistic action of heat and nisin. Lett. Appl. Microbiol. 30:249-253.

29. **Pirhonen, T. I., M. A. Andersson, E. L. Jääskeläinen, M. S. Salkinoja-Salonen, T. Honkanen-Buzalski, and T. M. L. Johansson.** 2005. Biochemical and toxic diversity of *Bacillus cereus* in a pasta and meat dish associated with a food-poisoning case. Food Microbiol. 22:87-91.

30. **Rödel, W., and R. Scheuer.** 2007. Recent results on the hurdle technology - measuring of combined hurdles. Mitteilungsblatt der Fleischforschung Kulmbach 46:3-10.

31. **Shaheen, R., W. A. Anderson, C. Apetroaie, A. Schulz, M. Ehling-Schulz, V. M. Ollilainen, and M. Salkinoja-Salonen.** 2006. Potential of selected infant food formulas for production of *Bacillus cereus* emetic toxin cereulide. Int. J. Food Microbiol. 107:287-294.

32. **Szabo, R. A., Speirs, J. I., and M. Akhtar.** 1991. Cell culture detection and conditions for production of a *Bacillus cereus* heat-stable toxin. J. Food Prot. 54:272-276.

33. **Te Giffel, M. C., and M. H. Zwietering.** 1999. Validation of predictive models describing the growth of *Listeria monocytogenes*. Int. J. Food Microbiol. 46:135-149.

34. **Ter Steeg, P. F., J. C. Hellemons, and A. E. Kok.** 1999. Synergistic actions of nisin, sublethal ultrahigh pressure, and reduced temperature on bacteria and yeast. Appl. Environ. Microbiol. 65:4148-4154.

35. **Tokarskyy, O., and D. L. Marshall.** 2008. Mechanism of synergistic inhibition of *Listeria monocytogenes* growth by lactic acid, monolaurin, and nisin. Appl. Environ. Microbiol. 74:7126-729.

36. **Wijtzes, T., F. M. Rombouts, M. L. T. Kant-Muermans, K. van 't Riet, and M. H. Zwietering.** 2001. Development and validation of a combined temperature, water activity, pH model for bacterial growth rate of *Lactobacillus curvatus*. Int. J. Food Microbiol. 63:57-64.

37. **Zwietering, M. H., T. Wijtzes, J. C. de Wit, and K. van 't Riet.** 1992. A decision support system for prediction of the microbial spoilage in foods. J. Food Prot. 55:973-979.

Summary

Consumers expect safe food within the given shelf life. To ensure food stability and safety, several growth limiting factors, referred to as hurdles, are used. When a combination of hurdles is used, generally, the intensity of the hurdles may be lower compared to the intensity of those hurdles when used individually to achieve the same effect. There are two opposite views of how antimicrobial factors combine; there are interactive effects between hurdles (synergy), or there are combined effects which are multiplicative (gamma hypothesis). For food safety management, it is important to understand if combinations are synergistic or not, to avoid making fail-dangerous or overly fail-safe predictions. Therefore, one aim of this PhD project was to validate the gamma hypothesis for specific combinations of hurdles commonly used in food production. Since the relationship between growth and toxin production of *B. cereus* is little understood, a second aim was to investigate the production of emetic toxin in more detail. Several new lines of research were set-up to deliver on these aims.

To test the gamma hypothesis, large data sets regarding the effects of individual and combined hurdles on the maximum specific growth rate (μ_{max}) had to be established. Chapter 2 of this thesis therefore provides an overview and comparison of methods which can be used for quick and reliable generation of growth data and estimation of growth parameters. The plate count method was compared to two optical density (OD) methods, namely, the 2-fold dilution (2FD) method and the relative rate to detection (RRD) method. The plate count method and both OD-methods gave comparable estimates and μ_{max}-values derived by the 2FD method and by the RRD method were of the same order of magnitude. Some marked differences between the two OD-approaches were apparent as well, since the 2FD method allowed for the derivation of values for lag time (λ) from the data, and this was not possible with the RRD method. However, the RRD method gave many more data points per experiment and in particular also gave more data points close to the growth boundary. It was shown that all three proposed methods can be used for parameter estimation, but that the RRD method was best to use for the validation/ falsification of the gamma hypothesis.

The use of the 2FD method revealed an increase in λ at near growth boundary conditions. Little insight exists in the processes occurring in the cell during the lag phase and specifically it is unclear which parameters are responsible for the start of the growth

phase. Chapter 3 therefore studied the physiological parameters in *B. cereus* cells upon exposure to near-growth-boundary acid stress and identified markers for the transition between lag phase and growth, using fluorescent probes combined with flow cytometry. Determination of cell counts and optical density revealed lag phases of 1, 2 and 5 h, in cultures shifted to pH 7, pH 5.3 (set with lactic acid) and pH 4.9 (set with sulfuric acid), respectively. ATP levels were constant during the lag phase and increased after the onset of growth, while the percentage of PI-stained cells and cells with a significant membrane potential decreased during the lag phase. The activity of the electron transfer chain and esterases were generally low during the lag phase and increased after the onset of growth, which allows for assessment of transition between lag phase and growth phase. Our results showed that, independent of the duration of the lag phase, the same processes in the cells could be observed under different growth conditions.

Chapters 4 and 5 tested the validity of the gamma hypothesis for combinations of pH and undissociated acid and for combinations of pH and water activity (a_w) lowering solutes. The undissociated acids tested were acetic acid, lactic acid, propionic acid and formic acid, and the a_w lowering solutes tested were sodium chloride, potassium chloride and glucose. Models describing the effect of the hurdles on μ_{max} were selected from literature and fitted to the experimental data. Based on a predefined set of criteria the best model was selected, which was the model of Rosso *et al.* for pH dependency and the model of Luong *et al.* for undissociated acid and a_w lowering solute. The pre-set criteria were: 1) the mean square error value for the model fit should be below 0.01, ensuring a high level of fit; 2) the standard deviations for individual model parameters should be smaller than the parameter estimates themselves, since standard deviations higher than the respective parameter estimates indicate large variation, and 3) the model parameters should preferably have biological meaning or at least be interpretable. The gamma model was found to have good predictive performance for combinations of pH and undissociated acids, and the performance was less when a synergy factor was included in the model. For combinations of pH and a_w lowering solutes, however, neither the gamma model nor one of the synergy models had a good predictive performance. The gamma hypothesis could therefore not be validated nor rejected in the latter case. It is considered important to define pre-set criteria before commencing experimentation for model validation/falsification, since such a systematic approach is required to be confident in the correctness of the individual components of the combined (synergy)

models. When non-optimal models to describe single hurdle effects are combined into a gamma model, this might drive creation of synergy models. In effect poorer performance of the individual hurdles would be accepted, resulting in a bias towards synergy factor models.

The *B. cereus* strain used in this research was an emetic toxin producing strain. However, the emetic toxin cereulide was not commercially available at the onset of the work, which effects the accurate quantification of this compound since to that point the structurally similar compound valinomycin was the only available alternative to make calibration curves. Chapter 6 describes a new chemical synthesis route for cereulide production, which makes sufficient amounts of the appropriate reference material available to deploy as a standard for accurate cereulide quantification by LC-MS, as done in Chapter 7. The new synthesis route consisted of 10 steps and had an overall yield of 28.5 %; an improvement compared to the yield of synthesis routes used by others before. The synthetic cereulide showed biological activity towards boar semen and HEp2-cells. Recovery experiments undertaken with acetonitrile on cereulide-spiked foods showed recovery rates close to 100 % over a wide concentration range. Using this new cereulide avoids the use of valinomycin, which underestimates the cereulide content by 10%. The effect of addition of salt on growth and cereulide production was determined in BHI using the cereulide standard. From the data obtained it was concluded that the time to onset of cereulide production was dependent on the growth parameters μ_{max} and λ of the culture. Cereulide production was found to start at least 10 hours after the culture had reached stationary phase. For the tested strain of emetic *B. cereus*, thus, cereulide production seemed not to be related to the level of cells.

In conclusion, the RRD method and the criteria for model selection as proposed can be used for future validation of the gamma hypothesis. The gamma hypothesis could not be validated nor rejected for all combinations evaluated here, but the criteria for model selection can be used to re-test available data from literature with other test organisms, other hurdle combinations and other models. The use of a cereulide standard contributes to food safety since it will allow making good assessments regarding the level of cereulide present in food products. Knowledge about the processes in the cell during lag phase and initiating the onset of growth can play an important role in the prevention of outgrowth and subsequent cereulide production, and the information gathered in this thesis in this regard may support further studies.

Samenvatting

Consumenten verwachten dat voedsel veilig is totdat het de houdbaarheidsdatum heeft bereikt. Om er voor te zorgen dat er geen micro-organismen in het product gaan groeien of groei voldoende te beperken, worden groeilimiterende factoren gebruikt, zogenaamde 'horden'. In plaats van één factor kan ook een combinatie van factoren worden gebruikt, wat bijvoorbeeld kan resulteren in het gebruik van lagere concentraties toevoegingen (additieven). Er zijn twee opvattingen over de werking van combinaties van factoren. De eerste aanname is dat er interactie optreedt tussen de factoren (synergie), en de andere hypothese is dat er geen interactie is en dat het effect van de factoren een vermenigvuldiging van de enkelvoudige effecten is (gammahypothese). In dit proefschrift is de gammahypothese nader bestudeerd voor het toxineproducerende micro-organisme *Bacillus cereus* F4810/72. Tevens is het effect van zout als additief op de toxineproductie onderzocht.

Voor dit onderzoek waren veel gegevens (data) nodig over het effect van additieven op de groeisnelheid (μ_{max}) van het micro-organisme. Hoofdstuk 2 van dit proefschrift geeft een overzicht en vergelijking van methoden die gebruikt kunnen worden om snel en betrouwbaar groeidata te kunnen genereren. De uitplaatmethode is vergeleken met twee methoden gebaseerd op metingen van de optische dichtheid (OD) van het groeimedium; de tweevoudige verdunnings (2FD) methode en de relatieve snelheid tot detectie (RRD) methode. De uitplaatmethode geeft vergelijkbare resultaten met beide OD-methoden en de schattingen van de μ_{max}-waarden van de 2FD-methode en de RRD methode hebben dezelfde ordegrootte. Verschillen tussen beide OD-methoden zijn dat bij de 2FD-methode zowel μ_{max} als de lagfase (λ) worden geschat en bij de RRD-methode alleen μ_{max}, en dat de RRD-methode meer datapunten geeft en vooral ook meer datapunten rond de groeigrens. Dit onderzoek toont aan dat alle drie de methoden gebruikt kunnen worden om datapunten te verkrijgen, maar dat voor het testen van de gammahypothese het beste gebruik kan worden gemaakt van de RRD-methode.

Het gebruik van de 2FD-methode liet zien dat de lagfase toeneemt wanneer *B. cereus* gekweekt wordt vlakbij zijn groeigrens. De processen die zich afspelen in de cel tijdens de lagfase en die er voor zorgen dat *B. cereus* uiteindelijk gaat groeien waren tot dusver onbekend. Hoofdstuk 3 bestudeert de processen in de cellen wanneer ze worden blootgesteld aan zuurstress in niveaus vlakbij de groeigrens en identificeert

welke veranderingen in processen kunnen aantonen of cellen zich in de lagfase of in de groeifase bevinden. De processen in de cel zijn bestudeerd met fluorescente labels en "flow cytometry". De toevoeging van melkzuur tot een pH van 5.3 en de toevoeging van zwavelzuur tot een pH van 4.9 resulteerde in een toename van de lagfase tot respectievelijk 2 uur en 5 uur, ten opzichte van de cellen die bij neutrale pH (pH 7) waren gekweekt en een lagfase van 1 uur hadden. Het ATP-niveau in de cultuur was constant tijdens de lagfase en nam toe tijdens de groeifase, terwijl het percentage cellen met een beschadigd celmembraan afnam tijdens de lagfase. De activiteit van de elektronenoverdrachtsketen en esterases was constant tijdens de lagfase en nam toe tijdens de groeifase, waardoor deze processen gebruikt kunnen worden om te bepalen in welke fase cellen zich bevinden. Onze resultaten laten zien dat, onafhankelijk van het soort zuur dat wordt gebruikt en de lengte van de lagfase, dezelfde processen in de cellen kunnen worden waargenomen.

Hoofdstuk 4 en 5 beschrijven het testen van de gammahypothese voor combinaties van pH en ongedissocieerd zuur en combinaties van pH en wateractiviteit (a_w) verlagende stoffen. De ongedissocieerde zuren die zijn getest zijn azijnzuur, melkzuur, propionzuur en mierenzuur en de a_w verlagende stoffen die getest zijn, zijn natriumchloride (keukenzout), kaliumchloride en glucose. Wiskundige modellen die het effect van de additieven op de groeisnelheid van micro-organismen beschrijven, zijn verzameld uit de literatuur en gefit op de experimentele data. Op basis van vastgestelde selectiecriteria is het beste model gekozen; het model ontwikkeld door Rosso voor het pH-effect en het model ontwikkeld door Luong voor de effecten van ongedissocieerd zuur en a_w-verlagende stoffen. De criteria waren: 1) de gemiddelde kwadratensom moet kleiner zijn dan 0.01 om te kunnen spreken van een goede fit; 2) de standaardafwijkingen voor elke parameterschatting moeten kleiner zijn dan de schatting zelf, omdat afwijkingen groter dan de schatting duiden op grote variaties van de parameter. Verder heeft de parameter bij voorkeur biologische betekenis. Bij het testen van combinaties van pH-effecten en ongedissocieerde zuureffecten bleek dat het gammamodel goede voorspellingen gaf van het gecombineerde effect en dat modellen met een synergiefactor minder goede voorspellingen gaven. Zowel het gammamodel als beide synergiemodellen waren niet in staat het effect van combinaties van pH effecten en a_w-verlagende stoffen op de groeisnelheid van *B. cereus* te voorspellen. In dit geval kon de gammahypothese dus niet bevestigd worden, maar ook niet worden afgewezen. Dit bewijst tevens dat het belangrijk is om van tevoren criteria vast te stellen om modellen te selecteren voor het

testen van de hypothese, omdat anders de kans bestaat dat er modellen gekozen worden die het effect van één of meer van de afzonderlijke additieven niet goed beschrijven. Het selecteren van een niet-optimaal model voor het additief kan er anders toe leiden dat er synergiemodellen gecreëerd gaan worden, terwijl er geen sprake is van synergie. Het gebruik van andere modellen had andere conclusies opgeleverd.

De *B. cereus* stam die gebruikt is in dit onderzoek produceert een toxine, genaamd cereulide. Dit toxine kon niet als zuivere stof worden gekocht, wat betekent dat er geen kalibratiegrafieken konden worden gemaakt om de productie van cereulide door *B. cereus* onder allerlei omstandigheden te kunnen kwantificeren. Vaak wordt daarom valinomycine, een stof die veel lijkt op cereulide, gebruikt voor de kalibratiegrafieken. Hoofdstuk 6 beschrijft een nieuwe chemische synthesestrategie, die resulteerde in een zuivere stof die gebruikt kan worden voor het maken van kalibratiegrafieken. De synthese bestaat uit 10 stappen en levert een opbrengst op van 28 procent. Het bleek dat het synthetische cereulide biologisch actief was, aangezien varkenssperma of HEp2-cellen erdoor beschadigd werden. Het gebruik van valinomycine voor kalibratiegrafieken, in plaats van synthetisch cereulide, zorgt voor een overschatting van 10 procent, in geschatte hoeveelheid cereulide uit een monster met onbekende hoeveelheid. Het effect van zout op groei en cereulideproductie is beschreven in hoofdstuk 7. Uit deze resultaten kan worden geconcludeerd dat het moment waarop een bacteriecultuur cereulide gaat produceren, afhangt van de groeisnelheid en de duur van de lagfase. Ongeveer 10 uur nadat de cultuur zijn stationaire fase heeft bereikt, start de productie en de cereulideproductie lijkt niet proportioneel ten opzichte van het aantal cellen.

Er kan worden geconcludeerd dat de RRD methode en de criteria die zijn opgesteld voor de selectie van de modellen kunnen worden gebruikt voor het testen van de gammahypothese. De gammahypothese kon niet worden bevestigd of worden verworpen, maar de voorgestelde criteria kunnen worden gebruikt om literatuurdata waar de hypothese ook werd getest opnieuw te testen met, indien van toepassing, betere modellen. Het bestaan van cereulide met bekende concentratie maakt het mogelijk om cereulide in voedsel beter te kunnen kwantificeren, wat bijdraagt aan de voedselveiligheid doordat er betere risicoanalyses kunnen worden gemaakt. De kennis over de processen in de cel tijdens de lagfase en transitie naar de groeifase kan een belangrijke rol gaan spelen bij het voorkomen van groei van het micro-organisme en achtereenvolgens de cereulideproductie.

Acknowledgments

I am blessed to have the opportunity to study and to defend my PhD thesis. Next to my own input to make this opportunity reality, I would not have been able to realize it without the help of other people. I would like to thank Martine Reij, Marcel Zwietering and Leon Gorris for the supervision of my research. Also thanks to Tjakko Abee and Han Joosten for being part of my advisory committee. I would like to thank Paul in 't Veld, Richard Blaauw, Monika Ehling-Schulz and Andreja Rajkovic for their contribution to my synthetic cereulide manuscript. Maarten Mols, thank you for your help with the lag phase research, which resulted in one manuscript. Also several students were involved in my PhD research; Aneta Linka, Fan Wang, Linlin Fan, Maarten Overes, Karin Metselaar and Piet van der Zaal, thank you for your contribution to my research.

I would like to thank my colleagues for the great time I had in the laboratory. Also the PhD trips to Canada and Switzerland with the PhD students were great fun. Thank you all for this experience! Some people in special deserve my appreciation. Ida, it was nice sharing the office with you and thank you for being my paranymph. Petra, your company in lab 402 was very much appreciated. I missed our conversations in my last year.

During my PhD research I also had a lot of support from people outside academia. Working at 'Bever Zwerfsport' and at 'Sportcentrum de Plataan' and contact with those colleagues was something I really needed to remain a person who is able to stay connected to the world and non academic issues. Thank you all for the great years I had in Rotterdam and I still have in Wageningen.

I would like to thank my friends and family, who live literally all over the world, for their support and friendship: Amanda, Aniek, Anneke, Babet, Danielle, Jenneke, Loes, Lisanne, Marije, Marlou and Mariska. Marjan and Ben, thank you for the nice diners, evenings and excursions. Sylvia, thank you for the many cups of tea you made me to cheer me up. I am happy that you are one of my paranymphs.

Mum and dad, from the moment I started studying in Wageningen you have supported me in everything. You always used to say that parents who are blessed with their children, have children who are blessed with their parents. One way or another, I feel blessed with you and thanks for everything! Wouter, thank you for your support and love throughout the past years. We can not tell how the future will be, but I don't care where we are going, as long as you are next to me!

Els

Dankwoord

Ik voel me gezegend met de kans die ik heb gekregen om te studeren en te promoveren. Naast mijn eigen inspanningen om deze kansen waar te maken, was dit niet gelukt zonder hulp van anderen. Ik wil daarom Martine Reij, Marcel Zwietering en Leon Gorris bedanken voor hun bijdragen aan mijn onderzoek. Ook dank aan Tjakko Abee en Han Joosten voor hun bijdragen tijdens het overleg van de begeleidingscommissie. Dank aan Paul in 't Veld, Richard Blaauw, Monika Ehling-Schulz en Andreja Rajkovic voor hun bijdragen aan het artikel over synthetisch cereulide. Maarten Mols, dank je wel voor je hulp bij het onderzoek en manuscript over parameters tijdens de lagfase. Aneta Linka, Fan Wang, Linlin Fan, Maarten Overes, Karin Metselaar en Piet van der Zaal; bedankt voor de bijdragen aan mijn onderzoek in de vorm van een afstudeervak.

Mijn collega's wil ik bedanken voor de leuke tijd tijdens mijn promotieonderzoek. De AIO-reizen naar Canada en Zwitserland had ik niet willen missen; dank aan alle AIOs voor die leuke ervaring. Ik wil Ida bedanken voor het delen van het kantoor en alle gesprekken en ik ben blij dat jij één van mijn paranimfen bent. Petra, het delen van het lab was een feestje en ik heb je gezelschap in mijn laatste jaar zeker gemist.

Tijdens mijn promotieonderzoek heb ik ook veel steun gehad van mensen buiten de academische wereld. Het werken bij Bever Zwerfsport en bij Sportcentrum de Plataan was voor mij van grote waarde om me ook met andere zaken dan onderzoek bezig te kunnen houden. Bedankt allemaal voor de geweldige tijd die ik heb gehad in Rotterdam en die ik nog steeds heb ik Wageningen.

Ik wil mijn vrienden en familie bedanken (die werkelijk overal ter wereld wonen) voor hun steun en vriendschap: Amanda, Aniek, Anneke, Babet, Danielle, Jenneke, Loes, Lisanne, Marije, Marlou en Mariska. Marjan en Ben, bedankt voor de gezellige etentjes, avonden en excursies. Sylvia, bedankt voor de vele koppen thee en goede gesprekken en het feit dat jij mijn paranimf wilt zijn.

Pap en mam, vanaf het moment dat ik ging studeren, hebben jullie mij altijd gesteund. Jullie zeggen altijd dat ouders die het getroffen hebben met hun kinderen doorgaans kinderen hebben die het getroffen hebben met hun ouders. Hoe het ook zij, ik heb het getroffen met jullie en bedankt voor alle steun!

Wouter, bedankt voor je steun en liefde de afgelopen jaren. We kunnen de toekomst niet voorspellen, maar dat maakt ook niets uit, zolang jij er maar bent!

Els

List of publications

1. **Biesta-Peters, E. G., M. W. Reij, H. Joosten, L. G. M. Gorris, and M. H. Zwietering.** 2010. Comparison of two optical density methods and a plate count method for estimation of growth parameters of *Bacillus cereus*. Appl. Environ. Microbiol. 76 (5): 1399-1405.

2. **Biesta-Peters, E. G., M. W. Reij, L. G. M. Gorris, and M. H. Zwietering.** 2010. Comparing nonsynergistic gamma models with interaction models to predict growth of emetic *Bacillus cereus* when using combinations of pH and individual undissociated acids as growth-limiting factors. Appl. Environ. Microbiol. 76 (17):5791-5801.

3. **Biesta-Peters, E. G., M. W. Reij, R. H. Blaauw, P. H. in 't Veld, A. Rajkovic, M. Ehling-Schulz, and T. Abee.** 2010. Quantification of the emetic toxin cereulide in food products by liquid chromatography-mass spectrometry using synthetic cereulide as a standard. Appl. Environ. Microbiol. 76 (22): 7466-7472.

4. **Biesta-Peters, E. G., M. Mols, M. W. Reij, and T. Abee.** 2011. Physiological parameters of *Bacillus cereus* marking the end of acid-induced lag phases. Int. J. Food Microbiol. 148 (1): 42-47.

5. **Biesta-Peters, E. G., M. W. Reij, M. H. Zwietering, and L. G. M. Gorris.** 2011. Comparing non-synergy gamma models and interaction models to predict growth of emetic *Bacillus cereus* for combinations of pH and water activity lowering solutes. Appl. Environ. Microbiol. 77 (16).

6. **Biesta-Peters, E. G., M. W. Reij, H. Joosten, L. G. M. Gorris, and M. H. Zwietering.** Kinetics of cereulide production by *Bacillus cereus* F4810/72 as influenced by water activity. Submitted for publication.

Curriculum Vitae

Elisabeth Geertruida (Els) Biesta-Peters was born on October 10, 1982 in Schiedam, The Netherlands. She grew up in Vlaardingen where she attended “basisschool de Ark” for primary education from 1986-1995. She received her "VWO diploma" in 2001, after finishing her secondary education attended at “CSG Aquamarijn, afdeling ‘t Groen” in Vlaardingen. In 2001 she started her bachelor studies in Food Technology at Wageningen University. Her thesis was carried out at the Laboratory of Product Design and Quality Management at Wageningen University. After her graduation in 2004 she started her master studies in Food Safety at the same university. Her thesis was carried out at the Laboratory of Food Microbiology at Wageningen University. For her internship she travelled to Canada, where she worked for four months at the Canadian Research Institute for Food Safety in Guelph, Canada. She graduated in 2006, whereafter she started her PhD project at the Laboratory of Food Microbiology at Wageningen University. Her PhD project was entitled '*Bacillus cereus*: emetic toxin production and gamma hypothesis for growth'. The results of that project are described in this thesis. Els currently works as senior scientist at the Laboratory of Food and Feed Safety of the New Food and Consumer Product Safety Authority (de nieuwe Voedsel en Waren Autoriteit) in Zutphen. She is also an instructor at “Sportcentrum de Plataan” in Wageningen.

Overview of completed training activities

Discipline specific activities
Courses
Reaction Kinetics in Food Science (2006), VLAG, Wageningen
Genetics and Physiology of Food-Associated Microorganisms (2007), VLAG, Wageningen
Management of Microbiological Hazards in Foods (2007), VLAG, Wageningen
Distance learning modules HACCP and Food Preservation (2007), VLAG, Wageningen
Food Fermentation (2008), VLAG, Wageningen

Meetings
Int. Conference Predictive Modelling in Foods (2007), Athens, Greece (poster)
NVVM conference day (2007, 2008), Wageningen
FIMM conference day (2007, 2008), Ede, Wageningen
VLAG thematic meeting: NMR and MRI applications (2008), VLAG, Wageningen
Int. Conference Predictive Modelling in Foods (2009), Washington, USA (oral presentations)
SGM Autumn Meeting (2010), Nottingham, UK (oral presentation)

Training periods
Nestlé Research Centre (2007), Vers-Chez-Le-Blanc, Switzerland
PTU Munich (2007, 2009), Freising, Germany
VWA (2009), Eindhoven, The Netherlands

General courses
Training and Supervising Thesis Students (2007), OWU, Wageningen
PhD Competence Assessment (2007), WGS, Wageningen
Project and Time Managements (2008), WGS, Wageningen
Scientific Writing (2008), Centa, Wageningen
Philosophy and Ethics of Food Science and Technology (2010), VLAG, Wageningen
De kunst van het vragen stellen (2008), OWU, Wageningen
Advanced Course Guide to Scientific Artwork (2010), library WUR, Wageningen

Other activities
Preparing project proposal (2006)
Seminars Laboratory of Food Microbiology (2006-2011)
VLAG PhD week (2007), VLAG, Bilthoven, The Netherlands
Supervising BSc and MSc students (2007-2010)
PhD trip of Laboratory of Food Microbiology to Canada (2008)
Organisation of PhD trip to Canada (2008)
PhD trip of Laboratory of Food Microbiology to Switzerland (2010)

This project was sponsored by Nestlé Research Centre, Lausanne, Switzerland

Cover design by Els Biesta-Peters

The hurdle technology picture (invitation) was kindly provided by Henk Van Ruitenbeek
The portrait picture on page 185 was kindly provided by 'Fred van de Heetkamp fotografie' after permission of 'Sportcentrum de Plataan'

Printed by Ipskamp Drukkers B.V., Enschede, The Netherlands